



**TURUN
YLIOPISTO**
UNIVERSITY
OF TURKU

SMOULDERING INFLAMMATION IN MULTIPLE SCLEROSIS

**A PET imaging study on prediction of disease
progression and effects of treatment**

Marcus Sucksdorff



**TURUN
YLIOPISTO**
UNIVERSITY
OF TURKU

SMOULDERING INFLAMMATION IN MULTIPLE SCLEROSIS

A PET imaging study on prediction of disease
progression and effects of treatment

Marcus Sucksdorff

University of Turku

Faculty of Medicine
Department of Clinical Medicine
Clinical Neurosciences
Turku Doctoral Programme in Clinical Research
Turku PET Centre
Division of Clinical Neurosciences, Turku University Hospital

Supervised by

Professor Laura Airas
Division of Clinical Neurosciences
Turku University Hospital and
University of Turku
Turku, Finland

Professor Juha O. Rinne
Turku PET Centre
Turku University Hospital and
University of Turku
Turku, Finland

Docent Eero Rissanen
Division of Clinical Neurosciences
Turku University Hospital and
University of Turku
Turku, Finland

Reviewed by

Professor Jukka Peltola
Department of Neurology
Tampere University Hospital and
Tampere University
Tampere, Finland

Docent Johanna Krüger
Research Unit of Clinical Medicine, Neurology
University of Oulu and
Neurocenter, Neurology
Oulu University Hospital
Oulu, Finland

Opponent

Professor Pentti Tienari
Translational Immunology
Research Programs Unit,
University of Helsinki,
Department of Neurology, Brain Center,
Helsinki University Hospital
Helsinki, Finland

The originality of this publication has been checked in accordance with the University of Turku quality assurance system using the Turnitin OriginalityCheck service.

ISBN 978-951-29-9529-5 (PRINT)
ISBN 978-951-29-9530-1 (PDF)
ISSN 0355-9483 (Print)
ISSN 2343-3213 (Online)
Painosalama, Turku, Finland 2023

To the loving memory of my mother

UNIVERSITY OF TURKU

Faculty of Medicine

Department of Clinical Medicine

Clinical Neurosciences

MARCUS SUCKSDORFF: Smouldering Inflammation in Multiple Sclerosis
– A PET Imaging Study on Prediction of Disease Progression and Effects
of Treatment

Doctoral Dissertation, 137 pp.

Doctoral Programme in Clinical Research

November 2023

ABSTRACT

Background: Multiple sclerosis (MS) is the most common inflammatory and neurodegenerative autoimmune disease of the central nervous system in young adults, where the inflammatory reaction causes destruction of the myelin sheath surrounding the neurons in addition to irreversible damage to the neuronal axons. A large proportion of people with MS continue to experience disease accumulation throughout the years, despite proper disease modifying therapy (DMT). The DMTs presently available fail to effectively prevent the disease accrual in progressive forms of MS. According to neuropathological studies, the diffuse inflammation in the area surrounding the MS lesions and in the normal appearing white matter (NAWM) is related to activated microglial cells. Overactivation of microglial cells is known to correlate with disease severity. Microglial activation can be detected by using *in vivo* positron emission tomography (PET) imaging with radioligands that bind to the translocator protein (TSPO). The TSPO-molecule upregulates mostly in activated microglia. Therefore, it has been considered as a “real-time” marker of the inflammatory activity in MS.

Aims of the study: The main aims of this thesis were to evaluate the effect of DMTs (fingolimod and natalizumab) on the microglial activity in the MS brain and to evaluate the role of activated microglia in predicting future disease progression by using PET imaging with TSPO binding ¹¹C-PK11195 radioligand.

Results: Fingolimod- and natalizumab treatment decreased microglial activity in brain regions critical to MS disease progression. Higher microglial activation in the perilesional area and NAWM predicted later disease progression independent of relapse activity.

Conclusions: The results demonstrate that TSPO-PET is a promising imaging method to identify the diffuse neuroinflammation in progressive MS, to predict future MS related disease progression independent of relapses and to evaluate the effect of DMTs.

KEYWORDS: progressive multiple sclerosis, biomarker, prediction, microglia, TSPO-PET, MRI, DMT

TURUN YLIOPISTO

Lääketieteellinen tiedekunta

Kliininen laitos

Kliiniset neurotieteet

MARCUS SUCKSDORFF: Kytevä inflammaatio MS-taudissa –

PET-kuvantamistutkimus ennustamaan taudin etenemistä ja hoitovastetta

Väitöskirja, 137 s.

Turun kliininen tohtoriohjelma

Marraskuu 2023

TIIVISTELMÄ

Tausta: MS-tauti on yleisin nuorten aikuisten tulehduksellinen, keskushermostoa rappeuttava autoimmuunisairaus, jossa tulehdusreaktio aiheuttaa hermosoluja ympäröivän myeliinivaipan tuhoutumista sekä itse hermosolujen viejähaarakkeiden, aksonien vaurioitumista. Suurella osalla potilaista tauti etenee vuosien saatossa, asianmukaisesta taudinkulkuun vaikuttavasta lääkityksestä huolimatta. Etenevän MS-taudin hoitoon ei toistaiseksi ole käytettävissä lääkitystä, joka estäisi tehokkaasti taudin etenemistä. Neuropatologisten tutkimusten mukaan MS-taudille tyypillisten tulehduspesäkkeitä ympäröivien alueiden sekä normaalilta näyttävän valkean aineen (normal appearing white matter; NAWM) diffuusiin tulehdukseen liittyy mikrogliasolujen aktivoituminen, jonka voimakkuus korreloi taudin vaikeusasteeseen. Mikrogliasolujen aktiivisuutta voidaan mitata positroni-emissiotomografia (PET) -kuvauksella, käyttämällä translokaatioproteiini -molekyyliin (TSPO) sitoutuvia radioaktiivisesti leimattuja merkkiaineita. TSPO-molekyyli ilmentyy pääosin aktivoituneissa mikrogliasoluissa, jonka vuoksi tätä pidetään tulehdusreaktion markkerina.

Tavoitteet: Väitöskirjan keskeisenä tavoitteena oli arvioida miten MS-taudin kulkuun vaikuttavat lääkitykset (fingolimodi ja natalitsumabi) muuttavat aivojen mikrogliasolujen aktiviteettia ja miten mikrogliasolujen aktiviteetti korreloi taudin myöhempään etenemiseen käyttäen aktivoituneisiin mikrogliasoluihin sitoutuvaa ¹¹C-PK11195 -merkkiainetta.

Tulokset: Fingolimodi- ja natalitsumabihoito vähensivät mikrogliasolujen aktiivisuutta MS-taudin etenemiselle kriittisillä aivoalueilla. Korkeampi mikrogliasolujen aktivaatio NAWM:ssa ja tulehduspesäkkeitä ympäröivillä alueilla ennusti taudin myöhempää etenemistä pahenemisvaiheista riippumatta.

Johtopäätökset: Tulosten perusteella voidaan todeta, että TSPO-PET-kuvantaminen on lupaava menetelmä tunnistamaan aivojen laaja-alainen inflammaatio etenevässä MS-taudissa, ennustamaan taudin etenemistä pahenemisvaiheista riippumatta sekä arvioimaan taudin kulkuun vaikuttavien lääkitysten hoitovastetta.

AVAINSANAT: etenevä MS-tauti, biomarkkeri, ennuste, mikrogliasolut, PET, MRI, taudin kulkuun vaikuttava lääkehoito

Table of Contents

| | |
|---|-----------|
| Abbreviations | 8 |
| List of Original Publications | 11 |
| 1 Introduction | 12 |
| 2 Review of the Literature | 14 |
| 2.1 Multiple sclerosis..... | 14 |
| 2.1.1 Epidemiology | 14 |
| 2.1.2 Pathogenesis | 15 |
| 2.1.3 Genetic and environmental risk factors | 16 |
| 2.1.4 Clinical features, diagnostic criterions, and outcome measures | 18 |
| 2.1.5 Smouldering MS and progression independent of relapses (PIRA)..... | 21 |
| 2.2 The treatment of MS | 23 |
| 2.2.1 Disease modifying therapies (DMTs)..... | 23 |
| 2.2.2 Treatment options for RRMS..... | 27 |
| 2.2.3 The benefits of an early induction of high-efficacy DMTs in RRMS | 30 |
| 2.2.4 Treatment options for progressive MS..... | 31 |
| 2.3 The role of microglia in MS..... | 33 |
| 2.3.1 Microglia..... | 33 |
| 2.3.2 Neuropathological studies revealing microglial activation..... | 34 |
| 2.3.3 Translocator protein (TSPO) expression as a marker of detecting microglial activation..... | 34 |
| 2.3.4 PET imaging detecting microglial activation in MS | 35 |
| 2.3.5 MRI imaging modalities detecting microglial activation in MS..... | 43 |
| 2.4 Positron emission tomography (PET) | 44 |
| 2.4.1 Principles of positron emission tomography (PET) | 44 |
| 2.4.2 PET scanner and acquisition of image data | 45 |
| 2.4.3 Modelling and quantification of the detected radioligand binding signal | 46 |
| 2.4.4 The variability in the TSPO uptake | 47 |
| 3 Aims | 49 |
| 4 Materials and Methods | 50 |

| | | |
|----------|---|------------|
| 4.1 | Materials | 50 |
| 4.1.1 | Study participants and procedures | 50 |
| 4.1.2 | Study I..... | 52 |
| 4.1.3 | Study II..... | 53 |
| 4.1.4 | Study III..... | 54 |
| 4.2 | Methods | 54 |
| 4.2.1 | MRI imaging | 54 |
| 4.2.2 | PET imaging and ¹¹ C-PK11195 radioligand production | 55 |
| 4.2.3 | Image processing and analysis | 55 |
| 4.2.4 | Modelling of ¹¹ C-PK11195 image data..... | 56 |
| 4.2.5 | Statistical methods | 56 |
| 5 | Results | 60 |
| 5.1 | Study I: Fingolimod treatment reduces microglial activation at the site of focal inflammatory lesions | 60 |
| 5.2 | Study II: Natalizumab treatment reduces microglial activation in the NAWM and at the rim of chronic lesions | 62 |
| 5.3 | Study III: Increased microglial activation predicts later disease progression independent of relapses during an average follow-up of over 4 years | 66 |
| 6 | Discussion | 71 |
| 6.1 | Interpretation of the study results and methodological considerations | 72 |
| 6.1.1 | The effect of DMTs on TSPO uptake..... | 72 |
| 6.1.2 | The longitudinal change in TSPO uptake in untreated patients with progressive MS..... | 74 |
| 6.1.3 | TSPO uptake as a predictor of MS progression..... | 75 |
| 6.1.4 | Methodological considerations of the baseline results | 76 |
| 6.1.5 | TSPO-PET as a prognostic tool of disease progression | 76 |
| 6.2 | Limitations..... | 79 |
| 6.3 | Clinical implications and future directions | 81 |
| 7 | Summary/Conclusions | 84 |
| | Acknowledgements | 85 |
| | References | 88 |
| | Original Publications..... | 103 |

Abbreviations

| | |
|-------|--------------------------------------|
| AIC | Akaike Information Criterion |
| ARR | Annualised relapse rate |
| AUC | Area under curve |
| BBB | Blood brain barrier |
| BP | Binding potential |
| BTK | Bruton's tyrosine kinase |
| CDP | Confirmed disability progression |
| CIS | Clinically isolated syndrome |
| CNS | Central nervous system |
| CSF | Cerebrospinal fluid |
| CT | Computer tomography |
| DIT | Dissemination in time |
| DIS | Dissemination in space |
| DMT | Disease modifying therapy |
| DTI | Diffusor tensor imaging |
| DV | Distribution volume |
| DVR | Distribution volume ratio |
| DWI | Diffusor weighted imaging |
| EAE | Experimental autoimmune encephalitis |
| EBV | Epstein-Barr virus |
| EDSS | Expanded Disability Status Scale |
| EMA | European Medicines Agency |
| FA | Fractional anisotropy |
| FLAIR | Fluid attenuated inversion recovery |
| FSS | Functional systems score |
| GFAP | Glial fibrillary acidic protein |
| GM | Grey matter |
| HAB | High affinity binder |
| HC | Healthy control |
| HLA | Human leukocyte antigen |
| HRRT | High resolution research tomography |

| | |
|------|---|
| HSCT | Hematopoietic stem cell transplantation |
| IgG | Immunoglobulin G |
| IRL | Iron lesion rim |
| IQR | Interquartile range |
| i.v. | Intravenous |
| LAB | Low affinity binder |
| LOR | Line of response |
| LST | Lesion segmentation tool |
| MAB | Mixed affinity binder |
| MD | Mean diffusivity |
| MRI | Magnetic resonance imaging |
| MS | Multiple sclerosis |
| MSIF | Multiple Sclerosis International Federation |
| MSSS | Multiple Sclerosis Severity Score |
| NAGM | Normal appearing grey matter |
| NAWM | Normal appearing white matter |
| NEDA | No evidence of disease activity |
| OR | Odds ratio |
| PBR | Peripheral benzodiazepine receptor |
| PET | Positron emission tomography |
| PF | Parenchymal fraction |
| PIRA | Progression independent of relapses |
| PML | Progressive multifocal leukoencephalopathy |
| p.o. | Peroral |
| PPMS | Primary progressive MS |
| PVE | Partial volume effect |
| QSM | Quantitative susceptibility mapping |
| RAW | Relapse-associated worsening |
| RCT | Randomised clinical trial |
| RD | Radial diffusivity |
| RIS | Radiologically isolated syndrome |
| ROI | Region of interest |
| RRMS | Relapsing remitting multiple sclerosis |
| SIP | Sphingosine-1-phosphate |
| s.c. | Subcutaneous |
| SD | Standard deviation |
| SEL | Slowly expanding lesion |
| SPM | Statistical parametric mapping |
| SPMS | Secondary progressive multiple sclerosis |
| SUV | Standardised uptake value |

| | |
|-------|------------------------------|
| SVCA | Supervised cluster algorithm |
| TAC | Time activity curve |
| TSPO | Translocator protein |
| VLA-4 | Very late antigen 4 |
| WM | White matter |
| 9HPT | 9-Hole Peg Test |

List of Original Publications

This dissertation is based on the following original publications, which are referred to in the text by their Roman numerals I-III:

- I Sucksdorff M*, Rissanen E*, Tuisku J, Nuutinen S, Paavilainen T, Rokka J, Rinne J, Airas L. Evaluation of the Effect of Fingolimod Treatment on Microglial Activation Using Serial PET Imaging in Multiple Sclerosis. *Journal of Nuclear Medicine*, 2017;58(10):1646–1651.
- II Sucksdorff M, Tuisku J, Matilainen M, Vuorimaa A, Smith S, Keitilä J, Rokka J, Parkkola R, Nylund M, Rinne J, Rissanen E, Airas L. Natalizumab treatment reduces microglial activation in the white matter of the MS brain. *Neurology Neuroimmunology & Neuroinflammation*, 2019;6(4): e574.
- III Sucksdorff M, Matilainen M, Tuisku J, Polvinen E, Vuorimaa A, Rokka J, Nylund M, Rissanen E, Airas L. Brain TSPO-PET predicts later disease progression independent of relapses in multiple sclerosis. *Brain*, 2020;143:3318–3330.

*Contributed equally to this work

The original publications have been reproduced with the permission of the copyright holders.

1 Introduction

Multiple sclerosis (MS) is the most common autoimmune disease of the central nervous system (CNS) in young adults, with both neuroinflammation and neurodegeneration contributing to the pathobiology of the disease (Compston & Coles, 2008; Ransohoff, Hafler, & Lucchinetti, 2015; Weinstein, Owens, & Gandhi, 2022). The initial cause of MS is not entirely understood, but it is suggested to start in the peripheral tissues by the adaptive immune response of T- and B-cells as a result of a diverse interaction of genetic, environmental and hormonal contributors (Comi et al., 2021; Dendrou, Fugger, & Friese, 2015; Olsson, Barcellos, & Alfredsson, 2017). Subsequently, the peripheral T-cells and B-cells in addition to the plasma cells and macrophages infiltrate the blood-brain-barrier (BBB) and migrate into the CNS resulting in multifocal demyelination (Frohman, Racke, & Raine, 2006).

The clinical manifestation of MS is heterogeneous. In 85–90% of cases MS starts as a relapsing-remitting disease. The hallmarks in relapsing remitting MS (RRMS) are the neurological symptoms i.e., MS relapses, that occur in various forms depending on the anatomical location of the lesions, are followed by a full or partial recovery. On average within 15–20 years from the onset of the disease, a large proportion of RRMS patients proceed to develop secondary progressive MS (SPMS), where slowly cumulating symptoms lead to progressive and irreversible disability (Compston & Coles, 2008; Eriksson, Andersen, & Runmarker, 2003; Koch, Kingwell, Rieckmann, Tremlett, & Neurologists, 2010; Tremlett, Yinshan Zhao, & Devonshire, 2008; Tutuncu et al., 2013; Vukusic & Confavreux, 2003; Weinshenker et al., 1989). Progressive loss of walking ability, bladder dysfunction and increasing cognitive impairment are typical in SPMS. However, progression can also occur already from the onset of the disease (primary progressive multiple sclerosis, PPMS) (Thompson et al., 2018).

The inflammatory activity in RRMS can efficiently be controlled by disease modifying treatments (DMTs), which primarily target the peripheral immune system. These treatments reduce the number of relapses and slow down the progression of the disease. However, there is no effective treatment available to prevent the cumulative disability in progressive forms of MS. In addition to being a

leading cause of disability and early retirement especially among young adults, the socioeconomic impact of MS is also considerably high (Filippi et al., 2018; Hollenbach & Oksenberg, 2015). Therefore, more research is urgently warranted to find alternative methods for the therapeutic development of treatments for the progressive forms of MS.

Conventional magnetic resonance imaging (MRI) is the cornerstone method in MS diagnostics and in monitoring the disease activity. However, especially in later MS there is increasing evidence of a diffuse widespread immunopathological process ongoing in the CNS outside the focal lesions that cannot be detected with conventional MRI. This smouldering disease component is characterised by the presence of chronic active lesions and overactivation of the microglia (Giovannoni et al., 2022; Guerrero & Sicotte, 2020), it is associated with signs of neurodegeneration (Correale, Gaitán, Ysraelit, & Fiol, 2017) and is termed in the present nomenclature as “smouldering MS”.

Microglia are myeloid cells of the CNS and have a crucial role as intrinsic defensive cells of the human brain. Nevertheless, overactivation of microglia has been implicated in the pathology of a wide range of neurodegenerative and neuroinflammatory diseases, including MS (Colonna & Butovsky, 2017). Positron emission tomography (PET) provides a method to detect microglial activation *in vivo* using radioligands binding to the translocator protein (TSPO), a protein structure expressed on the outer mitochondrial membrane of the activated microglia.

A better understanding of the mechanisms that underlie the disease progression and develop neurodegeneration in MS could be the key element in obtaining alternative methods to monitor disease progression and to develop future treatment options particularly targeted towards progressive MS.

The aim of this thesis was to evaluate the effect of DMTs on neuroinflammation in MS patients and to examine the possible predictive role of microglial activation in later MS disease progression by using *in vivo* PET imaging with TSPO radioligand ¹¹C-PK11195.

2 Review of the Literature

2.1 Multiple sclerosis

2.1.1 Epidemiology

MS is a chronic autoimmune disease of the brain and spinal cord, where the immune system attacks the protective myelin sheath surrounding the nerve cell axons. This results in multifocal inflammatory lesions in the CNS, which in addition to neurodegeneration are the hallmarks of the disease (Ransohoff et al., 2015).

It is estimated that MS affects more than 2.8 million people worldwide, with a prevalence of 50–300 per 100,000 people (Multiple Sclerosis International Federation (MSIF) 2021). Although MS is found in all parts of the world, its prevalence rates vary considerably in populations depending on the geographical location and ethnicity. The highest rates are in North America and Europe, and the lowest in sub-Saharan Africa and East Asia in latitudes near to the equator (D. L. Rotstein et al., 2018). Interestingly, MS is almost unheard of in certain populations such as the Inuits, New Zealand Maoris and Australian Aborigines (Multiple Sclerosis International Federation (MSIF) 2022). In Finland, the prevalence of MS is estimated to be 200/100 000 (Laakso et al., 2019). However, strong regional differences occur with an age-standardised prevalence of 251/100 000 in Southwest Finland compared to the age-standardised prevalence of 150/100 000 in North Karelia (Pirttisalo, Soilu-Hänninen, & Sipilä, 2019). In addition, a clear and stable increase in the age-standardised prevalence of MS has been observed over the past five decades in different hospital districts of Finland (Pirttisalo et al., 2020). The age at onset of the disease typically ranges from 20 to 40 years, with a female-to-male sex ratio of 2–3:1 (Brownlee, Hardy, Fazekas, & Miller, 2017). Being the commonest non-traumatic disabling disease to affect young adults and often leading to early retirement, the socioeconomic impact of the disease is considerably high (Kobelt et al., 2017).

2.1.2 Pathogenesis

MS is a chronic autoimmune neurological disease associated with CNS inflammation and neurodegeneration mediated by both the adaptive and the innate immune system (Frischer et al., 2009). The pathogenesis behind MS is complex. The present most proposed hypothesis for RRMS is that the disease starts from the peripheral tissues by the adaptive immune response of T cells, B cells and monocytes as a result of a diverse interaction of genetic, environmental and hormonal contributors. Subsequently, the T cells, B cells and monocytes, in addition to plasma cells and macrophages infiltrate the BBB and enter the CNS. The activated cells recognise their antigens, become reactivated and produce cytokines, and together with their toxic mediators further activate local tissue elements such as microglia and astrocytes (Lassmann, 2018). This process leads to the formation of focal inflammatory lesions and neurodegeneration. Once the acute focal inflammation resolves within an average of 4–6 weeks, the lesions in the white matter (WM) may evolve into chronic active lesions or chronic inactive lesions, or they may partially remyelinate. Inflammation is more emphasised in RRMS whereas neurodegenerative events increase in progressive forms of MS (Lassmann, 2018). However, neurodegeneration already exists from the onset of the RRMS disease (Kutzelnigg & Lassmann, 2014).

In RRMS, new inflammatory lesions are dominant and are often associated with contrast enhancing lesions in MRI (B. A. C. Cree et al., 2021). Demyelination and neurodegeneration are driven by the inflammatory process of T cells, B cells and macrophages and this is seen by the beneficial effect of anti-inflammatory disease modifying therapies (DMTs) (Stys, Zamponi, van Minnen, & Geurts, 2012). The pathological studies during the last years have, however, demonstrated that the inflammatory process seen in the relapsing stage of the disease is in a similar way also present in the progressive stage of the disease (Correale et al., 2017; Hochmeister et al., 2006; Lassmann, 2018). The difference being that in the relapsing form of the disease the inflammatory process is associated with severe BBB damage, with leakages of proteins into the brain tissue whereas in the progressive phase of the disease there is only minor or absent BBB damage (Correale et al., 2017; Hochmeister et al., 2006; Lassmann, 2018). This leads to a compartmentalised inflammation trapped in the CNS behind a relatively intact BBB, where the traffic of activated T cells, B cells and monocytes from the periphery into CNS is tuned down and the diffuse innate immune cell activation within the CNS becomes dominant (Lassmann, 2014; Machado-Santos et al., 2018). In the progressive phase of the disease, the CNS pathology shifts from focal to diffuse CNS injury associated with innate immune cell activation (Lassmann, 2018). Consequently, this compartmentalised disease process in the CNS in progressive MS might explain the

shortcomings of the current DMTs which are predominantly designed to target the peripheral immune response.

2.1.3 Genetic and environmental risk factors

The fundamental cause of MS is not entirely understood, but it is suggested to be a result of interactions between susceptibility genes and environmental factors. Many studies have highlighted evidence of a genetic component to the disease with a risk of 2–5% among first-degree relatives of MS patients and with a risk of 17–30% among monozygotic twins of MS patients (Sadovnick et al., 1993; Westerlind et al., 2014). Genome-wide association studies have identified over 200 genes linked to MS, with the strongest association observed with changes in the human leukocyte antigen (HLA) system (Bashinskaya, Kulakova, Boyko, Favorov, & Favorova, 2015). The alleles of HLA can either increase or decrease the risk of MS, with the strongest association observed with the HLA DRB1*15:01 allele with an average odds ratio (OR) of 3 compared to the strongest known protective gene variant HLA A02 with an OR of 0.6 (Brynedal et al., 2007; Sawcer et al., 2011). The combined expected OR at an individual level is likely defined based on the sum of risk gene variants and protective gene variants. For example, the combined OR with the presence of HLA DRB1*15:01 and absence of HLA A02 was shown to be approximately 5 (Brynedal et al., 2007; Sawcer et al., 2011).

The most common environmental factors consistently associated with an increased risk of developing MS include previous Epstein-Barr virus (EBV) infection, cigarette smoking and vitamin D deficiency.

EBV infection, especially during adolescence or later has shown to be the strongest known risk factor for developing MS. According to a meta-analysis published 2007, the risk of developing MS was about 10-fold greater among individuals who experienced an undiagnosed EBV infection in childhood confirmed with later EBV antibody positivity and at least 20-fold greater among individuals who developed mononucleosis compared with those who were EBV-negative (Ascherio & Munger, 2007). Furthermore, individuals infected with EBV in adolescence had a 2.3-fold risk of developing MS in later life compared to those infected with EBV in early childhood (Ascherio & Munger, 2007). More evidence of the crucial role of EBV in developing MS was published in 2022 in a study with a cohort comprising over 10 million young adults on active duty in the US military, with 955 individuals later diagnosed with MS during their period of service. Risk of MS was increased 27-fold with EBV-antibody positive versus EBV-negative results with bloods samples collected at a median of 1 year before MS onset. Furthermore, those individuals who had an EBV-antibody seroconversion during the follow-up had 32-fold risk of developing MS versus those individuals with persistent EBV

seronegativity. The risk of MS was not increased after infection with other viruses, including the similarly transmitted cytomegalovirus (Bjornevik et al., 2022). In addition, a large study revealed that over 99% of MS patients were seropositive for EBV and the OR for MS was 0.00 in seronegative individuals (Pakpoor et al., 2013). Furthermore, recent studies suggest that persistent EBV infection of the CNS drives the ongoing MS disease activity (Serafini, Rosicarelli, Veroni, Mazzola, & Aloisi, 2019; Serafini et al., 2017). However, considering that the prevalence of EBV-antibody positivity in the population is 95% and the overall risk of MS during a lifetime is under 0.5%, it is evident that other risk factors are also necessary as regards developing MS.

A systematic review and meta-analysis indicated that smoking increases the risk of MS by 50% and conversion to SPMS by 80%, with a cumulative effect on duration and intensity (Degelman & Herman, 2017). In addition, smoking can explain up to 40% of the worldwide increased incidence of MS in women (Palacios, Alonso, Brønnum-Hansen, & Ascherio, 2011). Smoking has also been shown to associate with increased MRI lesion load and brain atrophy (Zivadinov et al., 2009).

Several studies have highlighted the correlation between vitamin D and the development of MS as well as disease activity (Munger et al., 2004; Runia, Hop, de Rijke, Buljevac, & Hintzen, 2012). Additionally, an inverse correlation between vitamin D status and MS activity have been reported (Simpson et al., 2010). Higher serum levels of 25-hydroxyvitamin have been shown to predict decreased MS relapse activity and rate of progression during a 5-year follow-up (Ascherio et al., 2014).

Apart from EBV, smoking and D-vitamin deficiency, several other environmental factors have shown to a lesser degree a correlation with increased risk of developing MS. Obesity during childhood and adolescence increase the risk of MS especially among girls (Munger, Chitnis, & Ascherio, 2009; Wesnes et al., 2015). In addition, results from observational epidemiologic studies have highlighted a correlation with the development of MS and/or more rapid disease worsening conditions including shift work (Magrini et al., 2006), lack of physical exercise (Baird, Sasaki, Sandroff, Cutter, & Motl, 2020; Wesnes et al., 2018), poor diet (Marck, Aitken, Simpson, Weiland, & Jelinek, 2019), excessive alcohol intake (Jakimovski, Guan, Ramanathan, Weinstock-Guttman, & Zivadinov, 2019), poor sleep (Benjamin, 2020), comorbidities (Marrie, 2017), concomitant medications (Morrow, Rosehart, Sener, & Welk, 2018) and even air pollution (Heydarpour et al., 2014).

Taken together, EBV antibody positivity is the greatest known risk factor for MS, as all the other known or suspected risk factors has an OR under 4 with developing the disease. However, MS is a multifactorial disease and the risk of MS at an individual level likely consists of a complex interaction between the presence

of risk/protective gene variants and different environmental factors, each exerting a small impact on the overall risk. Therapeutic treatments aiming to decrease EBV activity and vaccine development against EBV may be key elements in reducing the incidence of MS in the future.

2.1.4 Clinical features, diagnostic criteria, and outcome measures

The clinical presentation of MS is heterogeneous. In 85–90% of cases the disease starts as RRMS, which is characterised by acute worsening of neurological symptoms (relapses) followed by a full or partial recovery (remission). In approximately 85% of RRMS patients, the first symptoms begin with an isolated optic neuritis, a brainstem syndrome, or a partial myelitis.

The diagnostic criteria for MS have been revised during recent years to attain a diagnosis at an earlier stage of the disease allowing early effective treatment. The current revised McDonald criteria (2017) are based on dissemination of MRI -detectable lesions in space (DIS) and in time (DIT), that are in accordance with clinical neurological symptoms (Thompson et al., 2018). During an active inflammation in the CNS, as during a relapse, the BBB is disrupted allowing gadolinium to enter the CNS and leak into an active MS lesion. Detecting lesions both with and without gadolinium enhancement in MRI brings evidence of DIT, thus making a diagnosis of MS possible already after the first clinical relapse. In addition to previous diagnostic criteria, the presence of cerebrospinal fluid (CSF) oligoclonal bands is also included as an alternative to fulfil DIT in the revised 2017 McDonald criteria. The modification of the criteria denotes that a higher proportion of patients with a less active disease course are diagnosed with MS. This revision strives for increased sensitivity (to identify previously undiagnosed MS patients, or to look for evidence of an earlier diagnosis), while still sustaining an equal level of specificity (to exclude patients who do not truly have MS). The revised 2017 McDonald MS diagnostic requirements are presented in Table 1.

Table 1. The 2017 McDonald diagnostic criteria for MS (Thompson et al., 2018).

| CLINICAL PRESENTATION | ADDITIONAL DATA NEEDED FOR MS DIAGNOSIS |
|--|---|
| ≥2 relapses and either objective clinical evidence of ≥2 lesions or objective clinical evidence of one lesion together with reasonable historical evidence of a previous relapse | None |
| ≥2 relapses and objective clinical evidence of one lesion (shows DIT) | DIS shown by: ≥1 T2 lesion typical of MS (periventricular, cortical or juxtacortical, infratentorial or spinal cord) or await a further relapse showing damage to another part of the CNS |
| 1 relapse and objective clinical evidence of ≥2 lesions (shows DIS) | DIT shown by: oligoclonal bands in the CSF or simultaneous presence of asymptomatic gadolinium-enhancing and non-enhancing lesions at any time or MRI evidence of a new lesion since a previous scan or await a further relapse |
| 1 relapse and objective clinical evidence of one lesion (CIS) | DIS shown by: ≥1 T2 lesion typical of MS (periventricular, cortical or juxtacortical, infratentorial or spinal cord), or await a further relapse showing activity in another part of the CNS DIT shown by: oligoclonal bands in the CSF or simultaneous presence of asymptomatic gadolinium-enhancing and non-enhancing lesions at any time or MRI evidence of a new lesion since a previous scan or await a further relapse |
| Insidious neurological progression suggestive of MS (PPMS) | Continued progression for 1 year (from previous symptoms or by ongoing observation) plus any 2 of 3 of the following criteria: ≥1 T2 lesions in the brain typical of MS (periventricular, cortical or juxtacortical or infratentorial), ≥2 T2 lesions in the spinal cord, oligoclonal bands in the CSF |

Abbreviations: DIT= dissemination in time; DIS= dissemination in space; CIS= clinically isolated syndrome; CNS= central nervous system; CSF= cerebrospinal fluid; MRI= magnetic resonance imaging; PPMS= primary progressive multiple sclerosis

The first clinical episode is classified as a clinically isolated syndrome (CIS). Due to the recent modification of the McDonald criteria, a CIS can be labelled as MS when it fulfils the MRI criteria for DIT and DIS or is accompanied by DIS and the presence of CSF oligoclonal bands (Thompson et al., 2018). Patients with CIS that do not fulfil the McDonald MS criteria are recommended to be followed up intensively as they frequently develop MS (Filippi et al., 2022). Moreover, the increased usage of MRI brain scans has more often led to incidental findings compatible with demyelinating lesions. For these findings (without any history of acute neurological symptoms) the term radiologically isolated syndrome (RIS) is used. Patients with RIS are recommended to be followed up regularly as the risk of conversion to MS is elevated (Lebrun, 2015). A recent randomised, double-blinded, placebo-controlled study using dimethyl fumarate to treat people with RIS resulted

in a risk reduction of more than 80 percent. This reduction was relative to the placebo in preventing a first clinical event connected to CNS demyelination during a 96-week follow-up (Okuda et al., 2023). A critical issue in the future would be to identify people with CIS or RIS that have the highest risk of developing MS and hence could be classified as preclinical MS, leading to a therapeutic intervention at the earliest phase of MS.

The most frequently used standardised rating system in the evaluation and follow up of clinical disability in MS is the Expanded Disability Status Scale (EDSS) (Kurtzke, 1983). The EDSS is nonlinear, with a scale ranging from 0 to 10, with 0 corresponding to no disability and 10 to death due to MS. Functional system (FS) scores form the basis of the EDSS assessment. There are eight FS scores in total: visual, brainstem, pyramidal, cerebellar, sensory, bowel and bladder, cerebral and ambulation, which are scored separately based on detailed definitions (neurostatus.net). The EDSS has settled its role as a routine tool capturing disability both in clinical work and in research settings. However, the EDSS is not sufficiently sensitive to capture subtle changes in disability (Thompson & Hobart, 1998). In addition, in the middle and upper scale, the EDSS focuses mainly on ambulatory deficits and is less sensitive to other deficits related to MS such as cognitive impairment. Moreover, a relatively high inter- and intra-rater variability may impact the rating score outcomes (Goodkin et al., 1992).

In addition to the EDSS, another frequently used rating system in MS population studies to stratify MS patients based on their rate of progression is the Multiple Sclerosis Severity Score (MSSS), which combines the EDSS and disease duration (Roxburgh et al., 2005). However, the prognostic ability at patient level remains unproven with individual MSSS scores often varying over time (Gross, Sillau, Miller, Farrell, & Krieger, 2019; Pachner & Steiner, 2009). Therefore, clinicians should be cautious when using MSSS to evaluate progression at an individual level.

SPMS is diagnosed retrospectively according to the Lublin criteria by an insidious worsening of neurologic function independent of relapses over the previous 3–12 months after an initial relapsing disease course (Lublin et al., 2014). Moreover, a recently proposed more specific definition of SPMS is the Lorscheider criteria, where the definition consists of (1) a progression of disability unrelated to relapses of 1 EDSS step in patients with an EDSS < 6 or 0.5 EDSS steps in patients with EDSS ≥ 6; (2) an EDSS score ≥ 4 including a pyramidal FS score of ≥ 2 and (3) a clinically confirmed progression ≥ 3 months, including confirmation within the leading FS (Lorscheider et al., 2016). However, progression can also occur already from the onset of the disease (primary progressive multiple sclerosis, PPMS) (Thompson et al., 2018). PPMS and SPMS related symptoms include progressive loss of walking ability, bladder dysfunction and increasing cognitive impairment.

Based on earlier natural history studies, there is high inter-individual variability in the disease course of the patients converting to SPMS. The shift of the disease course to SPMS takes place on average at 40–50 years of age with approximately 50–65% of the RRMS patients converting to SPMS; the average time from disease onset to the beginning of the progressive phase being 5–30 years (Barzegar et al., 2021; Compston & Coles, 2008; Eriksson et al., 2003; Koch et al., 2010; Tremlett et al., 2008; Tutuncu et al., 2013; Vukusic & Confavreux, 2003; Weinshenker et al., 1989). Importantly, the aforementioned studies are mainly from the pre-treatment era. Therefore, several recent studies have indicated that rates of disease worsening and evolution to SPMS may be substantially lower in the present day (Bergamaschi et al., 2016; Brown et al., 2019; B. A. Cree et al., 2016). This is presumably due to the early use of high efficacy DMTs from the onset of the disease (Bergamaschi et al., 2016; Brown et al., 2019; B. A. Cree et al., 2016).

Apart from the impact of early and appropriate use of DMTs (reviewed in Chapter 2.2) and other factors, such as the changes in the diagnostic criteria, improvement in the general state of health in the population and other environmental factors (for example decreased tobacco smoking) have led to a more favourable prognosis for RRMS. The strengthened diagnostic criteria have allowed an MS diagnosis for many patients at the first clinical demyelinating event, thus permitting earlier treatment whereas the remaining patients with CIS have a more benign prognosis (Filippi et al., 2022).

Nevertheless, clinical evaluation remains the key element in the physicians' daily work with individual patients. The revised McDonald MS criteria provide tools for physicians to capture the disease at a very early stage, but if the clinical picture is not properly interpreted or the MRI findings are over-interpreted, the risk of overdiagnosis increases. Considering the high socioeconomic impact of the disease, the specificity of the diagnosis should be as high as possible (less false MS diagnoses). Therefore, the clinical evaluation of the disease (especially in the diagnosis phase) should be ensured by experienced neurologists and radiologists in the MS field.

2.1.5 Smouldering MS and progression independent of relapses (PIRA)

RRMS is traditionally characterised by relapses caused by the activation of the adaptive immune system with or without residual worsening. Despite the advanced treatment options to effectively halt the inflammatory activity, many RRMS patients will still experience disease accumulation over time (Coles et al., 2006; Kappos et al., 2020). These patients undergo disability progression unrelated to relapses and without signs of radiological activity including contrast enhancing T1 lesions, enlarged T2 lesions or new T2 lesions in conventional MRI. This phenomenon is often referred to

as smouldering MS (Giovannoni et al., 2022). This long-term progression independent of relapses (PIRA) is mainly considered to be sustained by a primary diffuse insidious smouldering pathological process in the CNS behind an intact BBB characterised by chronic neuroinflammation and neurodegeneration. PIRA is essentially considered to be a clinical manifestation of the smouldering disease process.

There is, as yet, no complete consensus of what causes smouldering MS, but both focal inflammatory dependent and independent pathological drivers thought to be potentially responsible for smouldering MS have recently been under intensive research in the MS field. According to the current understanding, relapse-related demyelination and cell energy deficits are often followed by a long-term neuroinflammatory and neurodegenerative process including activated microglia and astrogliosis, ongoing energy deficits, and antibody-mediated damage leading to insidious disability progression. This detrimental process in the CNS can further be accompanied by viral infections, ageing mechanisms, lifestyle factors and comorbidities (Giovannoni et al., 2022). Here, chronic active lesions (i.e., smouldering or expanding) with activated microglia at the rim of the lesions are an important manifestation of smouldering MS and participate in the non-relapsing biological progression of the disease. In contrast to conventional MRI, novel innovative MRI modalities and PET-derived biomarkers have made it possible to detect and to some extent quantify chronic active lesions. The detection of chronic active lesions with above mentioned imaging modalities and the role of activated microglia in smouldering MS is discussed in detail in Chapter 2.3 in this thesis.

Several MRI, neuropathological and observational cohort studies suggest that this smouldering pathological process is present at every stage of the disease (Chard et al., 2002; De Stefano et al., 2010; De Stefano et al., 2011; Trapp et al., 1998). An observational cohort study consisting of over 5100 patients with CIS or early RRMS with the first EDSS evaluation within one year from the disease onset demonstrated that with a mean follow-up of over 11 years, PIRA occurred in over 1400 (27.6%) patients, and a longer exposure to DMTs was associated with a lower risk of both PIRA and relapse-associated worsening (RAW). The study highlighted, that insidious progression without relapses appears even in the earliest phases of the disease (Portaccio et al., 2022). In addition, a large clinical trial dataset with over 27000 MS patients and a follow-up of 15 years, demonstrated that PIRA and RAW contributed equally to the overall disability accumulation in RRMS (including early RRMS) whereas in SPMS and PPMS, PIRA was the dominant driver of disease worsening (Lublin et al., 2022). Moreover, the baseline features of patients with RRMS who experienced either PIRA or RAW events were not substantially different, highlighting the clinically relevant role of relapse-free progression also in RRMS (Lublin et al., 2022). In addition, a recently published study consisting of over 1100 MS patients demonstrated, that patients with PIRA had an 8-fold greater

risk of reaching EDSS 6.0 compared to those without PIRA during a median 10.5-year follow-up after the first demyelinating event (Tur et al., 2023). Importantly, patients presenting with PIRA within 5 years of the first demyelinating event had a 26-fold greater risk of reaching EDSS 6.0 compared to patients whose first PIRA appeared later in the disease, highlighting the association of early PIRA with long-term disability (Tur et al., 2023).

Taken together, a complete understanding of the underlying mechanisms behind the development of the insidious smouldering pathological process are still to be unsolved. The appearance of silent long-term progression during the RRMS phase in association with brain atrophy but without an association with radiological inflammatory activity suggests that the biological process underlying SPMS possibly starts far earlier than generally recognised (B. A. C. Cree et al., 2019). Hypothetically, either a diffuse injury caused by the compartmentalised neuroinflammation driven by the overactivated microglia and/or focal lesions too small to be detected by current imaging methods leads to irreversible tissue loss. The findings in Study III of this thesis support the hypothesis that the compartmentalised glial-cell driven inflammation is a significant underlying process contributing to disease accumulation in smouldering MS.

2.2 The treatment of MS

2.2.1 Disease modifying therapies (DMTs)

The primary mechanism of action for all current DMTs in MS is to diminish inflammation, which is seen as a reduced number of relapses and a decreased accumulation of new MS lesions. This contributes in preventing or slowing down the disease progression. The first DMTs became available in the early 1990s, when interferon-beta 1b was approved for treatment of MS. Since then, the selection of treatment options has extended immensely with the availability of glatiramer acetate, natalizumab and fingolimod in the 2000s, teriflunomide, dimethyl fumarate, alemtuzumab, siponimod, ocrelizumab and cladribine in the 2010s and ofatumumab, ozanimod and ponesimod in the 2020s leading to more individualised care of MS patients. All available DMTs primarily impact the peripheral adaptive immune system, with varying effects on disease activity and profile of adverse effects. Present DMTs are divided into groups classified as moderate efficacy and high efficacy on inflammatory activity. As of May 2023, European Medicines Agency (EMA) had approved altogether 20 DMTs in the treatment of MS.

The groups with their proposed mechanism of action, administration route and indication are summarised in Table 2.

Table 2. Currently available DMTs with their proposed mechanism of action, administration route and indication. Modified from (Wiendl et al., 2021) and (Rae-Grant et al., 2018).

| | |
|---|---|
| Interferon betas (beta-1a and -1b) | <p>Proposed mechanism of action: Not fully clarified. The anti-inflammatory effects of interferon betas are largely believed to result from the inhibition of T-lymphocyte proliferation, a shift of cytokine response from an inflammatory response to an anti-inflammatory profile, and reduced migration of inflammatory cells across the BBB.</p> <p>Administration route: Subcutaneously or intramuscular</p> <p>Frequency of administration: From every two days to every two weeks</p> <p>MS type: Active RRMS</p> |
| Glatiramer acetate | <p>Proposed mechanism of action: Not fully clarified. Glatiramer acetate supposedly regulate the peripheric immune response with an effect in the balance of Th1- and Th2-lymphocytes.</p> <p>Administration route: Subcutaneously</p> <p>Frequency of administration: Once a day or three times per week</p> <p>MS type: Active RRMS</p> |
| Teriflunomide | <p>Proposed mechanism of action: Teriflunomide selectively and reversibly inhibits dihydro-orotate dehydrogenase, which is a key mitochondrial enzyme in the pyrimidine synthesis pathway. This leads to a reduction in proliferation of activated T and B lymphocytes without causing cell death.</p> <p>Administration route: Oral (tablets)</p> <p>Frequency of administration: Once a day</p> <p>MS type: Active RRMS</p> |
| Dimethyl fumarate | <p>Proposed mechanism of action: Not fully clarified. Dimethyl fumarate is believed to act centrally by altering the nuclear factor erythroid 2 related factor 2 transcriptional pathway, which is involved in the cellular response to oxidative stress. The treatment decreases the oxidative stress, and it has both anti-inflammatory and neuroprotective effects.</p> <p>Administration route: Oral (tablets)</p> <p>Frequency of administration: Twice per day</p> <p>MS type: Active RRMS</p> |
| Diroximel fumarate | <p>Proposed mechanism of action: Not fully clarified. Diroximel fumarate is believed to act centrally by altering the nuclear factor erythroid 2 related factor 2 transcriptional pathway, which is involved in the cellular response to oxidative stress. The treatment decreases the oxidative stress, and it has both anti-inflammatory and neuroprotective effects.</p> <p>Administration route: Oral (tablets)</p> <p>Frequency of administration: Twice per day</p> <p>MS type: Active RRMS</p> |
| Fingolimod | <p>Proposed mechanism of action: Fingolimod modulates the sphingosine 1-phosphate receptor, thus preventing the egress of autoreactive lymphocytes from the lymph nodes towards the CNS.</p> <p>Administration route: Oral (tablets)</p> <p>Frequency of administration: Once a day</p> <p>MS type: Active RRMS</p> |
| Ponesimod | <p>Proposed mechanism of action: Ponesimod modulates the sphingosine 1-phosphate receptor, thus preventing the egress of autoreactive lymphocytes from the lymph nodes towards the CNS.</p> <p>Administration route: Oral (tablets)</p> <p>Frequency of administration: Once a day</p> <p>MS type: Active RRMS</p> |
| Ozanimod | <p>Proposed mechanism of action: Ozanimod acts as a sphingosine 1-phosphate receptor agonist, sequestering lymphocytes to peripheral lymphoid organs and thus preventing the egress of autoreactive lymphocytes from the lymph nodes towards the CNS.</p> <p>Administration route: Oral (tablets)</p> <p>Frequency of administration: Once a day</p> <p>MS type: Active RRMS</p> |

| | |
|---------------------|---|
| Natalizumab | <p>Proposed mechanism of action: Natalizumab is a humanized IgG4 antibody directed against the alpha chain of the VLA-4 integrin and inhibits migration of autoreactive inflammatory cells into the CNS.</p> <p>Administration route: Intravenously/ subcutaneously</p> <p>Frequency of administration: Every four to every six weeks</p> <p>MS type: Highly active RRMS</p> |
| Alemtuzumab | <p>Proposed mechanism of action: Alemtuzumab is a humanized monoclonal antibody directed against CD52, a cell surface antigen present at high levels on especially T and B lymphocytes. The therapeutic effect is suggested to come by a depletion and repopulation of these cells.</p> <p>Administration route: Intravenously</p> <p>Frequency of administration: Once a year for two years, thereafter based on individual consideration</p> <p>MS type: Highly active RRMS</p> |
| Mitoxantrone | <p>Proposed mechanism of action: Mitoxantrone is a synthetic anthracenedione derivative, that interacts with nuclear DNA and is a potent immunosuppressive agent targeting proliferating immune cells, inhibiting proliferation and inducing apoptosis of T lymphocytes, B lymphocytes, macrophages and other antigen-presenting cells.</p> <p>Administration route: Intravenously</p> <p>Frequency of administration: Every three months (maximum lifetime dose 120mg)</p> <p>MS type: Highly active RRMS</p> |
| Cladribine | <p>Proposed mechanism of action: Cladribine targets the T- and B-lymphocytes by interfering the DNA synthesis and repair through incorporation into DNA and through inhibition of enzymes involved in DNA metabolism. This leads to DNA strand breaks and ultimately to cell death.</p> <p>Administration route: Oral (tablets)</p> <p>Frequency of administration: Two courses of treatment throughout two years</p> <p>MS type: Highly active RRMS</p> |
| Ublituximab | <p>Proposed mechanism of action: Ublituximab is a humanized monoclonal antibody targeting the cell surface antigen CD20 expressed by B-lymphocytes. Ublituximab is involved in the depletion of B cells via antibody-dependent cellular cytotoxicity.</p> <p>Administration route: Intravenously</p> <p>Frequency of administration: Every six months</p> <p>MS type: Active RRMS, highly active RRMS</p> |
| Ocrelizumab | <p>Proposed mechanism of action: Ocrelizumab is a humanized monoclonal antibody targeting the cell surface antigen CD20 expressed by B-lymphocytes. Ocrelizumab selectively targets the circulating CD20-positive immature and mature B cells by binding to the surface proteins of the cells and depletes them but spares CD20-negative plasma cells.</p> <p>Administration route: Intravenously</p> <p>Frequency of administration: Every six months</p> <p>MS type: Active RRMS, highly active RRMS, Active PPMS</p> |
| Ofatumumab | <p>Proposed mechanism of action: Ofatumumab is a humanized monoclonal antibody targeting the cell surface antigen CD20 expressed by B-lymphocytes. Ofatumumab selectively targets the circulating CD20-positive immature and mature B cells by binding to the surface proteins of the cells and depletes them but spares CD20-negative plasma cells.</p> <p>Administration route: Subcutaneously</p> <p>Frequency of administration: Every four weeks</p> <p>MS type: Active RRMS, highly active RRMS</p> |
| Siponimod | <p>Proposed mechanism of action: Siponimod is a sphingosine 1-phosphate receptor modulator that selectively binds the sphingosine 1-phosphate receptor subtypes 1 and 5, thus preventing the egress of autoreactive lymphocytes from the lymph nodes towards the CNS.</p> <p>Administration route: Oral (tablets)</p> <p>Frequency of administration: Once a day</p> <p>MS type: Active SPMS</p> |
| Rituximab | <p>Proposed mechanism of action: Rituximab is a genetically engineered chimeric monoclonal antibody targeting the cell surface antigen CD20 expressed by B-lymphocytes. Rituximab binds to the CD20 leading to elimination of CD20-expressing B-cells and T-cells.</p> <p>Administration route: Intravenously</p> <p>Frequency of administration: Every six months</p> <p>MS type: Active RRMS, highly active RRMS, active PPMS (OFF-label usage)</p> |

Abbreviations: DMT= disease modifying therapy; CNS= central nervous system; RRMS= relapsing-remitting multiple sclerosis; PPMS= primary progressive multiple sclerosis; SPMS= secondary progressive multiple sclerosis.

The treatment should be planned on a patient-specific basis considering the prognosis, the efficacy and long-term safety profile of the treatment, as well as the individual factors such as comorbidity, desired pregnancy and other desires of the patient. Moreover, the major costs of DMTs to the government, to the healthcare system, to the insurance provider, or to the individual can cause a major barrier to the access of DMTs (Weinstein et al., 2022).

The predictors of a poor prognosis that should be considered when choosing the treatment are listed in Table 3.

Table 3. Predictors of poor prognosis in MS. Modified from (D. Rotstein & Montalban, 2019).

| |
|--|
| <p>Demographics and environmental factors</p> <ol style="list-style-type: none"> 1. Low vitamin D levels 2. Smoking 3. Older age 4. Male sex 5. Comorbidity 6. Not of European decent <p>Clinical factors</p> <ol style="list-style-type: none"> 1. PPMS disease type 2. Polysymptomatic onset 3. Poor recovery from the first relapse 4. Brainstem, cerebellar or spinal cord onset 5. A shorter interval between the first and second relapses 6. A high relapse rate 7. A higher EDSS score at diagnosis 8. Early cognitive deficits <p>MRI observations</p> <ol style="list-style-type: none"> 1. A high number of T2 lesions 2. A high T2 lesion volume 3. The presence of gadolinium enhancing lesions 4. The presence of infratentorial/spinal cord lesions 5. The presence of new T2 lesions in the early phase of the disease 6. Whole brain lesions 7. Grey matter lesions <p>Biomarkers</p> <ol style="list-style-type: none"> 1. A high number of T2 lesions 2. The presence of IgM and IgG oligoclonal bands in the CSF 3. High levels of neurofilament light chain in the CSF and serum 4. High level of IgG-index in the CSF 5. Retinal nerve fibre layer thinning detected with optical coherence tomography |
|--|

Abbreviations: PPMS= primary progressive multiple sclerosis, EDSS= Expanded Disability Status Scale, CSF= cerebrospinal fluid, IgM= immunoglobulin M, IgG= immunoglobulin G

In the Finnish Current Care Guidelines for MS therapy, the choice of treatment initiation is guided by disease activity (Multiple Sclerosis Current Care Guidelines 2020, www.kaypahoito.fi). RRMS is defined as active or highly active based on the relapse rate and findings of new, enlarging T2 or gadolinium enhancing lesions in

the MRI. A wide range of DMTs are approved for treating patients with RRMS and is accordingly suggested (Table 2), also taking into account the predictors of poor prognosis (Table 3). However, the current selection of DMTs for progressive forms of MS is narrow with only ocrelizumab indicated for active PPMS and siponimod indicated for active SPMS, both having a rather modest effect on disease progression (Table 2).

2.2.2 Treatment options for RRMS

The most widely used primary outcomes for previous pivotal Phase 3 randomised, placebo-controlled clinical trials of DMTs have been the annualised relapse rate (ARR) and progression of disease (measured using the EDSS score). Furthermore, a combined endpoint outcome measure that is increasingly used both in clinical trials and clinical work is “no evidence of disease activity” (NEDA). NEDA is defined as a lack of clinical relapses, absence of disability progression and no new or enlarging lesions on MRI (Giovannoni, Bermel, Phillips, & Rudick, 2018).

The first DMTs designed to treat RRMS were the self-injectable interferon-betas and glatiramer acetate. They have a relatively modest effect on the disease by reducing the relapse rate by 29% to 34% compared with placebo (McGinley, Goldschmidt, & Rae-Grant, 2021). Nowadays, with the existence of more efficient oral DMTs and biological DMTs, the usage of interferon-betas and glatiramer acetate have decreased substantially.

The present oral DMTs for treatment of RRMS include dimethyl fumarate, teriflunomide, diroximel fumarate, fingolimod, ozanimod, ponesimod and cladribine (Wiendl et al., 2021).

Dimethyl fumarate was shown to reduce the relapse-rate, new T2 and gadolinium enhancing lesions on MRI and to slow down disease progression (Gold et al., 2012) and sustained a long-term efficacy/safety profile in a 13 year follow-up study (Gold et al., 2022). The effect of teriflunomide to decrease the ARR and to reduce the risk of disability progression measured by the EDSS was demonstrated in two phase III randomised clinical trials (RCTs) (Confavreux et al., 2014; O'Connor et al., 2011). In addition, teriflunomide sustained a positive safety profile in the long-term use (McGinley et al., 2021). The comparative studies in real-world effectiveness and treatment persistence between teriflunomide and dimethyl fumarate have shown rather equal results (Hillert, Tsai, Nouhi, Glaser, & Spelman, 2022; Kalincik et al., 2019). In addition, diroximel fumarate, a similar oral treatment to dimethyl fumarate with similar effect but with less gastrointestinal adverse events, was recently licensed (Jonasson & Sejbaek, 2020). Due to the limited effect in suppressing the inflammation in RRMS, interferon-betas, glatiramer acetate, dimethyl fumarate,

teriflunomide and diroximel fumarate have a treatment indication only for active RRMS, not for highly active RRMS.

Fingolimod is a sphingosine 1-phosphate (S1P) receptor modulator used in highly active RRMS. It blocks the T cells from exiting the lymph nodes and due to decreased amount of potentially autoreactive T cells entering the CNS, the T cell-mediated autoimmune reaction in the CNS is reduced (Cohen & Chun, 2011). Based on several observational cohort studies, the effect of fingolimod has shown to be superior to dimethyl fumarate and teriflunomide but inferior to the biological DMTs (Brown et al., 2019; Kalincik et al., 2017; Kalincik et al., 2019; Sharmin et al., 2021). However, the potential risk of severe MS disease activity clinically and radiologically after treatment cessation (rebound) (Barry, Erwin, Stevens, & Tornatore, 2019) has to some extent decreased the attractiveness of fingolimod during the recent years. This is especially because of the increasing biological DMT repertoire which has data available indicating a more robust long-term effect/risk profile. After fingolimod, additional S1P receptor modulators, ozanimod and ponesimod, have been approved to treat RRMS recently.

Natalizumab was the first biological DMT used for MS and is still considered to be one of the most effective treatments for MS. It is a humanised IgG4 antibody directed against the alpha chain of the very late antigen 4 (VLA-4) integrin and inhibits cell migration toward the CNS. Natalizumab demonstrated a 42% relative risk reduction in disability progression at 2 years and 68% reduction in the ARR at 1 year when compared to placebo in a study where over 900 RRMS patients were randomly assigned to receive natalizumab or placebo (Polman et al., 2006). Furthermore, MRI outcomes revealed a decrease in the number of T2-weighted lesions by 83% and a decrease in gadolinium enhancing lesions by 92% compared to placebo (Polman et al., 2006). In a subsequent study with over 700 treatment-naïve patients receiving either natalizumab or interferon-beta or glatiramer acetate, natalizumab demonstrated a 68% relative reduction in ARR compared to interferon-beta and glatiramer acetate (Spelman et al., 2016). In addition, in a study with almost 800 patients comparing the effectiveness between natalizumab and fingolimod after treatment failure with interferon-beta or glatiramer acetate, the ARR declined from 1.5 to 0.2 in natalizumab treated patients, compared with a reduction in ARR from 1.3 to 0.4 in fingolimod treated patients; this corresponds to a relative 50% lower post-switch relapse rate with the initiation of natalizumab compared with fingolimod (Kalincik et al., 2015). However, the usage of natalizumab is restricted with those patients that carry the JC-virus due to the risk of progressive multifocal leukoencephalopathy (PML) (Berger & Korolnik, 2005).

Alemtuzumab is an anti-CD52 monoclonal antibody, that has also shown to be an effective treatment for highly active MS (Cohen et al., 2012). However, the usage

of alemtuzumab has recently been restricted to some extent due to the long-term risk of developing autoimmune diseases (Guarnera, Bramanti, & Mazzon, 2017).

The usage and development of B cell therapies has dramatically changed the therapeutic field to treat MS during the past few years with ocrelizumab, ofatumumab and rituximab (used off-label) on the market. Ocrelizumab is a humanised monoclonal antibody selectively targeting CD20, a cell-surface antigen expressed on pre-B cells, mature B cells, and memory B cells, and administered as an intravenous infusion every 6 months (Sorensen & Blinkenberg, 2016). In a phase 3 RCT, with over 800 RRMS patients receiving ocrelizumab and over 800 RRMS patients receiving interferon-beta, patients treated with ocrelizumab had an at least 46% reduction in the ARR at 96 weeks compared to patients treated with interferon-beta (Hauser et al., 2017). Furthermore, patients treated with ocrelizumab showed a 94% reduction in the number of new gadolinium-enhancing lesions on MRI compared to patients treated with interferon-beta (Hauser et al., 2017). Ofatumumab, given as a subcutaneous injection monthly, showed a reduced ARR by 51% (0.11 vs. 0.22) and 58% (0.10 vs. 0.25) compared to teriflunomide in two phase 3 double-blind RCTs of over 1800 patients (Hauser et al., 2020). In addition, MRI endpoints showed a 94–97% decrease in the mean number of gadolinium-enhancing lesions on MRI and an 82–85% decrease in the mean number of new or enlarging T2-lesions per year with ofatumumab compared to teriflunomide (Hauser et al., 2020). Rituximab is a genetically engineered chimeric monoclonal antibody that recognises and binds to the CD20 protein on the surface of B lymphocytes causing elimination of CD20-expressing B-cells and T-cells. (Palanichamy et al., 2014). Rituximab has been shown to be effective in the treatment of RRMS based on a rater-blinded phase 3 RCT (rituximab vs. dimethyl fumarate) (Svenningsson et al., 2022), several observational studies (Chisari et al., 2022; D'Amico et al., 2019; Salzer et al., 2016), and a phase 2 RCT (Hauser et al., 2008). The phase 2 study did not move on to phase 3, (instead, ocrelizumab was developed based on the rituximab monoclonal antibody), but the usage of rituximab as an off-label treatment in MS has increased substantially during the past years (Chisari et al., 2022).

Recent studies have highlighted a favourable outcome with cladribine, an infrequently administered oral treatment that has an immunomodulative effect through selectively targeting, and thereafter repopulating lymphocyte subtypes (Giovannoni, Soelberg Sorensen, et al., 2018; Signori et al., 2020). An observational study with over 3000 patients demonstrated that patients treated with cladribine had a reduced ARR by 40–52% compared to patients with dimethyl fumarate, interferon-beta or glatiramer acetate (Signori et al., 2020). In addition, a subgroup analysis of the same study with an inclusion criteria of high disease activity (defined as ≥ 2 relapses the year prior to study) demonstrated that patients with cladribine had a

reduced ARR by approximately 70% compared to patients with interferon-beta, glatiramer acetate, and dimethyl fumarate (Signori et al., 2020).

Hematopoietic stem cell transplantation (HSCT) is used as an alternative off-label treatment in highly active RRMS. A recent observational study showed that in pairwise comparisons between patients with high disease activity and moderate disability receiving either HSCT or high efficacy DMT (fingolimod, natalizumab, and ocrelizumab), HSCT showed to be substantially superior to fingolimod and marginally superior to natalizumab in reducing the risk of relapses during a 5-year follow-up (Kalincik et al., 2023). The pairwise comparison between HSCT and ocrelizumab did not show difference in the relapse rates and disability outcomes over a shorter period of three years. A quarter of the patients in the HSCT group experienced febrile neutropenia with one treatment-related death (Kalincik et al., 2023). Due to the off-label status and a higher risk profile compared to highly active DMTs, current care guidelines of MS in Finland recommend the usage of HSCT only as “a rescue therapy” (Multiple Sclerosis Current Care Guidelines 2020, kaypahoito.fi). The ongoing phase II-III RCTs comparing the effect and adverse events of HSCT and high efficacy DMTs will shed light on the role of HSCT in the future treatment field of highly active MS (NCT03477500, NCT04971005, NCT04047628).

2.2.3 The benefits of an early induction of high-efficacy DMTs in RRMS

There are two treatment approaches used in the clinical setting. Historically, the most common treatment approach was escalation, starting with a DMT with a lower efficacy but with a potentially lower risk of adverse effects. However, this approach often resulted in undertreatment, defined as a breakthrough of the disease and accumulated disability. Hence, there has been significant interest in recent years to consider starting a DMT with a higher efficacy earlier in MS (Harding et al., 2019; Prosperini et al., 2020). This treatment approach is known as the early aggressive approach, aiming to provide better relapse control and delay accumulation of disability as early as possible in course of the disease. Several recent MS registry-based studies have indicated that early use of higher-efficacy DMTs have a beneficial effect on later disability progression and long-term disease course (Bergamaschi et al., 2016; Brown et al., 2019; B. A. Cree et al., 2016). A cohort study of over 1500 RRMS patients suggested that initial treatment with a higher-efficacy medication (fingolimod, alemtuzumab or natalizumab) was associated with a lower risk of conversion to SPMS compared with initial treatment with glatiramer acetate or interferon beta (Brown et al., 2019). In a large retrospective international observational study, patients receiving high-efficacy therapy (rituximab,

ocrelizumab, mitoxantrone, alemtuzumab, natalizumab) initiated within 2 years of disease onset had on average less disability after 6–10 years compared with patients receiving high-efficacy therapy later in the disease course (He et al., 2020). In the sixth year after disease onset, the mean EDSS scores were 2.2 vs. 2.9 between the groups and the difference persisted throughout each year of the 6–10-year follow-up period with EDSS scores of 2.3 vs. 3.5 after the tenth year of follow-up, respectively (He et al., 2020). In addition, in a large register study with almost 12000 patients fulfilling the inclusion criteria, using multivariable regression models adjusted for the time to first treatment, the risk for disability progression was lower for patients who started treatment within 1.2 years from the disease onset in comparison to those treated after this time interval (Iaffaldano et al., 2021). A follow-up study of 5 years including almost 600 MS patients demonstrated a smaller increase in the EDSS score at 5 years with those who received high-efficacy DMT initially compared to those who first received moderate-efficacy DMT, with a mean increase in EDSS score of 0.3 vs. 1.2, respectively (Harding et al., 2019). Moreover, the patient group that received high-efficacy DMT had initially more signs of an active disease compared to the patient group that received moderate-efficacy DMT, thus highlighting the better long-term outcomes of early intensive disease-modifying therapy compared to escalation therapy (Harding et al., 2019).

However, a limitation of the induction therapy approach is that patients are predisposed to higher risks of potentially severe adverse effects and due to the heterogenic nature of MS, some patients may not need such efficient treatment. Ongoing MS registry-based studies and RCTs will shed more light on the plausible benefits and disadvantages on the early use of higher-efficacy DMTs in the near future.

2.2.4 Treatment options for progressive MS

The present DMTs available have so far been disappointing in treating non-active progressive MS, where CNS compartmentalised processes are driving the pathology behind a mainly intact BBB (B. A. C. Cree et al., 2021; Kappos et al., 2018; Yong & Yong, 2022). Currently, EMA has approved an official indication in the treatment in progressive forms of MS for only two DMTs: ocrelizumab in active PPMS and siponimod in active SPMS.

Ocrelizumab was the first approved medication for use in the treatment of PPMS based on the results from the double-blind, placebo-controlled phase 3 ORATORIO, RCT of over 700 PPMS patients. The study showed that ocrelizumab treated patients exhibited moderately less disability progression than patients on placebo after 24 weeks (29.6% vs. 35.7%) (Montalban et al., 2017). Furthermore, in a 6.5-year follow-up study of the patients that participated in the ORATORIO trial, the earlier

and continuous ocrelizumab treatment provided sustained benefits on measures of disease progression compared with those initially receiving placebo but who were transferred to ocrelizumab in a later phase (Wolinsky et al., 2020). The effect of rituximab in PPMS was evaluated in a phase 2 RCT, where it did not significantly slow down the progression of the disease (Hawker et al., 2009). Nevertheless, in a subgroup analyses, rituximab showed a delay in time for the progression of the disease in younger (<51 years) patients and in patients with gadolinium enhancing lesions in MRI at baseline (Hawker et al., 2009). Therefore, the usage of B-cell depletion treatment might be most effective in PPMS patients who are younger and have higher inflammatory activity. Apart from ocrelizumab, rituximab is also used in PPMS as off-label treatment, using individual consideration (Chedid, Moisset, & Clavelou, 2022).

Siponimod, a selective S1P-receptor modulator, was the first EMA-approved medication for use in the treatment of SPMS. It significantly reduced 3-month confirmed disability progression (CDP) compared to placebo in a large double-blind, phase 3 RCT consisting of over 1600 SPMS patients with an equal safety profile to other S1P modulators (Kappos et al., 2018). However, the effect of disease accumulation was rather modest with 3-month CDP of 26% in the siponimod treated group compared with 32% in the placebo group, with a relative risk reduction of 21% in the 3-year follow-up (Kappos et al., 2018). The current usage of siponimod is restricted to SPMS patients with relapses and/or radiological activity. Rituximab is also used in SPMS as an off-label treatment, using individual consideration (Naegelin et al., 2019).

Study II presented in this thesis was an investigator-initiated substudy to a phase 3 double-blind placebo-controlled RCT (ASCEND) (Kapoor et al., 2018). The ASCEND study evaluated the effect of natalizumab on SPMS patients with a desired end point of reducing sustained disability progression unrelated to relapses. However, the study failed to meet the multicomponent end point, measured by the EDSS, Timed 25-Foot Walk, and 9-Hole Peg Test (9HPT). Nevertheless, natalizumab treatment did reduce a worsening of the hand function of the patients in this study, as measured by the 9HPT.

In line with the treatment effect on PPMS and SPMS, high efficacy DMTs seem to have only a relatively modest impact on PIRA. A pooled analysis of 2 double-blind parallel-group RCTs consisting of over 1600 RRMS-patients, comparing the effect of ocrelizumab and interferon β -1a throughout a 96-week treatment period with confirmed disability accumulation as the endpoint (defined by an increase in EDSS, Timed 25-Foot walk, or 9HPT), showed that most overall disability accumulation in RRMS is consequential to an underlying progressive disease course independent of relapse activity (Kappos et al., 2020). There were 18.5% PIRA events and 3% RAW events in the whole study group for the ocrelizumab -treated group,

whereas the proportion was 23.3% and 6.2% in the interferon β -1a -treated group, respectively (Kappos et al., 2020).

To summarise, the efficacy and benefits of current DMTs in progressive forms of MS appear to be partial and more limited compared to DMTs used in RRMS. The shortcomings or rather modest results of the DMT trials in progressive forms of MS likely originate from the large protein structure of the drugs and the pathophysiology of the disease. Progressive MS features a compartmentalised self-sustaining immune response in the CNS behind a mainly intact BBB, consisting of activated microglia cells, astrocytes and immune-independent processes that drive axonal dysfunction and neurodegeneration (Baecher-Allan, Kaskow, & Weiner, 2018). Treatments to prevent or delay the self-sustained immune system process in the CNS that underlies clinical progression and accumulation of disability remains a major challenge. Currently, the available DMTs primarily effect the peripheral adaptive immune system. Due to the large protein size, they likely have a limited permeability across an intact BBB to the CNS (Hagens et al., 2018). Considering this, future treatment approaches that combine an anti-inflammatory drug diminishing the peripheral adaptive immune system activity with a compound penetrating into the CNS with a direct effect on CNS-compartmentalised inflammation are urgently warranted.

2.3 The role of microglia in MS

2.3.1 Microglia

The central role of microglia in the CNS has been recognised in a substantial amount of research not only in MS but also in several other inflammatory and degenerative diseases (Stephenson, Nutma, van der Valk, & Amor, 2018). Microglia are myeloid cells of the CNS representing approximately 10–15% of the total cell population of the human brain and they are distributed in all areas of the brain (Kreutzberg, 1996). Microglia cells derive from myeloid precursors in the yolk sac, making them distinct from monocyte derived macrophages (Mosser, Baptista, Arnoux, & Audinat, 2017). They migrate during ontogeny into the developing nervous tissue, and mature into brain-resident microglial cells (Biber, Owens, & Boddeke, 2014).

Microglial cells have a crucial role as the intrinsic defensive cells of the human brain. They have protective and homeostatic functions such as antigen presentation to host immune cells, defense from foreign intruders and phagocytosis of unnecessary synapsis (Minghetti & Levi, 1998; Tremblay et al., 2011). Microglial cells clear debris, which is an important function for maintaining a healthy brain. Microglial cells are extremely versatile, and plastic and they can undergo rapid changes depending on the conditions. They continuously survey their

microenvironment for any injury or stimuli that might be harmful for the CNS (Holloway, Canty, King, & Ziebell, 2019).

Microglial cells also contribute to CNS pathology. They respond to changes in the microenvironment leading to a reactive phenotype that can have detrimental effects for the surrounding brain tissue (Voet, Prinz, & van Loo, 2019). Hence, in chronic neuroinflammation the equilibrium between the protective debris-clearing and the inflammation-propagated activated microglia becomes disrupted, leading to uncontrolled neuronal damage caused by overactivated microglia (Gao & Hong, 2008).

A better understanding of the complex activities of microglial cells is beneficial for finding new tools for novel treatment options not only for MS but also for a wide spectrum of other neurodegenerative diseases.

2.3.2 Neuropathological studies revealing microglial activation

It is assumed that activated microglial cells contribute to neuronal damage and tissue atrophy especially in progressive MS (Moll et al., 2011). In the progressive phase of the disease, the CNS pathology shifts from focal to diffuse CNS injury associated with microglial activation (Lassmann, 2018). Neuropathological studies have shown a correlation between the extent of disability and brain tissue pathology in areas of the brain which appear normal in a conventional MRI; that is in the so-called normal appearing white matter (NAWM), at the rim of demyelinating lesions and in the normal appearing grey matter (NAGM) (Frischer et al., 2009; Lassmann, Brück, & Lucchinetti, 2007; Lassmann, van Horsen, & Mahad, 2012; Popescu & Lucchinetti, 2012). Brain samples taken from patients with progressive MS seldom feature signs of acute inflammation. Instead of this feature, the dominating lesion types in progressive MS are the chronic active (i.e., smouldering or expanding) lesions with microglial activation at the edge of an otherwise burned-out plaque or alternatively inactive chronic lesions with no microglial activation at the plaque edge (Frischer et al., 2015). Importantly, the chronic active lesions are associated with signs of demyelination and axonal injury (Frischer et al., 2009; Gillen, Mubarak, Nguyen, & Pitt, 2018).

2.3.3 Translocator protein (TSPO) expression as a marker of detecting microglial activation

Activated microglia express the translocator protein (TSPO) molecule, which structurally is an 18 kDa protein with five alpha helices spanning the membrane lipid bilayer, which is located on the outer mitochondrial cell membrane. Besides

activated microglia, TSPO is expressed at a low level in the “resting” or surveying microglia cells. However, upon their activation the TSPO molecule is upregulated and is thus considered to be a sensitive “real-time” marker of the activation of these cells (Cosenza-Nashat et al., 2009) and consequently a putative marker of neuroinflammation commonly associated with neurodegenerative and neuroinflammatory diseases such as MS (Guilarte, 2019; Högel, Rissanen, Vuorimaa, & Airas, 2018). The microglial activation can be detected *in vivo* using positron emission tomography (PET) and radioligands binding to the TSPO molecule (see also Chapter 2.4.1 of the principles of PET and Chapter 2.3.4 for the review of TSPO-PET radioligands used in MS studies).

TSPO has many proposed functions depending on the tissue, including roles in the immune response, steroid biosynthesis, heme synthesis, programmed cell death and regulation of cell proliferation (Mukhin, Papadopoulos, Costa, & Krueger, 1989; Veenman & Gavish, 2012). In addition to activated microglia, TSPO expression in the CNS also arises to a lesser extent from astrocytes, blood-derived macrophages, endothelial and smooth muscle cells, and plasma proteins within the bloodstream (Cosenza-Nashat et al., 2009). In a neuropathological study, 25% of the TSPO expression arose from astrocytic binding in active WM lesions and chronic active lesion rims, whereas the respective percent was even 65% in the hypocellular centres of the chronic active and inactive lesions (Nutma et al., 2019). Moreover, TSPO expression from endothelial cells accounted for 5% in the WM (Nutma et al., 2019). In the recent study of the same group, the expression of microglia/macrophage cell markers was examined with an extended characterisation of TSPO expressing cells in post mortem MS brain samples to characterise the phenotype of the TSPO expressing cells. Nearly all TSPO expression from the NAWM, the active lesions and the perilesional area of chronic active lesions originated from microglia/macrophages (approximately 95%). Interestingly, in the pixel analysis of TSPO expression per cell the TSPO expression was equal between regions containing homeostatic microglia and regions containing activated microglia. This suggests that the increase in the TSPO expression likely arises both from an alteration in myeloid cell density and a phenotypic shift in microglia (Nutma et al., 2021).

2.3.4 PET imaging detecting microglial activation in MS

PET imaging using radioligands binding to the 18-kDa TSPO within microglia and macrophages, and to a lesser extent to astrocytes, has increasingly been used in MS research to evaluate microglial activation *in vivo* in various relevant regions of interest within the brain. The most widely used TSPO binding radioligand in previous MS studies has been ^{11}C -PK11195. It is a 1st generation TSPO radioligand

which has been available since late the 1980s when it was first used for imaging of human gliomas (Junck et al., 1989). The first *in vivo* human MS pilot brain study with ^{11}C -PK11195 was performed in 1997. The study consisting of two MS patients revealed that TSPO binding was increased in acute lesions and was low in chronic lesions (Vowinckel et al., 1997). The first larger ^{11}C -PK11195 PET study with 12 MS patients and 8 healthy controls (HCs) revealed increased TSPO binding in the NAWM, the thalamus and brain stem compared to HCs and increased TSPO binding in gadolinium enhancing lesions compared to non-enhancing lesions (Banati et al., 2000). Furthermore, an association between a higher percentage of TSPO binding in T1 lesions and a higher EDSS was detected making it the first cross-sectional PET study to reveal an association between microglial activation and MS level of disability (Banati et al., 2000). Subsequently, several cross-sectional TSPO-PET studies have demonstrated a correlation between disease accumulation and increased TSPO binding in various parts of the brain related to MS pathology including NAWM (Colasanti et al., 2014; Debruyne et al., 2003; Herranz et al., 2016; Rissanen et al., 2018; Versijpt et al., 2005), cortical grey matter (GM) (Herranz et al., 2016; Politis et al., 2012) and thalami (Herranz et al., 2016; Misin et al., 2022).

In recent years, special interest has been focused on the perilesional area of the white matter demyelinating lesions. Several recent studies have revealed a correlation between disease accumulation and increased perilesional TSPO binding (Lehto, Sucksdorff, et al., 2023; Nylund et al., 2022; Rissanen et al., 2018). Figure 1 demonstrates representative TSPO-PET and MRI images with both chronic active and chronic inactive lesions (Figure 1).

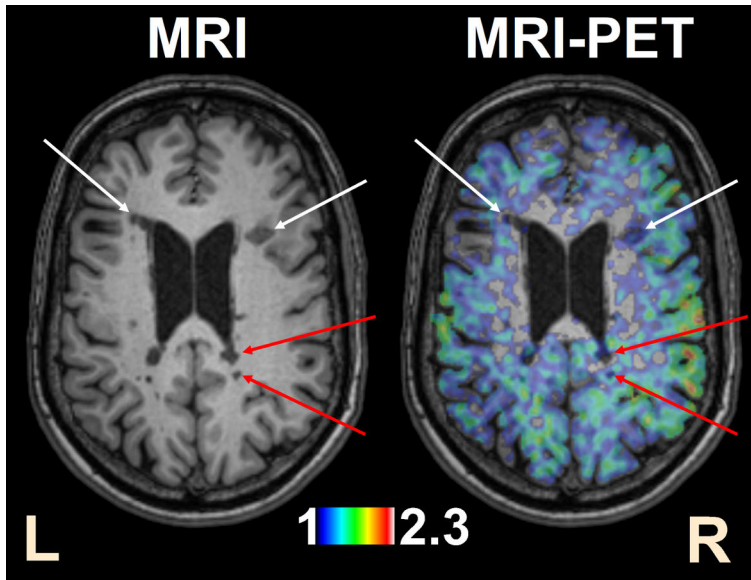


Figure 1. Visual demonstration of the T1 MRI image (left) and respective ^{11}C -PK11195 TSPO-PET image overlaid with the T1 image (right). Red arrows point to a chronic active T1-hypointense lesion with increased perilesional ^{11}C -PK11195 uptake demonstrative of microglial activation. White arrows point to a chronic inactive lesion with negligible radioligand binding. In the parametric PET image, the scaled colour bar indicates the voxel wise ratio representing the intensity of specific radioligand binding measured as DVR. DVR = distribution volume ratio; TSPO = translocator protein; PET = positron emission tomography.

Importantly, microglial activation seems to already have an impact on MS disease evolution at the earliest stage of the disease. A study by Giannetti et al. demonstrated that higher microglial activation increased the subsequent risk of clinically definite MS in patients with CIS during a 2-year follow-up. Thus, highlighting the already plausible detrimental effect of microglial activation at the very early stage of the disease in terms of the later disease evolution (Giannetti et al., 2015).

Apart from Study II, as presented in this thesis, the only TSPO-PET imaging study to report longitudinal inflammatory changes in progressive MS patients was published 2021. The study consisting of 14 progressive MS patients (with stable DMT at least 6-month prior to/ during the study) demonstrated an increase in the ^{11}C -PK11195 uptake in NAWM, thalamus, cortical GM and putamen during the 12-month follow-up (Kang, Pandya, Zinger, Michaelson, & Gauthier, 2021). This suggests that microglial activation in the brain may increase over time in patients with progressive MS and could play an active role in the pathogenesis of disease progression.

There is a huge potential in the usability of PET imaging for the quantification of the treatment effects of DMTs targeting microglial activation. Apart from the studies presented in this thesis (Study I and II), relatively few longitudinal PET studies evaluating the effect of DMTs on TSPO-expression have been published to date.

In the first study published by Ratchford et al., 9 previously untreated RRMS patients were evaluated before and after 1 year of glatiramer acetate treatment. The study demonstrated that treatment of RRMS with glatiramer acetate reduced ^{11}C -PK11195 binding significantly in both cortical GM and cerebral WM when using cerebellum as a reference region (Ratchford et al., 2012). The study by Kaunzner et al. evaluated the effect of natalizumab treatment on ^{11}C -PK11195 uptake in a total of 18 RRMS patients, detecting a significant decrease on ^{11}C -PK11195 uptake in both enhancing and non-enhancing lesions 6 months after initiation of natalizumab (Kaunzner et al., 2017). The researchers concluded that NAWM had a stable ^{11}C -PK11195 uptake over 6 months, and thereafter deemed the NAWM to be an ideal reference tissue (Kaunzner et al., 2017).

Previous longitudinal PET studies have also reported negative results of the effects of DMTs decreasing microglial activation in the MS brain. In a study by Bunai et al., a small patient-cohort of 6 clinically stable RRMS patients underwent serial PET imaging, where ^{11}C -DPA713 -binding (a 2nd generation TSPO-tracer) was evaluated before and after 1 year of receiving DMT (4 patients received fingolimod, 2 patients received interferon-beta). Compared to the first PET imaging, the one-year PET measurement revealed significantly elevated ^{11}C -DPA713 -binding in broader brain regions, suggesting that microglial activation may proceed in the entire brain of clinically stable MS patients even after receiving DMT (Bunai et al., 2018).

A visual demonstration of the change in microglial activation during a follow-up of one year in the brains of two separately chosen MS patients is presented in Figure 2.

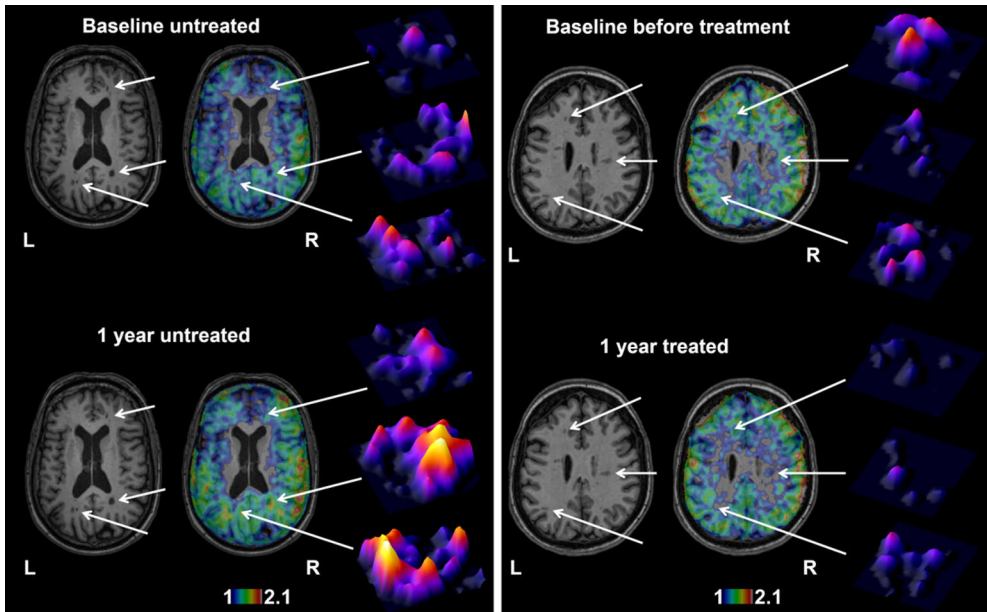


Figure 2. Visual demonstration of the change in microglial activation in an individual untreated SPMS patient and a natalizumab-treated RRMS patient. (A) Axial view of T1 MRI image and respective ^{11}C -PK11195 TSPO-PET image overlaid with the T1 image at baseline (top row) and after one year (bottom row) in an untreated 53-year-old woman with a disease duration of 29 years and EDSS score of 6.0 at baseline and 6.5 at follow-up. White arrows point to the perilesional ^{11}C -PK11195 uptake of chronic active T1-hypointense lesions that increases during the follow-up. The increased perilesional ^{11}C -PK11195 uptake can also be visualized using surface plots of the chosen lesions (on the right). (B) Axial view of T1 MRI image and respective ^{11}C -PK11195 TSPO-PET image overlaid with the T1 image at baseline (top row) and after one year (bottom row) of a natalizumab-treated 46-year-old woman with a disease duration of 7.6 years and EDSS score of 2. The perilesional ^{11}C -PK11195 uptake decreases during the follow-up (white arrows). The surface plots visualize the decreased microglial activation in the perilesional area of the chosen lesions (on the right). EDSS = Expanded Disability Status Scale; RRMS = relapsing-remitting MS; SPMS = secondary progressive MS; TSPO = translocator protein. Reprinted with the permission from Study II.

To date (as of May 2023), apart from the studies presented in this thesis, 19 TSPO-PET studies have been published using ^{11}C -PK11195 radioligand as the marker for detecting microglial activity. The main findings on the radioligand binding are presented in Table 4.

Table 4. Cross-sectional and longitudinal human PET imaging studies with first generation TSPO ligand ¹¹C-PK11195 in multiple sclerosis. Modified from (Airas, Nyland, & Rissanen, 2018).

| REFERENCE | STUDY POPULATION (N) | MAIN FINDINGS ON THE TSPO-BINDING |
|-----------------------|---|--|
| Vowinckel et al. 1997 | 2 (MS) | Increased TSPO-binding in a resolving acute WM lesion Low TSPO-binding in chronic T1 lesions. |
| Banati et al. 2000 | HC (8) RRMS (8) SPMS (1) PPMS (3) | Higher TSPO-binding in 30% of Gd+ than Gd- lesions Higher mean TSPO-binding in T1 hypointense lesions in RRMS patients during a relapse than without relapse. Higher mean TSPO-binding in thalami and brainstem of MS vs. HC. Higher percentage of T1-lesion TSPO-binding associated with higher EDSS. |
| Debruyne et al. 2003 | HC (7) RRMS (13) SPMS (7) PPMS (2) | Increased TSPO-binding in Gd+ active lesions. Increased TSPO-binding in T2 lesions at the time of relapse. Higher NAWM TSPO-binding associated with longer disease duration. |
| Versijpt et al. 2005 | HC (8) RRMS (13) SPMS (7) PPMS (2) | Lower TSPO-binding in T2 lesions associated with higher brain atrophy index. Higher TSPO-binding in NAWM associated with higher brain atrophy index. |
| Politis et al. 2012 | HC (8) RRMS (10) SPMS (8) | Higher cortical TSPO-binding in MS vs. HC. Higher TSPO-binding in WM of SPMS and RRMS vs. HC. Total cortical TSPO-binding correlated with EDSS, with a stronger association in SPMS compared to RRMS. |
| Ratchford et al. 2012 | RRMS (9) | Decreased TSPO-binding in the cortical GM and cerebral WM after 1 year of treatment of glatimer acetate. |
| Giannetti et al. 2015 | RRMS (10) SPMS (8) PPMS (1) | Higher TSPO-binding in T1-lesions in SPMS/PPMS vs. RRMS. Higher TSPO-binding in T1-lesions correlated with higher EDSS score in SPMS/PPMS but not in RRMS. Total TSPO-binding in T1-lesions predicted disability in the SPMS/PPMS patient group at 2 years after TSPO-imaging. |
| Giannetti et al. 2015 | HC (8) CIS (18) | Higher TSPO-binding in NAWM in CIS vs. HC. Higher mean TSPO-binding in NAWM in patients with T2 lesions than without. Higher TSPO-binding in deep WM but not in cortical GM in CIS vs. HC. Higher TSPO-binding in NAWM correlated to higher EDSS score. CIS patients who developed clinically defined MS by 2 years follow-up had higher TSPO-binding in NAWM at baseline. |
| Rissanen et al. 2014 | HC (8) CIS (18) HC (8) SPMS (10) | Increased perilesional TSPO-binding in 57% of T1-hypointense lesions. Mean TSPO-binding higher in NAWM vs. T2 lesional area in SPMS. Higher TSPO-binding in NAWM and thalami in SPMS vs. HC. |

| | | |
|-------------------------|-----------------------------------|---|
| Kaunzner et al. 2017 | RRMS (16) SPMS (2) HC (6) | Decreased TSPO-binding both in the enhancing and non-enhancing lesions 6 months after initiation of natalizumab. |
| Rissanen et al. 2018 | HC (17) RRMS (10) SPMS (10) | Higher TSPO-binding in NAWM in SPMS vs. RRMS and HC Higher TSPO-binding in the perilesional area in SPMS vs. RRMS. Higher TSPO-binding in NAWM associated with higher EDSS score. Higher TSPO-binding in NAWM associated with reduced WM tract integrity (demonstrated by lower FA and higher MD). |
| Bezukladova et al. 2020 | HC (15) RRMS (40) SPMS (15) | Higher TSPO-binding in NAWM in SPMS vs. RRMS and HC. Higher TSPO-binding in NAWM associated with reduced WM tract integrity (demonstrated by reduced FA and increased MD, AD, and RD). |
| Kang et al. 2021 | PMS (16) HC (16) | Increased TSPO-binding in the NAWM, thalamus, cortical GM and putamen during a 12-month follow-up. |
| Nylund et al. 2022 | RRMS (67) SPMS (24) | Patients with higher disability measured by EDSS displayed a higher proportion of rim-active lesions. The phenotyping of chronic lesions was based on a novel automated TSPO-PET analysis method. |
| Misin et al. 2022 | HC (18) RRMS (47) SPMS (19) | TSPO-binding was significantly higher in the thalamus among the patients with later worsening. Increased TSPO-binding in the thalamus predicted disability progression with 53% sensitivity and 94% specificity with an AUC value of 0.82. Patients with later disability progression had more atrophy in the thalamus, caudate, and putamen at baseline vs. patients with no subsequent worsening. |
| Saraste et al. 2022 | MS (48) | Decreased serum 3-hydroxykynurenine correlated with increased TSPO-binding in NAWM and thalamus, and with increased EDSS scores. |
| Lehto et al. 2023 | PPMS (1) | Decreased TSPO-binding in the perilesional area and thalamus after 18 months of treatment of rituximab. |
| Lehto et al. 2023 | RRMS (12) HC (12) | No significant alteration in the TSPO-binding was observed in any part of the brain after 1 year of treatment of teriflunomide. |
| Polvinen et al. 2023 | RRMS (59) SPMS (23) | Patients with a high proportion of chronic active (>10% rim-active lesions) and a low proportion of chronic inactive lesions (\leq 50% inactive lesions) predicted disease progression with an OR of 27 in the entire cohort (n=82) and an OR of 35 in the group free of relapses (n=21) with an EDSS follow-up of 5 years. The phenotyping of individual chronic lesions was based on their TSPO-PET binding status presented in the study Nylund et al., 2022. |

Abbreviations: TSPO= translocator protein; WM= white matter; Gd= gadolinium; HC= healthy control; CNS= central nervous system; EDSS= Expanded Disability Status Scale; RRMS= relapsing-remitting multiple sclerosis; PPMS= primary progressive multiple sclerosis; SPMS= secondary progressive multiple sclerosis; NAWM= normal appearing white matter; PMS = progressive multiple sclerosis; GM= grey matter; CIS= clinically isolated syndrome; FA= fractional anisotropy; MD= mean diffusivity; RD= radial diffusivity; AD= axial diffusivity; AUC= area under curve; OR= odds ratio

Despite its relatively high specificity for TSPO (Banati et al., 2014), the ^{11}C -PK11195 radioligand has its limitations such as a short half-life (20.1 min), a low brain uptake caused by a relatively low penetration through the BBB and a rather modest signal-to-noise ratio (Schweitzer, Fallon, Mann, & Kumar, 2010). To improve the signal-to-noise properties, 2nd generation TSPO ligands with higher affinity have been developed with promising results (Datta, Colasanti, Kalk, et al., 2017; Hamzaoui et al., 2023; Herranz et al., 2016).

A ^{11}C -PBR28 2nd generation TSPO-PET study consisting of 27 MS patients (15 SPMS and 12 RRMS) and 14 matched HCs revealed that MS patients exhibited abnormally high ^{11}C -PBR28 binding across the brain compared to matched controls (Herranz et al., 2016). Moreover, ^{11}C -PBR28 -uptake in the GM cortex, deep GM, and NAWM was greater in SPMS patients compared to RRMS patients and correlated with neurological disability and impaired cognitive performance (Herranz et al., 2016). A recent lesion-based 2nd generation [^{18}F]-DPA-714 TSPO-PET study performed on 36 MS patients and 19 HCs revealed that an unexpectedly high proportion of 59% of all non-gadolinium-enhanced MS lesions have a smouldering component (Hamzaoui et al., 2023). The lesion classification was based on [^{18}F]-DPA-714 uptake of each lesion according to innate immune cell content and localisation defined by a comparison of [^{18}F]-DPA-714 binding between patients with MS and HCs. The [^{18}F]-DPA-714 uptake in the lesions predicted atrophy and clinical progression during a 2-year follow-up. This suggests, that following the acute phase, a substantial proportion of lesions develop a chronic inflammatory component, promoting neurodegeneration and clinical progression (Hamzaoui et al., 2023).

However, genetically determined variation in the binding affinity for the 2nd generation tracers occurs due to the single nucleotide polymorphism rs6971 in the TSPO gene (Owen et al., 2012), bringing more variables into the already complex picture. The binding of the 2nd second-generation TSPO ligand in the brain of a low affinity binder (LAB) subject is too low to enable a reliable quantification of activated microglia (Kreisl et al., 2013). Moreover, the analysis of mixed affinity binders (MAB) and high affinity binders (HAB) must be stratified separately making the analysis and recruiting process more demanding (Kreisl et al., 2013).

Detection of microglial activation in the MS brain using TSPO-PET imaging has increased the understanding of MS pathogenesis and provides an alternative method to monitor disease accumulation, to predict disease progression (Study III) and to measure treatment response (Study I and II). However, there are still great challenges to be solved before TSPO-PET can be more widely used in clinical work or as a surrogate marker in therapeutic studies. First, TSPO-PET MS studies have often been relatively small in sample size making the study underpowered with a heterogenic study population and a cross-sectional study design. Second, the TSPO

binding image analysis methodology has been heterogenic across different PET centres throughout the world, making it challenging to carry out direct comparisons between the studies (Airas et al., 2018). Therefore, future multi-centre, longitudinal studies with larger patient cohorts using harmonised and validated TSPO-PET imaging methodology are warranted to maximise the benefits that PET imaging can bring in understanding the complexity behind MS pathology and to seek pathways for novel treatments.

2.3.5 MRI imaging modalities detecting microglial activation in MS

Recent innovative improvements in MRI technologies have generated promising methods to identify and to some extent quantify chronic active lesions *in vivo*. These methods include detection of paramagnetic iron rim lesions on susceptibility-sensitive MRI sequences and longitudinal follow-up of MRI to define expanding lesions on T1- and T2-weighted conventional MRI sequences (Absinta, Sati, & Reich, 2016).

Susceptibility-sensitive MRI enables a novel contrast mechanism in MRI. Here, methods to detect the rim of iron-laden activated microglia/macrophages on chronic active lesions are of main interest. Several combined pathologic-MRI studies have consistently demonstrated a paramagnetic rim (i.e iron lesion rim (IRL)) in chronic active lesions on susceptibility-weighted MRI, reflecting the pathologically confirmed iron-laden microglia at the rim of these lesions (Absinta et al., 2019; Dal-Bianco et al., 2017; Dal-Bianco et al., 2021). A recent study, comparing 67 MS patients with at least one IRL on MRI to 67 age- and sex-matched MS patients without IRLs, revealed that the patient group with iron IRLs had higher disability scores, significantly lower brain volumes and a significantly higher total T2 lesion volume (Wittayer et al., 2022). In addition, longitudinal studies have demonstrated a slow but gradual linear expansion on serial T1- and T2-weighted scans of IRLs (Dal-Bianco et al., 2017; Dal-Bianco et al., 2021). These rim iron-laden chronic active lesions with a known tendency to expand over time are also named slowly expanding lesions (SELs). A recent 9-year follow-up study demonstrated that the proportion of these SELs in the baseline brain MRI was associated with a worsening EDSS score and conversion from RRMS to SPMS (Preziosa et al., 2022). Importantly, *in vivo* evidence of the co-localisation between IRLs and TSPO-rim-positive lesions was demonstrated in a study by Kaunzner et al., where a multi-modality imaging approach with 30 MS patients was performed using both ^{11}C -PK11195 TSPO-PET and quantitative susceptibility mapping (QSM) (Kaunzner et al., 2019).

Despite being easily accessible, these novel MRI methods detecting chronic active lesions are not at present routinely incorporated in day-to-day clinical work and they have only recently begun to be included in clinical trials (NCT04025554; NCT04742400). The greatest issue limiting the usage of these novel MRI methods in daily clinical work and in clinical trials on a larger scale is the lack of standardisation in chronic active lesions identification, quantification, and monitoring. In addition, it is yet unclear how MRI-based iron rim identification and TSPO-PET imaging methods perform when compared directly on a larger scale and whether their complimentary use will improve the sensitivity of predicting MS progression. Moreover, to the best of my knowledge, there are no published MRI studies evaluating the possible decrease in the iron accumulation at the rim of IRLs after initiation of DMTs. Ongoing multi-modality serial MRI/TSPO-PET imaging studies evaluating the effect of DMTs and co-localisation on iron accumulation and TSPO-uptake on the rim of chronic active lesions will help to resolve these questions (NCT04925557; NCT04126772).

2.4 Positron emission tomography (PET)

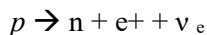
2.4.1 Principles of positron emission tomography (PET)

PET is a fine noninvasive and quantitative imaging technique, that enables visualisation and the measurement of rates in biochemical processes (e.g., enzyme reactions, ligand-receptor interactions, cellular metabolism, cell proliferation, gene expression) in tissues of living subjects (van den Hoff, 2005; Zanzonico, 2012). Whereas conventional MRI is sensitive regarding demonstrating focal anatomical abnormalities and diffuse atrophy in the human brain, it fails to detect pathological changes in neurodegenerative/neuroinflammatory diseases at a molecular level. PET imaging allows the detection of neurodegenerative/neuroinflammatory -disease related pathology at a molecular level *in vivo* (Masdeu, Pascual, & Fujita, 2022).

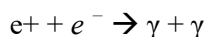
PET imaging uses biologically active molecules, termed tracers or radioligands, that interact with their specific targets within the CNS (Zanzonico, 2012). The radioligands are labelled with positron emitting radioisotopes, such as ^{11}C , ^{15}O and ^{18}F , which are produced using a cyclotron. The desired radioisotopes are produced as follows: Negative hydride ions are accelerated to a spiral path in a magnetic field of the cyclotron and after reaching the desired energy directed through a thin foil, which captures electrons of accelerated ions, thus producing the desired protons. The resulting protons are then directed to collide with stable isotopes, thus producing the desired radioisotopes (Pichler et al., 2018). The half-life of ^{11}C (the most widely used radioisotope in MS studies) is 20.3 min (Turkington, 2001). Due to the short half-

lives of the radioisotopes, a short cyclotron-to-camera-time is required. Therefore, the radioligands are mostly produced on-site.

At the beginning of the PET imaging, the tracer is injected intravenously into the patient, after which it is delivered to the targeted region via blood flow. The basis of positron emission relies on beta plus (β^+) decay. The radioactive isotopes decays by the emission of positrons. Inside the nucleus of the unstable radioactive isotope, a proton (p) is transformed into a neutron (n) while simultaneously emitting a positron (e^+) and an electron neutrino (ν_e):



After the β^+ decay, the emitted positron travels through matter losing its kinetic energy quickly and eventually collides with an electron (e^-). This collision is termed annihilation, resulting in two photons (γ), each with an energy of 511 keV, emitted in approximately opposite directions.



2.4.2 PET scanner and acquisition of image data

PET imaging is based on the detection of these annihilated photons (or gamma rays). After the annihilation, the photons travel at the speed of light in the opposite directions and can almost simultaneously be detected by the opposing sophisticated gamma-counter detectors positioned in the rings inside the PET scanner. The two photons are deduced to travel along an imaginary line connecting the opposite detectors. This line is called the line of response (LOR). Thus, the detection of two annihilated photons on the opposing detectors of the LOR is referred to as a true count. Importantly, a detection of a single annihilated photon on the LOR without a simultaneous event on the opposing detector is referred to as a false count. Though the exact location of the annihilations remains unknown, many detected true counts along the LORs allow the spatial distribution of the radioactive tracers to be reconstructed in a 3D image. A small part of the annihilated photons in the imaged ROI's are scattered, subsequently leading to a false LOR with an incorrect location of the event detected. Nevertheless, about 97% of the single events on the false LOR can be eliminated using an event window correction procedure. After the elimination of false counts, the remaining data of registered true counts is recorded in a 2D coordinate system. Each LOR is identified and located based on its angle and distance and can thereafter be plotted as a discrete point on a graph. The plotted curve of the LORs is called a sinogram due to its sinusoidal shape. The sinograms are collected as a function of time and further divided into time frames corresponding to the temporal distribution of the detected true counts. The sinogram data is furthermore reconstructed with attenuation correction and correction of isotope decay and

filtering (smoothing) resulting in a quantitative PET image representing the radioactivity of the decaying radioisotope of the PET tracer as a function of time; this is termed the time-activity curve (TAC) (Lammertsma, 2002).

Due to the relatively poor spatial resolution of the PET images (~ 2.5 mm), the reconstructed PET images are overlaid with the anatomically corresponding MR images to relate the radioligand kinetics to the anatomical structures. As a result of the limited spatial resolution, each voxel can represent a combination of different structures with different radioligand distribution. This phenomenon is named the partial volume effect (PVE) and degrades the quantitative accuracy of PET image. Due to PVE, the intensity of a particular voxel reflects the radioligand concentration not only of the tissue within the voxel but also from the surrounding area. PVE becomes more important when the target investigated is smaller, especially when it is less than two times the spatial resolution of the PET scanner (Erlandsson, Buvat, Pretorius, Thomas, & Hutton, 2012). Different partial volume correction techniques have been developed to correct the spill over effect caused by the relatively poor spatial resolution of PET images. These techniques are either included in the image reconstruction from the beginning or applied later to the reconstructed images (Erlandsson et al., 2012).

2.4.3 Modelling and quantification of the detected radioligand binding signal

Mathematical modelling needs to be obtained in order to quantify the values that describes the biological properties of the region of interests (ROI's) in the best way. Compartment models are commonly used to quantify and optimise the analysis process of the PET data. Here, applying kinetic models that are based on assumptions of a compartmental system are key elements. The most widely used kinetic modelling method for the evaluation of the nuclear medicine imaging data is the Logan plot (Logan, 2000; Logan et al., 1996; Logan et al., 1990). It is an algorithm for the quantitative analysis of reversibly binding neuroreceptors using PET, with simple mathematical implementation and fast computation (Logan et al., 1990). The modelling methods are then implemented by fitting the model equation to the measured TAC, in order to optimise and smooth the quantitative values that describes the biological properties.

A reference region with a negligible specific binding in the brain is required to obtain reliable PET data and to enable the usage of mathematical modelling in optimising and smoothing the PET data. Many neurodegenerative/neuroinflammatory diseases influence the whole brain (including MS), making it difficult to find a disease-free reference region in the brain. To minimise the estimate bias due to specific binding in the reference region, a supervised cluster algorithm

(SuperPK software) approach has been widely used in PET studies to detect neuroinflammation (including Studies I–III presented in this thesis) (Turkheimer et al., 2007; Yaqub et al., 2012). Here, a supervised cluster algorithm with 4 predefined kinetic tissue classes with negligible radioligand binding is utilised. The reference tissue-input Logan method with a time interval from 20 to 60 minutes is applied to the regional TACs using the supervised cluster algorithm reference input (Turkheimer et al., 2007; Yaqub et al., 2012).

The final results of the specific binding of the radioligand in the pre-specified ROI's describing the underlying biological properties are reported with varying outcome measures. The distribution volume ratio (DVR), the binding potential (BP) and the standardised uptake value (SUV) are the three most widely used outcome measures in PET studies evaluating neuroinflammation/neurodegeneration. DVR is a linear function of receptor availability and is widely used as a model parameter in imaging studies (including Studies I–III in this thesis (Logan et al., 1996) and can be estimated as follows: The ratio of distribution volume (DV) in target ROI to the DV in the reference region ROI. Estimates from Logan plots aim to reduce the bias and variance in DVR. The ultimate parameter of interest in the *in vivo* kinetic modelling is the non-displaceable specific binding of the radioligand in ROI as a function of time. The SUV is a simple and robust way of determining activity in PET imaging. It is a semiquantitative measure and is defined as the radioligand binding in the ROI, divided with the injected dose per unit whole body volume. Consequently, SUV measurement does not allow pharmacokinetic modelling, but on the other hand, does not require dynamic imaging or blood samples. BP is also a parameter used quantifying specific radioligand binding. It is a combined measure of the density of the receptors free of a specific binding and the affinity of the specific binding and is defined as the ratio of specifically bound radioligand in the ROI and non-displaceable radioligand at equilibrium (Innis et al., 2007).

Regardless of the varying mathematical modelling, quantification methods and outcome measures used in PET studies, the essential matter is to address the quantitative values that describes the biological properties of the ROIs in the most reliable way with the help of the procedures mentioned above.

2.4.4 The variability in the TSPO uptake

As far as I know, no test-retest ¹¹C-PK11195 TSPO-PET study with MS patients has yet been published. There have only been a few ¹¹C-PK11195 TSPO-PET studies performed for HCs and one study performed for patients with Alzheimer's disease with a low number of 4 to 6 participants taking part in the studies. Varying results from good to rather modest test-retest reproducibility were reported in HCs with a variability in the ¹¹C-PK11195 TSPO uptake in the GM (from 5% to 27%), WM

(from 4% to 44%) and thalamus (from 8% to 29%) (Jučaitė et al., 2012; Kaunzner et al., 2017; Plavén-Sigraý et al., 2018). Moreover, a variability of 11% was reported in the GM of patients with Alzheimer's disease (Turkheimer et al., 2007). Notable, the high variability in the aforementioned studies with HCs might reflect the low ^{11}C -PK11195 TSPO uptake in young study participants, as ageing may increase the TSPO uptake (Damani et al., 2011). Study participants with low ^{11}C -PK11195 TSPO uptake are more prone to the impact of artefacts decreasing the signal-to-noise ratio of the ligand and increasing the risk of worse test-retest reproducibility. To date, the only test-retest study in MS patients has been performed with the 2nd second-generation TSPO ligand ^{11}C -PBR28 (Park et al., 2015). Here, a rather good test-retest reproducibility of 4 disease stable MS patients was reported with a variability ranging from 7 to 9% across GM, NAWM and MS lesions (Park et al., 2015).

3 Aims

The general aims of this study were 1) to evaluate the effect of DMTs on neuroinflammation *in vivo* in MS patients using functional neuroimaging with specific radioligand binding to activated microglial cells and 2) to examine the possible predictive role of microglial activation in later MS disease progression. The specific aims of the sub-studies, referred to with the Roman numerals **I–III**, were as follows:

- I** To evaluate whether fingolimod treatment decrease microglial activation in different parts of the MS brain during a 6-month follow-up using longitudinal ^{11}C -PK11195 TSPO-PET imaging.
- II** To evaluate whether natalizumab treatment decrease microglial activation in different parts of the MS brain during a 12-month follow-up using longitudinal ^{11}C -PK11195 TSPO-PET imaging, and to further compare the results with an age-sex matched untreated MS patient cohort imaged with the same longitudinal protocol.
- III** To examine the usefulness of ^{11}C -PK11195 TSPO-PET imaging for predicting the later MS disease course during a 4-year follow-up period using the change in the EDSS score as an outcome measure.

4 Materials and Methods

4.1 Materials

4.1.1 Study participants and procedures

All studies were performed as an investigator initiated academic research project in Turku PET Centre and in the outpatient clinic of the Division of Clinical Neurosciences at the University Hospital of Turku, Finland. The studies were approved by the Ethics Committee of the Hospital District of Southwest Finland and all participants provided written informed consent according to the World Medical Association's Declaration of Helsinki.

The patients were recruited from the neurology outpatient clinics and HCs were recruited through information posted on notice boards of Turku University Hospital and via the MS patient organisation. Initially, the study physician contacted the potential study participants by telephone, and if they agreed, they were sent the study information material by mail or email. The possible risks of the study were explained to the study participant in detail. With a targeted injection dose of 500 MBq, the average effective radiation dose per injection was estimated to be 2.40 mSv. The total average effective radiation dose for those study participants on whom PET imaging was performed twice was 4.80 mSv and for those on whom PET imaging was performed three times was 7.20 mSv. The average radiation dose per annum for Finns is 3.2 mSv (Säteilyturvakeskus, STUK). For comparison, values of the radiation dose caused by one head computer tomography (CT) scan (routinely used in clinical practice) is estimated to be 1.3 mSv. Consequently, the radiation dose was considered acceptable to the study participants. It was also explained, that if some significant coincidental finding was detected in the MRI or in the clinical evaluation, the study participant would be directed to further investigations or treatment if needed.

During the first visit, the study physician went through the study information material with the study participant, and an appropriate time was reserved for questions and discussion. The study participants were informed of their right to withdraw from the study at any time and for any reason. The study physician also had the responsibility to evaluate whether the study participant had sufficient

cognitive capacity to understand the purpose of the study. After having read and understood the study information material, the study participant provided written informed consent prior to entering the study.

The overall number of participants in the studies in this thesis consisted of 69 MS patients (45 RRMS and 24 SPMS patients) and 18 age-sex matched HCs.

The following inclusion criteria were used for the study participants with MS:

1. Age between 18-65 years (Study **I–III**)
2. Definite MS diagnosis according to the revised McDonalds criteria (Polman et al., 2011) (Study **I–III**)
3. Definite MS diagnosis according to the revised McDonalds criteria (Polman et al., 2011) for more than 5 years prior to enrolment (Study **I**)

Exclusion criteria in Studies **I–III** included clinical relapse and/or corticosteroid treatment within 30 days of evaluation, gadolinium contrast enhancement in baseline MRI, active neurological or autoimmune disease other than MS or another comorbidity considered significant, inability to tolerate PET or MR imaging, and a current or desired pregnancy following study enrolment. In addition, in Study **III** the exclusion criteria included a clinical relapse and/or corticosteroid treatment within 30 days prior to the EDSS re-evaluation. Inclusion criteria for HCs included an age between 18–65 years with no previous history of neurological symptoms or diagnoses.

In most cases, brain MRI imaging (see Chapter **4.2.1**) supervised by the study physician was performed during the first visit after the written informed consent was provided. The PET imaging (see Chapter **4.2.2**) was performed preferably within two weeks from the MRI imaging, depending on the imaging time schedule. The study physician carried out the neurological status using the EDSS and a careful general inspection and cardiovascular status for all the study participants. Summary and baseline characteristics of all the study participants are presented in Table 5.

Table 5. Summary and baseline characteristics of all the study participants included in the studies.

| | Number of study participants and MS subtype | Age (years) | Females/males | Disease duration prior to imaging (years) | Baseline EDSS |
|---------|---|------------------|---------------|---|-----------------|
| Study 1 | 10 RRMS | 42 ± 9 | 9/1 | 8 ± 4 | 2.7 ± 0.5 |
| | 8 HC | 50 ± 8 | 6/2 | N/A | N/A |
| Study 2 | The natalizumab treated group | 6 SPMS / 4 RRMS | 6/4 | 14 ± 9 | 3.5 (2.6–3.9) * |
| | No treatment group | 10 SPMS / 1 RRMS | 7/4 | 15 ± 7 | 6.0 (3.8–6.0) * |
| | | 8 HC | 50 ± 8 | 6/2 | N/A |
| Study 3 | 45 RRMS / 24 SPMS | 46 ± 10 | 50/19 | 13 ± 7 | 3.0 (2.5–4.5) * |
| | 18 HC | 43 ± 11 | 13/5 | N/A | N/A |

Abbreviations: RRMS = relapsing-remitting multiple sclerosis; SPMS = secondary-progressive multiple sclerosis; HC = healthy control; SD= standard deviation, EDSS = Expanded Disability Status Scale, N/A= not applicable. Values are the mean (±SD where indicated) of the variables unless otherwise stated. *Median and interquartile range (IQR).

The procedures of the Studies I–III were as following:

4.1.2 Study I

Eleven patients with RRMS were imaged using PET and MRI at baseline. A minimum washout period of 1 month after a possible previous DMT was required before baseline images. Treatment with oral 0.5 mg fingolimod was initiated shortly after the baseline images. One patient withdrew from the study after baseline images and was excluded from the final analysis. Ten patients were imaged both at baseline and after 24 weeks of fingolimod treatment. Seven patients also underwent PET and MRI images after 6–8 weeks of fingolimod treatment. EDSS, a safety evaluation and the recording of relapses were performed at baseline, and then after 6–8 weeks and 24 weeks of fingolimod treatment. The baseline PET was compared with the historical PET data, with identical imaging methodology from 8 HCs. A flowchart of the study is demonstrated in Figure 3.

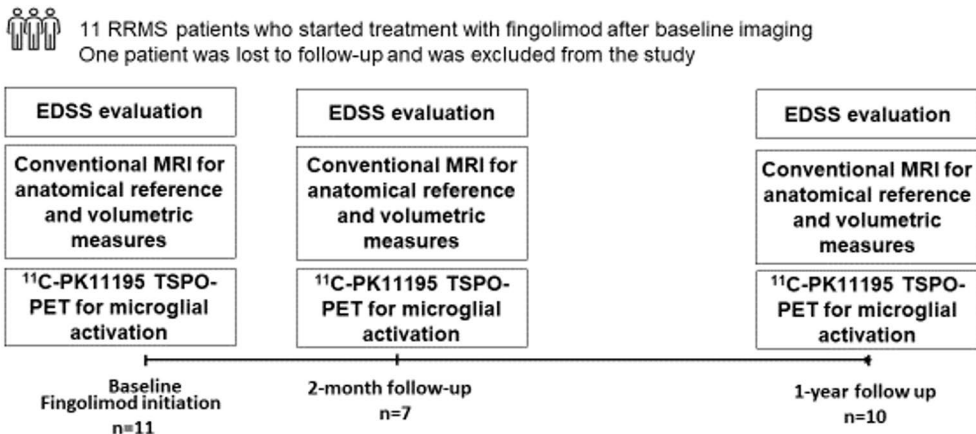


Figure 3. A flowchart of the Study I timeline.

4.1.3 Study II

Ten patients were imaged using PET and MRI at baseline before initiation of natalizumab treatment, and then one year later (6 SPMS and 4 RRMS patients). A minimum washout period of 2 months after a possible previous DMT was required before baseline images. Eleven patients without any DMT were imaged for comparison using the same protocol (10 SPMS patients and 1 RRMS patient). EDSS evaluation and recording of relapses were performed at baseline and after one year for every patient. Safety monitoring was performed regularly at one-month intervals. All patients were re-evaluated for EDSS within a median of 4.1 years after baseline images. The baseline PET images were compared with the historical PET data, and with the identical imaging methodology from 8 HCs. A flowchart of the study is demonstrated in Figure 4.

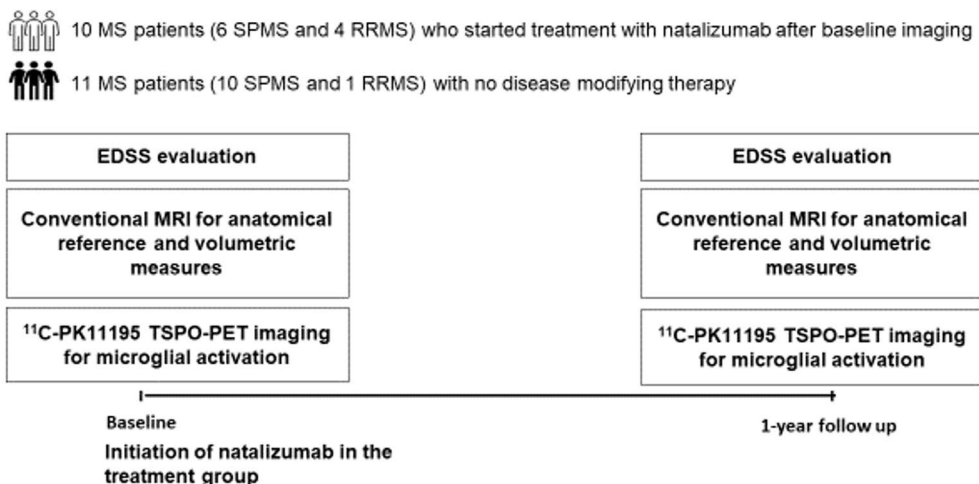


Figure 4. A flowchart of the Study II timeline.

4.1.4 Study III

The study cohort consisted initially of 73 multiple sclerosis patients (49 RRMS and 24 SPMS patients). PET and MRI images were performed at baseline. All patients had initially participated in some of our previous/ongoing PET studies. EDSS was evaluated at the baseline and at an average of 4.1 years later. The ARR was also determined for the follow-up period and for the disease history from the diagnosis to the time of PET imaging. Four RRMS patients were lost to follow-up and were excluded from this study. The PET images were compared with historical PET data, with identical imaging methodology from 18 HCs. A flowchart of the study is demonstrated in Figure 5.

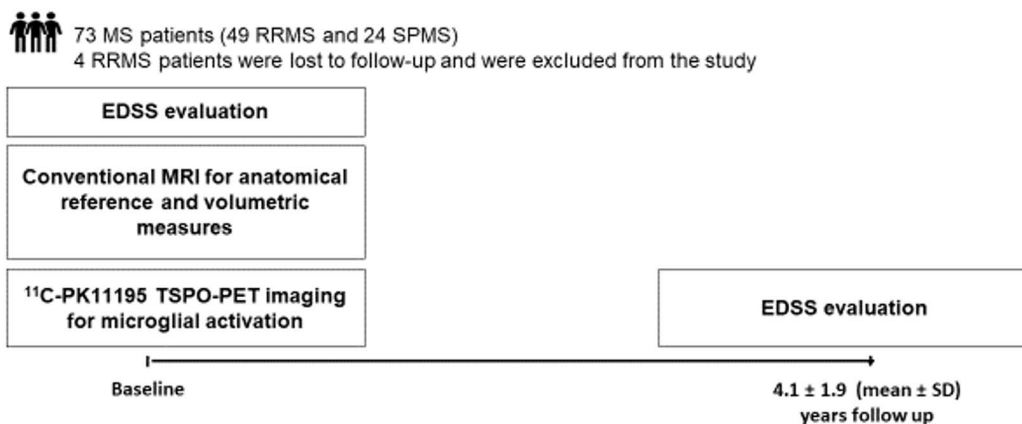


Figure 5. A flowchart of the Study III timeline.

4.2 Methods

4.2.1 MRI imaging

Brain MRI was carried out to evaluate MS pathology, to exclude individuals with anatomical abnormalities and to obtain anatomic reference for the PET image analysis. Brain MRI imaging was performed with a 3-T Ingenuity TF PET/MRI scanner (Philips) on all MS patients and HCs participating in the studies, apart from a HC group of eight persons used in Study **I and II**, for whom MRI was performed with a Gyroscan Intera 1.5-T Nova Dual scanner (Philips). The imaging protocol included axial T2, 3-dimensional (3D) fluid-attenuated inversion recovery (FLAIR), 3D T1, and gadolinium enhanced 3D T1 weighted sequences.

4.2.2 PET imaging and ^{11}C -PK11195 radioligand production

All PET examinations in Studies **I–III** were performed using the brain-dedicated high resolution ECAT HRRT scanner (Siemens/CTI, Knoxville, TN, USA). HRRT is a dual-layer, crystal-detector scanner with a reconstructed image resolution of approximately 2.5 mm (de Jong et al., 2007).

The tracer ^{11}C -PK11195 was applied in all the studies (**I–III**). The radiochemical synthesis of ^{11}C -(R)-PK11195 ((R)-[N-methyl- ^{11}C]-1-(2-chlorophenyl)-N-(1-methylpropyl)-3-isoquinolinecarboxamide) is described in detail in (Rissanen et al., 2014). The tracer production was performed with the cyclotron in the Turku PET Centre and followed the EU regulations. The target radioactivity dose of the administered ^{11}C -PK11195 was 500 MBq in every study in this thesis. No significant differences of the administered dose of ^{11}C -PK11195 occurred between the groups or between different timepoints in Studies **I–III** (data not shown).

First, a transmission scan lasting 6 minutes using the ^{137}Cs point source was performed for attenuation correction of the PET emission data. Thereafter, 60-min dynamic imaging was started simultaneously with an intravenous bolus injection of the tracer. An individually shaped thermoplastic mask was used to minimise spontaneous head movement artefacts during the scan.

4.2.3 Image processing and analysis

The dynamic PET images were preprocessed in a similar manner for each study participant in this thesis. First, the PET image reconstruction was performed using 17 frames (2×15, 3×30, 3×60, 7×300 and 2×600 seconds, total of 3600 seconds). The dynamic data was then smoothed using a Gaussian 2.5 mm post reconstruction filter and thereafter possible displacements between frames were corrected using mutual information realignment in statistical parametric mapping (SPM8, version 8; Wellcome Trust Centre for Neuroimaging, a software running in MATLAB (The Mathworks, Natick, MA)).

In the longitudinal Studies **I** and **II**, the T1 MRI image at the first time point was co-registered in SPM8, to the sum image of realigned motion corrected PET frames of the same timepoint for each study participant. All the follow-up MRI images were then co-registered to the T1 MRI image of the first session. MS lesions were identified using the Lesion Segmentation Tool (LST) (a toolbox running in SPM8) for each timepoint. After being checked and manually corrected slice by slice, the resulting lesion mask images were further used to fill the corresponding T1 MRI image with the lesion-filling tool in the LST. The filled T1 lesion masks were then used for segmenting GM and WM volumes using the FreeSurfer 5.3 software. Similarly, the volumes of T2 lesion masks obtained with the LST were manually corrected slice by slice and thereafter used for the T2 lesion load evaluation. In

addition, the LST masks for every patient at each time point were further combined to a unified lesion ROI. An average filled T1 image was calculated from the filled T1 images of all MRI sessions, and was used for ROI delineation for the WM, cortical GM, striatum, thalamus, and cerebellum using the Freesurfer 5.3 software. Finally, the lesion ROI was removed from the WM ROI resulting in NAWM ROI. Additionally, in Study **II**, a perilesional ROI with a distance of 3 to 6 mm to the lesion mask border was created by dilating the lesion mask image 3 mm and 6 mm and then removing the core from the resulting image.

In Study **III**, the process of volumetric analysis proceeded with the same protocol as in Studies **I** and **II**, apart from the T2 lesion masks being created before T1 lesion masks using LST. This was a base for a manually corrected combined T1 lesion mask, which then was used to create the perilesional ROI. The resulting T1 lesion ROI mask image was used (similarly to Studies **I** and **II**) to fill the corresponding T1 image with the lesion-filling tool in LST and was further used for segmenting GM, WM, and thalamus with Freesurfer 5.3 software. The perilesional ROI in Study **III** was created by dilating the T1 lesion ROI mask image by six voxels (corresponding to 6 mm of width) and then removing the core from the resulting image. In addition, a NAWM ROI was created by removing the T1 lesion ROI and the six-voxel perilesional ROI from the WM ROI.

4.2.4 Modelling of ^{11}C -PK11195 image data

The outcome measure in Studies **I-III** evaluating the specific binding of ^{11}C -PK11195 in pre-specified ROIs of the participants brains (describing the underlying biological properties) was reported as DVRs (see Chapter **2.4.3**). A non-invasive reference region input was obtained using the supervised cluster algorithm approach with 4 predefined kinetic tissue classes (SuperPK software) (see Chapter **2.4.3**) (Turkheimer et al., 2007; Yaqub et al., 2012). The ROI specific binding of ^{11}C -PK11195 were optimised and smoothed by using the reference tissue-input Logan method, with time interval from 20 to 60 minutes (see Chapter **2.4.3**) (Logan et al., 1996).

4.2.5 Statistical methods

The study specific statistical methods are described below.

Study I

All ROI-level statistical analyses of ^{11}C -PK11195 DVR and clinical parameters were conducted with SPSS software (IBM SPSS Statistics, version 23, Armonk, NY,

USA). The Shapiro-Wilk test was used in evaluating the data distribution. Normally distributed group characteristics were reported as mean and SD, whereas nonnormally distributed variables were reported as medians [interquartile range (IQR)]. The baseline imaging parameters comparisons between HCs and MS patients were evaluated using an analysis of covariance. Age was used as a covariate due to different, but overlapping, distributions of age. Correlational analysis between the changes in the volumes and DVRs in the ROIs were examined using a Spearman correlation to rule out the possible effect of volumetric changes in the DVR estimates.

The longitudinal PET data were analysed using repeated-measures ANOVA with Bonferroni adjustment. The pairwise comparisons were performed using the nonparametric Mann-Whitney U test or related-samples Wilcoxon signed-rank test. The nonparametric tests were chosen due to the low number of study participants (10 MS patients, 8 HCs). The Spearman's correlation test was used in analysing the associations between variables of interest. P -value < 0.05 was considered statistically significant for all analyses unless otherwise stated.

Study II

All ROI-level statistical analyses of ^{11}C -PK11195 DVR and clinical parameters were conducted with R software (version 3.5.2), with variables reported as median [IQR]. Due to the low number of study participants in all groups (10 natalizumab-treated MS patients, 11 non-treated MS patients, 8 HCs), mainly nonparametric tests were used in the analyses. A Wilcoxon rank-sum test was used in the analysis of differences in the demographic variables between the MS patient groups. In addition, a χ^2 test was used due to the differences in proportions of patients with SPMS and females between the MS patient groups. The baseline imaging differences in DVR values and MRI parameters between the MS patient groups were compared with the Wilcoxon rank-sum test.

The longitudinal imaging data with changes of DVR values and MRI parameters between the images were analysed separately in both MS patient groups using the Wilcoxon signed-rank test. Since all the relationships between the variables could not be seen as linear, all correlations were performed as Spearman correlations. The partial correlations between the EDSS change and DVR values were adjusted for the time between the EDSS measurements as follows. The variables were regressed on the time difference, and the residuals of the model (i.e., the part in which the time difference impact has been removed) were used to calculate the partial correlations.

Study III

All ROI-level statistical analyses of ^{11}C -PK11195 DVR and clinical parameters were conducted with R software (version 3.6.1), with variables reported as mean (\pm SD) unless otherwise stated. A Wilcoxon rank-sum test was used to evaluate the differences in baseline imaging results between the whole MS patient group and HC group as well as in the initial comparisons of variables of interest between the MS patient subgroups with disease progression and no progression during the follow-up. A Spearman correlation was used to evaluate the relationships between the continuous variables, including baseline DVR values, baseline brain volumes and ARR variables.

A forward-type stepwise logistic regression was chosen to evaluate which variables most likely predicted EDSS increase during the follow-up. Modelling was initially done for the whole MS patient group and thereafter for the subgroup of patients free of relapses during the follow-up. Several clinical, conventional MRI volume and DVR values were considered when building the model, as follows:

1. DVR variables: NAWM, perilesional NAWM, T1 and T2 lesions, cortical GM, and thalamus.
2. Conventional MRI volume variables: T1 and T2 lesions, cortical GM, and thalamus as parenchymal fractions (PF), and whole brain volume.
3. Clinical variables: EDSS, gender, age, disease duration at baseline, time difference between the EDSS measurements, ARR preceding PET imaging, ARR during the follow-up, class of the DMT at baseline or at most 2 months before and class of the DMT within the first 3 years after MS onset.

The class of the DMTs were categorised as follows:

1. No DMT
2. Moderate efficacy DMTs (interferons, glatiramer acetate, dimethyl fumarate, fingolimod and teriflunomide)
3. High efficacy DMTs (natalizumab, alemtuzumab, ocrelizumab and rituximab)

Creating the model started with a model without any predictors. Subsequently, in each of the following steps the most suitable variable was added to the model according to Akaike Information Criterion (AIC). After establishing the final model with the lowest AIC value, the model was checked for its assumptions (e.g. multicollinearity, influential values). To obtain the OR, the estimates for the parameters were exponentiated. Due to the range of some continuous variables, the

ORs for a 0.1-unit increase were calculated for those variables instead of ORs for a 1-unit increase.

After this, the chosen model was validated using a leave-one-out cross validation, in which the probability of the disease progression for each observation was predicted using all the other observations. The contingency tables were used for calculating the specificity and sensitivity. The observation was classified as a 'predicted later disease progression', if the probability of EDSS increase based on the model was closer to one. Alternatively, if the probability of EDSS increase was closer to zero, the observation was classified as 'disease progression not predicted'. In addition, the receiver operating characteristic curve was estimated along with area under the curve (AUC) value. All tests were two-tailed and a P -value < 0.05 was considered statistically significant for all analyses.

5 Results

Altogether, the results originate from the clinical and imaging data consisting of 45 RRMS patients, 24 SPMS patients and 18 HCs (Table 5).

5.1 Study I: Fingolimod treatment reduces microglial activation at the site of focal inflammatory lesions

In the baseline TSPO-PET imaging analysis, a higher ^{11}C -PK11195 uptake was observed in the thalamus and in the combined NAWM and GM area among the MS patients ($n = 10$) compared to HCs ($n = 8$) (Figure 6). In other brain areas, no significant differences were found between the groups.

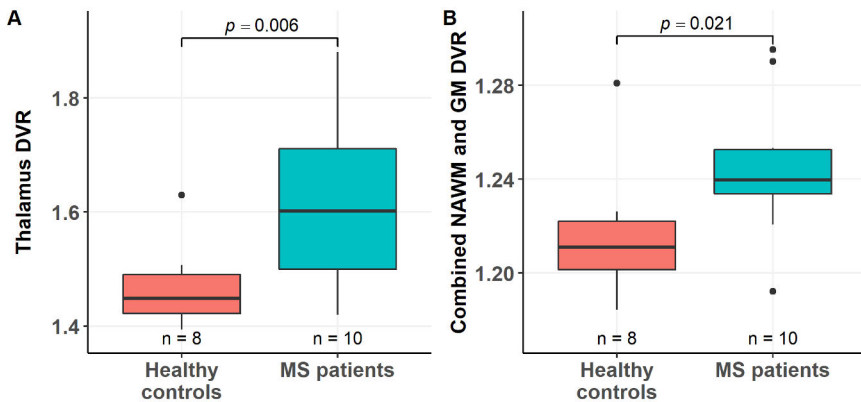


Figure 6. Boxplots of the ^{11}C -PK11195 distribution volume ratios (DVR) in the thalamus and in the combined normal appearing white matter (NAWM) and grey matter (GM) area of MS patients and healthy controls (HC) at baseline TSPO-PET imaging. Modified from the original publication I.

Higher ^{11}C -PK11195 uptake in the NAWM at baseline associated with longer disease duration and higher age (Figure 7). In addition, there was a non-significant trend for a correlation between longer treatment-free washout period before initiation of fingolimod and higher ^{11}C -PK11195 uptake in the NAWM at baseline (Figure 7).

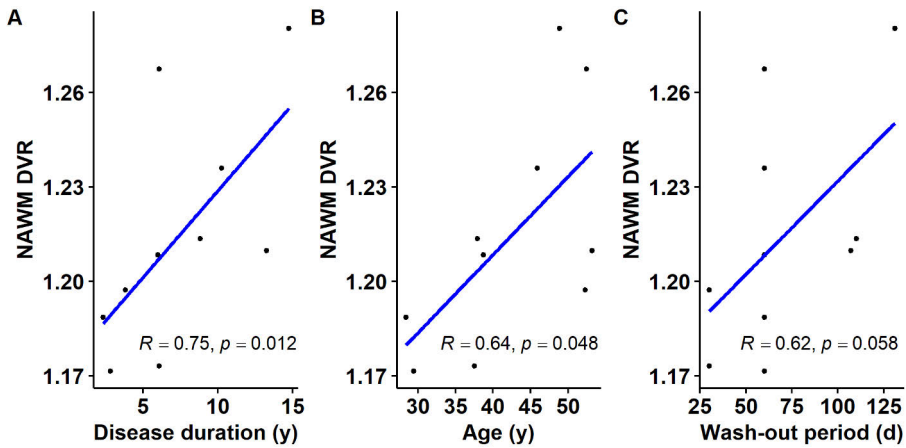


Figure 7. Scatterplots illustrating the association between the ^{11}C -PK11195 distribution volume ratios (DVR) in the normal appearing white matter (NAWM) at baseline TSPO-PET imaging and longer disease duration (**A**), higher age (**B**) and longer treatment-free washout period (**C**) of the MS patients. Modified from the original publication I.

In the serial TSPO-PET imaging analysis among the MS patients ($n = 10$), decreased ^{11}C -PK11195 uptake was observed in the combined T2 lesion area after 6 months of treatment with fingolimod (Figure 8).

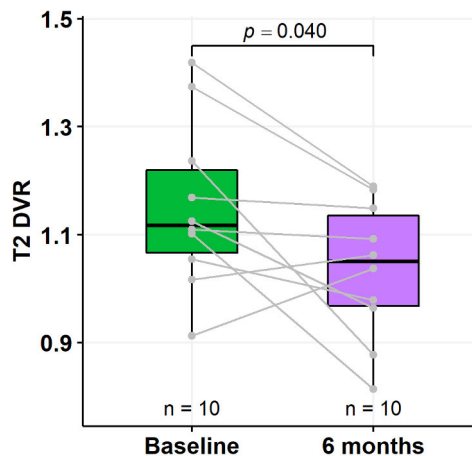


Figure 8. Boxplot of the ^{11}C -PK11195 distribution volume ratios (DVR) at baseline and at 6 months timepoint in the combined T2 lesion area of the MS patients. Modified from the original publication I.

In other brain areas, no significant changes were observed. Seven MS patients were scanned at all time points (at baseline, at 2 months and at 6 months after fingolimod initiation), with non-significant alterations observed in any of the ROIs

at the group level. However, a slight decrease in the uptake of ^{11}C -PK11195 was detected in 5 of the 7 patients in the NAWM and 6 of the 7 patients in cortical GM during the follow up between 2 months and 6 months of fingolimod initiation (Figure 9).

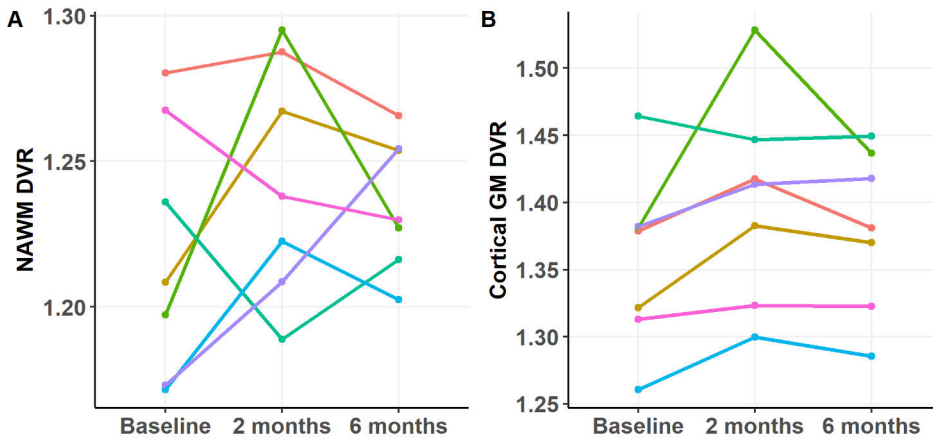


Figure 9. Longitudinal TSPO-PET imaging results demonstrating the ^{11}C -PK11195 distribution volume ratios (DVR) in MS patients in the normal appearing white matter (NAWM) (A) and cortical grey matter (GM) (B) at baseline, 2 months, and 6 months time points. Modified from the original publication I.

To achieve enough power for future ^{11}C -PK11195 TSPO-PET studies, the sample size needed to demonstrate a statistically significant alteration in ^{11}C -PK11195 uptake within the NAWM and this was calculated using the data from this study as follows: To reveal a $\pm 5\%$ treatment effect with a statistical significance of $P < 0.05$, the sample size and the respective statistical power for a 5% increase between baseline and 2 months are 13 and 0.907, respectively. For a 5% decrease both in 2- to 6-months and in 2-months to 1-year intervals, the sample size is 14 and power 0.913.

5.2 Study II: Natalizumab treatment reduces microglial activation in the NAWM and at the rim of chronic lesions

The main demographic features of the Study II, including conventional MRI data, clinical measures and comparison between the non-treated and natalizumab-treated MS patient cohorts are presented in Table 6. The baseline ^{11}C -PK11195 uptake comparison between the natalizumab-treated and non-treated groups showed no significant differences in any of the brain areas studied.

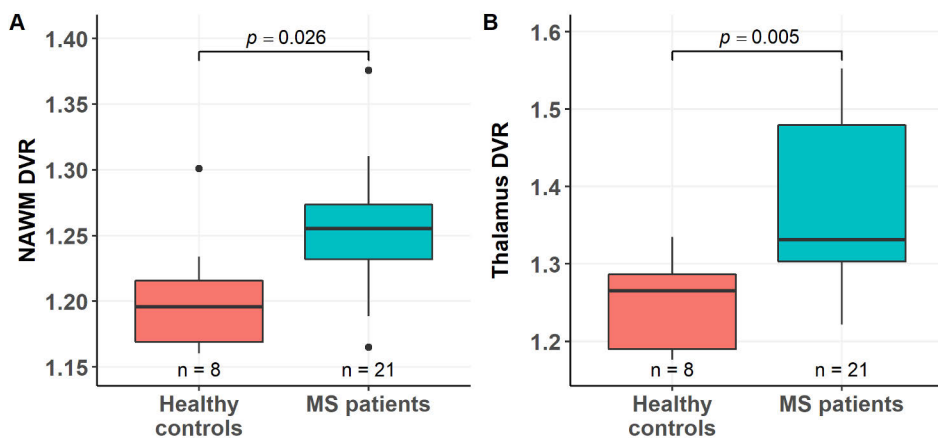
Table 6. Summary of the main demographic information and baseline imaging parameters of the study cohort. Modified from the original publication II

| | Natalizumab treated (n=10) | No treatment (n=11) | p value |
|---|----------------------------|---------------------|---------|
| SPMS (n=16) | 6 | 10 | 0.097 |
| RRMS (n=5) | 4 | 1 | |
| Age (years) | 49 ± 9 | 48 ± 10 | 0.700 |
| Female/Male (n) | 6/4 | 7/4 | 0.864 |
| Disease duration (years) | 14 ± 9 | 15 ± 7 | 0.600 |
| Years since SPMS diagnosis | 3.6 ± 1.8 | 3.4 ± 2.3 | 0.830 |
| EDSS at baseline (median and IQR) | 3.5 (2.6–3.9) | 6.0 (3.75–6.3) | 0.036* |
| Number of relapses 1 year prior to baseline imaging | 0.7 ± 0.8 | 0.3 ± 0.5 | 0.220 |
| T2 lesion volume (cm ³) | 14.8 | 28.9 | 0.018* |
| T1 lesion volume (cm ³) | 13.9 | 26.8 | 0.022* |
| GM volume (cm ³) | 437 | 433 | 0.916 |
| NAWM volume (cm ³) | 444 | 426 | 0.504 |

Abbreviations: RRMS = relapsing-remitting multiple sclerosis; SPMS = secondary-progressive multiple sclerosis; EDSS = Expanded Disability Status Scale; IQR = interquartile range; GM = grey matter; NAWM = normal appearing white matter

Values are the mean (± standard deviation (SD) where indicated) of the variables unless otherwise stated. * Denotes a statistically significant group difference at a level of $p < 0.05$.

In the baseline TSPO-PET imaging analysis, higher ¹¹C-PK11195 uptake was observed in the NAWM and in the thalamus among the MS patients ($n = 21$) compared to HCs ($n = 8$) (Figure 10), whereas in cortical GM no significant differences were found between the groups.

**Figure 10.** Boxplots of the ¹¹C-PK11195 distribution volume ratios (DVR) in the normal appearing white matter (NAWM) and thalamus of MS patients and healthy controls (HC) at baseline TSPO-PET imaging. Modified from the original publication II.

In the serial TSPO-PET imaging analysis, natalizumab treatment ($n = 10$) reduced the ^{11}C -PK11195 uptake in the NAWM, in the T1 and T2 lesional area and in the 3– to 6-mm perilesional area during a 1-year follow-up (Figure 11). Contrary to the natalizumab-treated group, increased ^{11}C -PK11195 uptake was observed in the MS patient group with no DMT. Here, the ^{11}C -PK11195 uptake increased in the 3– to 6-mm perilesional area and a trend toward the increase was observed in the NAWM during the 1-year follow-up (Figure 11). In other brain areas, no significant changes were observed in either MS group. The clinical disability using the EDSS score was unaltered in both MS groups after the 1-year follow-up.

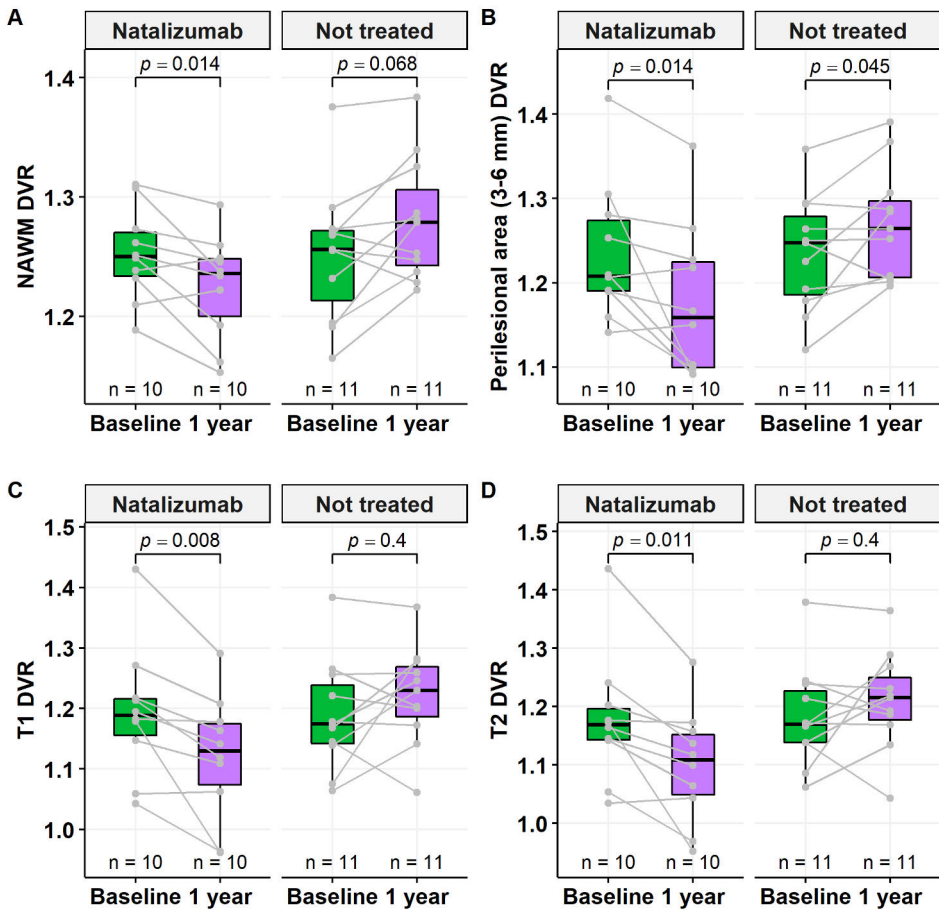


Figure 11. Boxplots of the ^{11}C -PK11195 distribution volume ratios (DVR) at baseline and at 1-year timepoint of untreated and natalizumab treated MS patients in the normal appearing white matter (NAWM) (A), 3- to 6mm perilesional area (B), T1-lesional area (C) and T2-lesional area (D). Modified from the original publication II.

The EDSS score was re-evaluated for the untreated group after an average follow-up of over 4 years. Higher baseline ^{11}C -PK11195 uptake in the NAWM and in the 3– to 6 mm perilesional area predicted disability progression using the EDSS score (Figure 12).

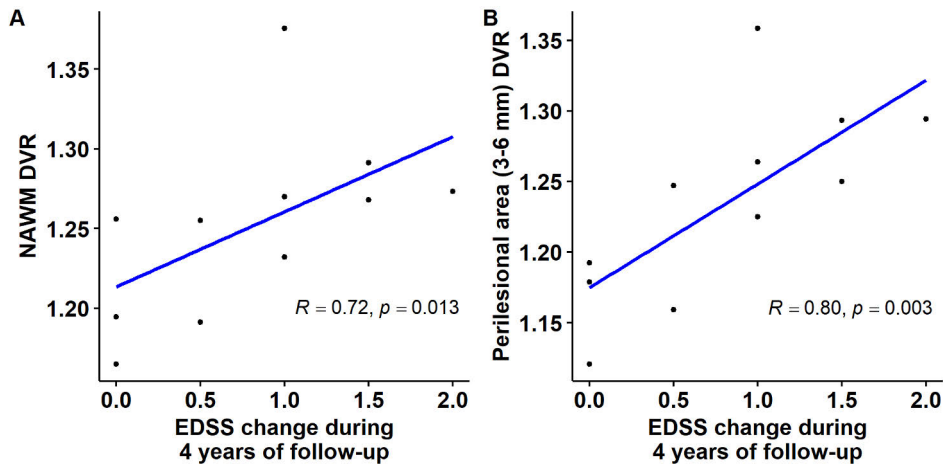


Figure 12. Scatterplots illustrating the association between the ^{11}C -PK11195 distribution volume ratios (DVR) in the normal appearing white matter (NAWM) (A) and in the 3 to 6 mm perilesional area (B) and Expanded Disability Status Scale (EDSS) score change during the 4-year follow-up of the untreated MS patient cohort. Modified from the original publication II.

5.3 Study III: Increased microglial activation predicts later disease progression independent of relapses during an average follow-up of over 4 years

In the baseline TSPO-PET imaging analysis, higher ^{11}C -PK11195 uptake was observed in the NAWM and in the thalamus among the MS patients ($n = 69$) compared to HCs ($n = 18$) (Figure 13), whereas in cortical GM no significant differences were found between the groups.

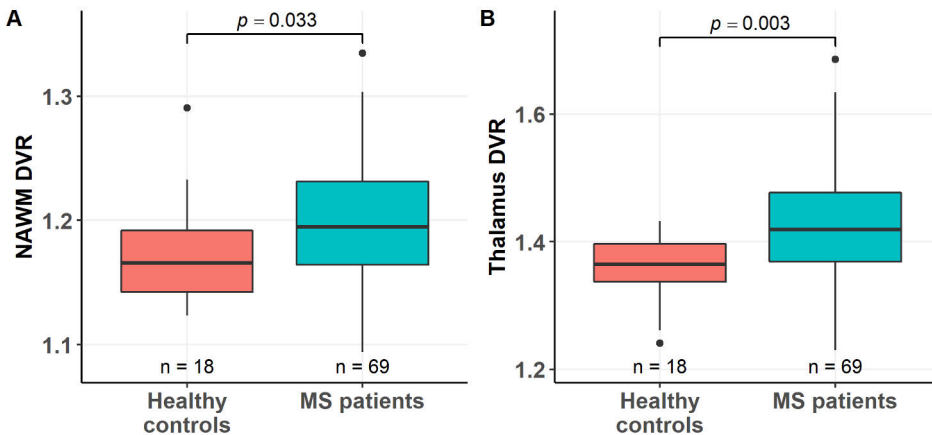


Figure 13. Boxplots of the ^{11}C -PK11195 distribution volume ratios (DVR) in the normal appearing white matter (NAWM) and thalamus of MS patients and healthy controls (HC) at baseline TSPO-PET imaging. Modified from the original publication III.

During an average of a 4.1-year follow-up, 20 (29%) patients experienced disease progression, whereas 49 (71%) patients remained clinically stable. The baseline ^{11}C -PK11195 uptake was significantly higher in the NAWM and in the perilesional NAWM in the patient group experiencing disease progression compared to the patient group clinically stable during the follow-up (Figure 14 A-B); however, in other brain areas, no significant differences were found between these subgroups. Altogether, 51 patients remained free of relapses during the follow-up. Of these, 11 patients experienced progression. The baseline ^{11}C -PK11195 uptake in the NAWM and in the 0– to 6mm perilesional area was significantly higher in the patient subgroup experiencing progression free of relapses compared to the respective ^{11}C -PK11195 brain uptake in the subgroup of 40 patients not experiencing progression or relapses during the follow-up (Figure 14 C–D). In other brain areas, no significant differences were found between these subgroups.

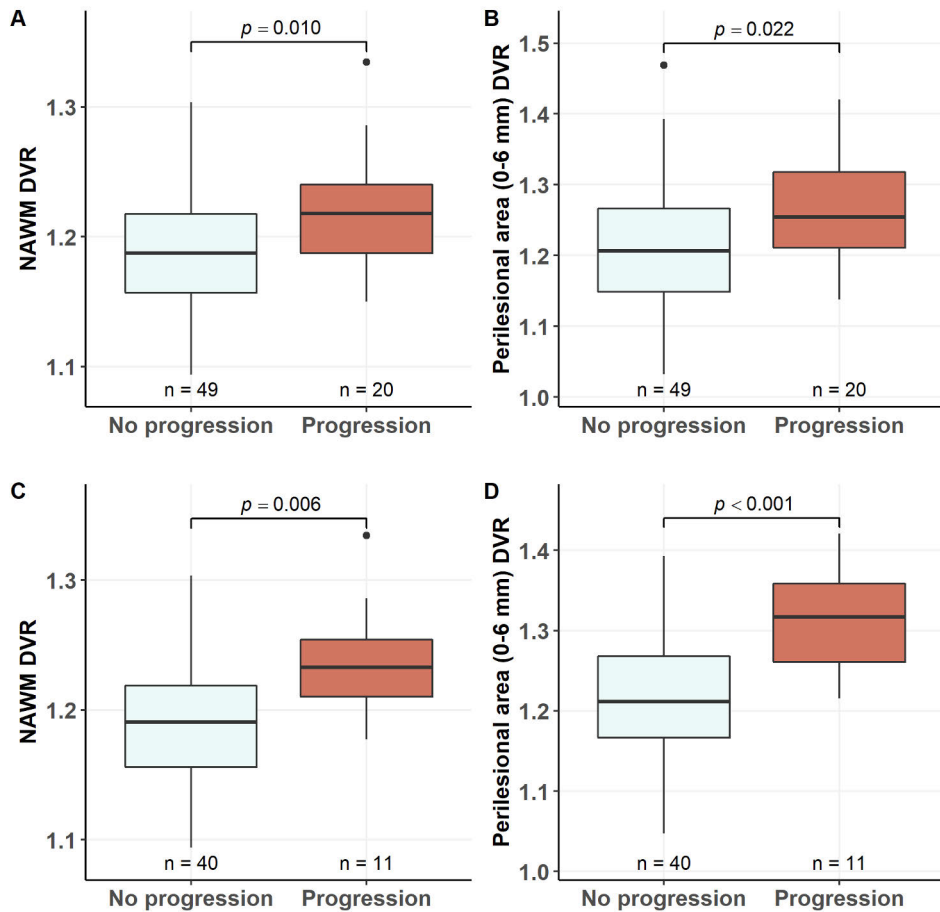


Figure 14. Boxplots of the baseline $^{11}\text{C-PK11195}$ distribution volume ratios (DVR) in the normal appearing white matter (NAWM) (A) and in the perilesional area (B) in MS patients with progression (n=20) and patients without progression (n=49) during an average follow-up of over 4 years. Respective DVR values in the NAWM (C) and in the perilesional area (D) in the MS patient group free of relapses (n=51) divided into subgroups of patients experiencing progression (n=11) and patients clinically stable (n=40) during an average follow-up of over 4 years. Modified from the original publication III.

In the baseline conventional MRI analysis, the T1 and T2 lesion load was greater in patients who experienced later disease progression (n=20), compared to those who did not progress (n=49) (Figure 15 A–B), whereas brain volumetric measurements in other brain regions did not correlate with later clinical progression. However, no significant differences were found between the patient group experiencing progression free of relapses (n=11) and the clinically stable patient group (n=40) during the follow-up in the baseline conventional MRI analysis (Figure 15 C–D).

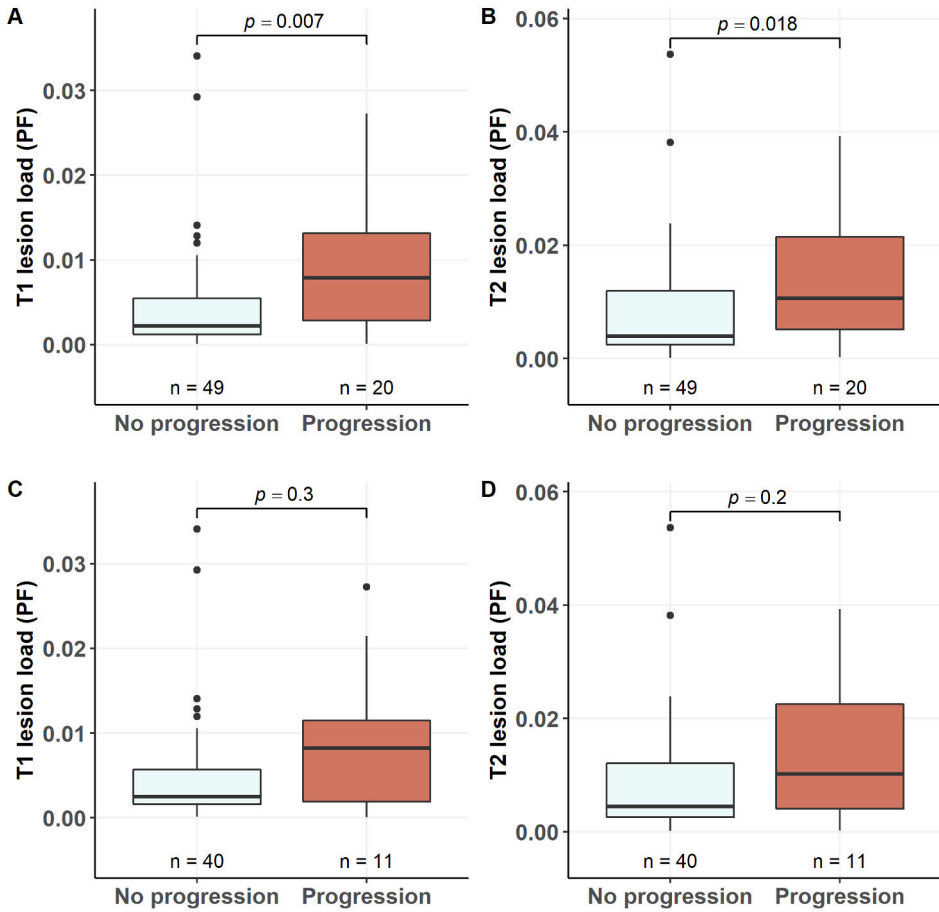


Figure 15. Boxplots of the baseline conventional MRI analysis of the T1 lesion load (A) and T2 lesion load (B) in MS patients with progression (n=20) and patients without progression (n=49) during an average follow-up of over 4 years. Respective T1 lesion load (C) and T2 lesion load (D) analysis in the MS patient group free of relapses (n=51) divided into subgroups of patients experiencing progression (n=11) and patients clinically stable (n=40) during an average follow-up of over 4 years. Modified from the original publication III.

A forward-type stepwise logistic regression model was used to determine the best variables predicting disease progression. In the entire MS patient group (n = 69), the following remained in the model as predictors: the EDSS at baseline, the ¹¹C-PK11195 uptake in the NAWM at baseline, the class of the DMT at baseline or at most 2 months before baseline, and the ARR during the follow-up. Higher baseline ¹¹C-PK11195 uptake in the NAWM was the strongest predictor of later progression (OR = 4.26), whereas high efficacy DMT (compared to no DMT) reduced substantially the odds of later disease progression (OR = 0.04) (Table 7). Additionally, a higher ARR during the follow-up increased the odds of later disease

progression (OR = 1.41) (Table 7). In the patient subgroup free of relapses, a higher baseline $^{11}\text{C-PK11195}$ uptake in the perilesional NAWM associated with later disease progression (OR = 4.57), whereas moderate efficacy DMT (compared to no DMT) reduced the odds of later disease progression (OR = 0.15) (Table 7). None of the conventional MRI parameters measured at baseline associated with later progression in any MS patient group when using the forward-type stepwise logistic regression model.

Table 7. The association between the baseline $^{11}\text{C-PK11195}$ distribution volume ratios (DVR) and later Expanded Disability Status Scale (EDSS) score progression during the follow-up period of over 4 years. A forward-type stepwise logistic regression model was used to define the best variables predicting disease progression. Testing was started with no variables in the model, each variable was then added separately and tested using the Akaike information criterion (AIC). The table presents the variables that improved the model fit to predict progression. Modified from the original publication III.

| | OR | p value |
|--|------|---------|
| All MS patients (n=69) | | |
| High EDSS at baseline | 1.39 | 0.102 |
| High ARR during follow-up | 1.41 | 0.012* |
| DMT (moderate efficacy) | 0.4 | 0.228 |
| DMT (high efficacy) | 0.04 | 0.038* |
| High DVR in NAWM | 4.26 | 0.048* |
| MS patients without relapses during the follow-up (n=51) | | |
| High DVR in the perilesional area | 4.57 | 0.013* |
| DMT (moderate efficacy) ^a | 0.15 | 0.044* |
| DMT (high efficacy) ^b | 0.52 | 0.616 |

Abbreviations: MS = multiple sclerosis; EDSS = Expanded Disability Status Scale; ARR = annual relapse rate; DMT = disease modifying therapy; DVR = distribution volume ratio; NAWM = normal appearing white matter; OR = odds ratio.

^a Class of the DMT at baseline or at most 2 months before: moderate efficacy DMT versus no DMT.

^b Class of the DMT at baseline or at most 2 months before: high efficacy DMT versus no DMT.

* Denotes statistically significant group difference at a level of $p < 0.05$.

The final logistic regression model predicted later progression in the entire MS patient group with 55% sensitivity and 90% specificity with an AUC value of 0.78, whereas in the patient group free of relapses during the follow-up the model predicted later progression with 55% sensitivity and 95% specificity with an AUC value of 0.75 (Figure 16).

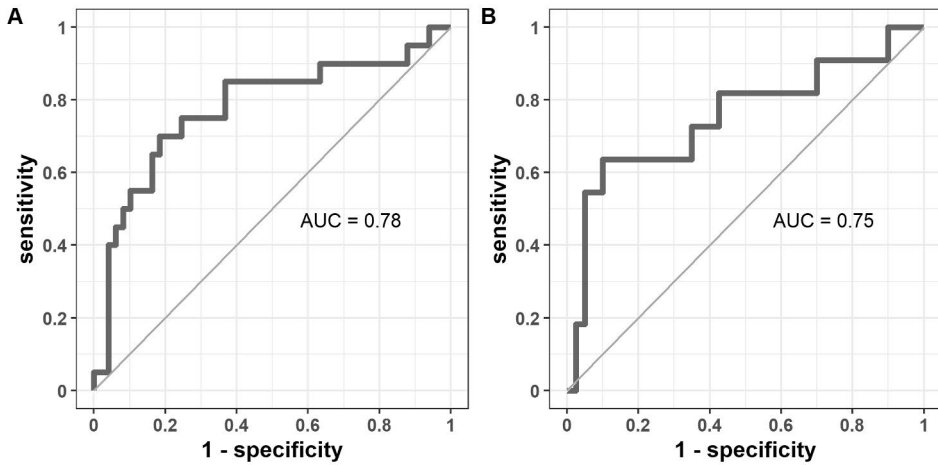


Figure 16. Receiver operating characteristic curves with an area under the curve (AUC) values. In the entire cohort (n=69) **(A)**, the final logistic regression model correctly predicted progression in 11/20 patients (sensitivity=55%) and no progression in 44/49 patients (specificity=90%) with an AUC value of 0.78. In the patient group free of relapses (n=51) **(B)**, the model correctly predicted progression in 6/11 patients (sensitivity=55%) and no progression in 38/40 patients (specificity=95%) with an AUC value of 0.75. Modified from the original publication III.

6 Discussion

To understand the biological processes that underlie disease progression and advance neurodegeneration could be the key element in obtaining more accurate tools to develop future treatments particularly targeted at progressive MS. The prognosis of MS is highly variable, from aggressive forms of MS to benign MS from the onset of the disease. Furthermore, the appearance of a smouldering form of MS with its clinical manifestation of PIRA already at the early phase of RRMS with an association to brain atrophy (B. A. C. Cree et al., 2019) highlights the hypothesis, that the same biological process underlying SPMS plausible begins much earlier in the disease spectrum than generally recognised. The transition from RRMS to SPMS is clinically insidious and pathologically associates with the activation of the CNS-resident microglial cells (Mayo, Quintana, & Weiner, 2012). Since conventional MRI fails to detect microglial activity, more sensitive methods to monitor this progressive MS related diffuse pathology of the CNS are needed. Here, TSPO-PET and novel MRI imaging modalities provide a method to detect microglial activation *in vivo*.

In this thesis, by using *in vivo* TSPO-PET imaging with TSPO binding ¹¹C-PK11195 radioligand,

1. The effect of DMTs on microglial activation in MS brain *in vivo* was evaluated (Study **I** and **II**)
2. The possible predictive role of microglial activation in later MS disease progression was examined (Study **II** and **III**)

6.1 Interpretation of the study results and methodological considerations

6.1.1 The effect of DMTs on TSPO uptake

There are high expectations of the usage of TSPO-PET as an imaging tool to measure the effect of DMTs in MS in the future. The serial TSPO-PET studies (Study **I** and **II**) presented in this thesis are among the first to evaluate the effect of DMTs on TSPO expression. As reviewed earlier, previous longitudinal TSPO-PET studies have shown varying results with reduced ^{11}C -PK11195 uptake in both cortical GM and cerebral WM after glatimer acetate treatment (Ratchford et al., 2012) and reduced ^{11}C -PK11195 uptake in focal inflammatory lesions after natalizumab treatment (Kaunzner et al., 2017).

Study **I** presented decreased ^{11}C -PK11195 uptake in the combined T2 lesion area after 6-months of treatment with fingolimod, with no significant changes in other brain areas. This result is consistent with previous larger studies using MRI imaging as an outcome measure with focal inflammatory activity reduction after initiation of fingolimod (Kappos et al., 2006). Our interpretation of Study **I** was that fingolimod treatment reduced the ^{11}C -PK11195 uptake in the lesion area presumably by preventing leukocyte trafficking from the periphery.

However, there are factors supporting the possible direct effect of fingolimod within the CNS of patients with MS. First, fingolimod is a lipophilic molecule structure and possibly crosses the intact BBB into the CNS to some extent despite its large molecule size. Based on a rat experimental autoimmune encephalomyelitis (EAE) model, pharmacologically relevant concentrations were found in the CNS of rats after oral administration of fingolimod (Foster et al., 2007). Second, microglia, oligodendrocytes, and astrocytes have demonstrated the capability of expressing sphingosine 1-phosphate, the target receptors of fingolimod (Chun & Hartung, 2010). Third, astrogliosis and demyelination have shown to be mediated by sphingosine 1-phosphate signalling in the CNS (Choi et al., 2011).

The findings presented in the EAE models raise hopes that fingolimod can have a direct effect to suppress the compartmentalized neuroinflammation in the CNS in addition to the peripheral effect of the drug to suppress the adaptive immune response. However, extrapolating the EAE model data to humans should be done with extra caution keeping in mind that the TSPO biology in human brain *in vivo* can greatly differ from the rat EAE models.

In the Study **I**, the ^{11}C -PK11195 uptake increased slightly in 5 of the 7 patients in the NAWM and in 6 of the 7 patients in the cortical GM after 2 months of treatment (Figure 9). These findings could be interpreted to reflect the still increasing inflammatory activity originating from the adaptive immune system after the

previous DMT cessation. Consistent with this, the patients also demonstrated a slight increase in T2 lesion load at the respective time point.

Moreover, in a rat EAE model, fingolimod reduced TSPO expression in the perilesional area with MS-like lesions monitored with the 2nd generation TSPO radioligand ¹⁸F-GE180 *in vivo* and this was confirmed with *ex vivo* autoradiography and immunohistochemistry (Airas et al., 2015). Regrettably, the perilesional area was not included as a ROI in Study I.

It is of note, that as a follow-up study with the same cohort used in Study I, we investigated the effect of 6-month fingolimod treatment on the integrity of the entire and segmented NAWM with diffusion tensor imaging (DTI) (Saraste et al., 2021). This is a nonconventional MRI technique that can be used to assess microstructural alterations in myelin and axons. Contrary to Study I, changes in the cingulate NAWM were observed with increased mean values for fractional anisotropy (FA) and decreased mean values for radial diffusivity (RD) suggesting microstructural fingolimod-induced improvements in the cingulate NAWM (Saraste et al., 2021). Although a correlation between the change in the integrity and ¹¹C-PK11195 uptake in the NAWM was not detected with the fingolimod treated patients in the study by Saraste et al., the previous cross-sectional study of our group highlighted a co-occurrence of microglial activity and microstructural WM damage with a correlation to clinical accumulation (Bezukladova et al., 2020).

Study II presented reduced ¹¹C-PK11195 uptake in the NAWM, in focal inflammatory lesions and in the perilesional area after a 12-month treatment with natalizumab, whereas increased ¹¹C-PK11195 uptake was observed in the untreated MS control group in the perilesional area in addition to a trend toward an increase in the NAWM during the 12-month follow-up (Figure 11).

As reviewed earlier, several neuropathological post mortem studies (Frischer et al., 2009; Kutzelnigg et al., 2005; Lassmann et al., 2012; Moll et al., 2011) and cross-sectional TSPO-PET imaging studies (Colasanti et al., 2014; Giannetti et al., 2015; Rissanen et al., 2018; Versijpt et al., 2005) have demonstrated a correlation between increased microglial activity in the NAWM and/or in the perilesional areas with disease accumulation. Therefore, finding and developing treatments that aim to decrease microglial activity in brain areas relevant for MS disease progression are of great interest.

Study II was the first study to report reduction in TSPO uptake after initiation of DMT both in the NAWM and at the rim of chronic active lesions; this suggests that the diffuse pathology associated with progressive MS can be therapeutically targeted using highly active anti-inflammatory medication. Due to the assumed restricted entering of natalizumab into the CNS through an intact BBB as reviewed earlier, we interpret that the reduced microglial activity after the initiation of natalizumab is mainly caused by the efficient blocking of inflammatory cell entry from the

periphery into the CNS rather than by a direct effect of natalizumab on the resident microglial cell population within the CNS.

The result concerning the reduction in ^{11}C -PK11195 uptake in focal inflammatory lesions after natalizumab treatment is in line with the previous study evaluating the effect of natalizumab on the ^{11}C -PK11195 uptake (Kaunzner et al., 2017). However, contrary to Study II, no change in the ^{11}C -PK11195 uptake in the NAWM was detected after natalizumab treatment, possibly due to the shorter follow-up time used compared to Study II (6 months vs 12 months) (Kaunzner et al., 2017). Similarly, Study I with a 6-month follow-up failed to detect reduced ^{11}C -PK11195 uptake in the NAWM after initiation of fingolimod. The median EDSS score remained unaltered with the natalizumab-treated during the 12-month follow-up in Study II. As reviewed earlier, Study II was a sub study to a phase 3 double-blind placebo-controlled randomised study (ASCEND), in which natalizumab treatment did not reduce sustained disability progression unrelated to relapses in a SPMS cohort (Kapoor et al., 2018). This progression was measured with a multicomponent endpoint including the EDSS, Timed 25-Foot Walk and 9HPT (Kapoor et al., 2018). Nevertheless, when the endpoints were analysed separately, natalizumab treatment did reduce a worsening of hand function, as measured by the 9HPT. This, in addition to the findings in Study II of reduced microglial activity following natalizumab treatment, highlights the plausible effect of natalizumab treatment even in an advanced MS patient cohort. However, the natalizumab-treated patient cohort in Study II was heterogenous (6 SPMS and 4 RRMS patients) and therefore the results cannot be directly incorporated to present a pure progressive MS patient cohort. In addition, we did not include the Timed 25-Foot Walk and 9HPT in Study II, which was a clear limitation.

6.1.2 The longitudinal change in TSPO uptake in untreated patients with progressive MS

For all I know, Study II was the first study to longitudinally evaluate the natural evolution of MS disease pathology in terms of microglial activity. The study was conducted with a prospectively followed untreated MS control cohort of eleven patients mostly presenting with a secondary progressive disease type. Increased ^{11}C -PK11195 uptake in the perilesional area in addition to a trend toward increase in the NAWM was detected during the 12-month follow-up (Figure 11). No significant changes in other brain areas were detected during the 12-month follow-up. This result suggests that microglial activation in brain areas relevant for progression can increase over time in patients with progressive MS and that this could be a key element in the pathogenesis of the insidious disease progression. This result is consistent with a recent study, consisting of 14 progressive MS patients that similarly

demonstrated increased ^{11}C -PK11195 uptake in the NAWM during a 12-month follow-up (Kang et al., 2021). However, in contrast to Study **II**, increased ^{11}C -PK11195 uptake was also detected in the cortical GM, the putamen and the thalamus, whereas perilesional areas were not evaluated (Kang et al., 2021). The discrepancy between the study results of the cortical GM, the putamen and the thalamus could possibly originate from the relatively low number of study participants, the rather short follow-up time, the difference in the demographic parameters of the study cohorts, in addition to the several confounding factors that can influence the evaluation of the ^{11}C -PK11195 uptake in cortical GM, as explained in Chapter **6.1.4**.

6.1.3 TSPO uptake as a predictor of MS progression

Higher baseline ^{11}C -PK11195 uptake in the NAWM and in the perilesional area predicted disability progression (measured with the EDSS) in the untreated MS patient cohort of eleven patients in Study **II** during follow-ups averaging over 4-years (Figure 12). This observation was, to my knowledge, the first to demonstrate that higher TSPO uptake predicts greater clinical disability. Inspired by this finding, we further evaluated the predictive value of baseline ^{11}C -PK11195 uptake on later disease accumulation in a larger MS cohort.

Study **III**, consisting of a relatively large cohort of 69 MS patients (45 RRMS, 24 SPMS), demonstrated that baseline ^{11}C -PK11195 uptake both in the NAWM and in the perilesional area was predictive of disease progression at 4 years (Figure 14). Moreover, increased baseline ^{11}C -PK11195 uptake both in the NAWM and in the perilesional area predicted later disability progression independent of relapse activity at 4 years (Figure 14). A correlation between the baseline ^{11}C -PK11195 uptake and later disease progression was not found in other brain areas investigated. The final logistic regression model (with the perilesional area as the strongest predictor used in the model) predicted later progression in the patient group free of relapses with 55% sensitivity and 95% specificity (Figure 16). The results of Study **III** strongly suggest that increased diffuse neuroinflammation targeted by TSPO-PET imaging is a critical pathological element contributing to the diffuse neuroaxonal damage and predicts more rapid development of the insidious progression independent of relapse activity. The strength of the study is its novel design with no comparative studies yet available. As reviewed earlier, higher TSPO uptake in the NAWM in a cohort of CIS subjects correlated with a higher risk of developing MS at 2 years. This highlights the plausible role of microglial activation on MS disease evolution already at the earliest stages of the disease (Giannetti et al., 2015). The findings of Study **III** are consistent with post mortem neuropathological studies, that highlight a correlation between disease accumulation and microglial activity in the NAWM and perilesional area (Frischer et al., 2009; Kuhlmann et al., 2017; Kutzelnigg et al., 2005; Lassmann

et al., 2012; Moll et al., 2011) in brain regions associated with later disease progression confirmed in Study **III**.

6.1.4 Methodological considerations of the baseline results

The baseline results of the increased ^{11}C -PK11195 uptake in the NAWM and the thalamus (Studies **I–III**) of MS patients compared to HCs are in line with previous studies (Datta, Colasanti, Kalk, et al., 2017; Datta, Colasanti, Rabiner, et al., 2017; Giannetti et al., 2015; Herranz et al., 2016; Kang et al., 2021; Politis et al., 2012; Rissanen et al., 2014). Furthermore, the correlation between increased ^{11}C -PK11195 uptake in the NAWM and in the perilesional area with disease accumulation presented in Study **III** are also in line with previous studies (Debruyne et al., 2003; Herranz et al., 2016; Rissanen et al., 2018). This indicates that the cohorts used in Studies **I–III** likely represent reliable average real life MS cohorts and that the baseline imaging study results can be replicable, which is counted as a strength of these studies.

However, significant differences in the baseline cortical GM ^{11}C -PK11195 uptake between the MS cohorts and HCs in Studies **I–III** were not detected. Previous PET studies addressing TSPO expression in the cortical GM have yielded variable results. While some studies have shown higher cortical GM TSPO radioligand binding in MS patients compared to HCs (Herranz et al., 2016; Politis et al., 2012; Singhal et al., 2019), other studies have failed to find differences in cortical TSPO-PET signal between MS patients and controls (Kaunzner et al., 2017; Misin et al., 2022). The various results regarding the TSPO uptake in cortical GM in different studies can originate from several confounding factors. The cortical GM is a thin layer more abundantly vascularised than WM (Hase et al., 2019) and is anatomically located close to the large meningeal blood vessels. This can lead to false TSPO signal affected from the endothelial TSPO expression (Cosenza-Nashat et al., 2009) as well as from the plasma protein TSPO expression within the bloodstream (Chen & Guilarte, 2008). Furthermore, the lower signal-to-noise ratio of the first-generation ^{11}C -PK11195 radioligand compared to later-generation ligands might also have an impact on the varying results in the studies for the detected TSPO expression in cortical GM (Ching et al., 2012).

6.1.5 TSPO-PET as a prognostic tool of disease progression

TSPO-PET imaging holds promise as an imaging biomarker for identifying those MS patients with the greatest likelihood of progression. The perilesional area especially is an intriguing ROI for capturing pathological signs to predict later

disease progression as reported in Study **II** and **III**. However, the interpretation of the results in Study **II** and **III** is hampered due to the lack of phenotyping of the lesions. The perilesional area in Study **II** and **III** is evaluated as a combined area surrounding all lesions, including the perilesional areas of chronic inactive lesions with none/negligible microglial activity and the perilesional areas of chronic active lesions with notable microglial activity.

To increase the accuracy of future PET studies corresponding more precisely to the underlying biological process in the MS brain, our group developed an automated TSPO-PET analysis method for comprehensive phenotyping of individual chronic lesions based on their microglial activity status *in vivo* (Nylund et al., 2022). Based on this novel approach, an association between a higher proportion of lesions with microglial activity at the lesion rim and increased disability measured by EDSS was demonstrated in a large cross-sectional setting consisting of 1510 white matter T1-hypointense lesions from 91 MS patients (Nylund et al., 2022). Importantly, the lesion distribution and disease duration in the Nylund et.al. study was largely consistent with the seminal neuropathology work by Frischer *et al.* (Frischer et al., 2015).

The lesion phenotyping approach was further used in the recently published large prospective study by our group, where ¹¹C-PK11195 TSPO-PET-imaging in 82 MS patients was performed with an EDSS follow-up of 5 years (Polvinen et al., 2023). Disability progression was detected in 21 patients (26%) during the follow-up with a significantly higher proportion of rim-active lesions and significantly lower proportion of inactive lesions compared to the patient group free of progression. Furthermore, the results were similar in the patient group free of relapses (n=60). By using the stepwise logistic regression modelling (similarly used in Study **III**), to identify the most important clinical and imaging-related predictors of later clinical disease progression, we showed that a high proportion of chronic active (>10% rim-active lesions) and a low proportion of chronic inactive lesions (≤50% inactive lesions) create a remarkably strong combined predictor for later disease progression in MS with an OR of 27 in the entire cohort and an OR of 35 in the group free of relapses. To summarise, those patients having a combination of abundant chronic active lesions and a low number of chronic inactive lesions, were more likely to experience later progression during the 5 years of follow-up; whereas patients with a small quantity of chronic active lesions were less likely to progress (Polvinen et al., 2023).

In addition, another recent prospective imaging study of our group consisting of 66 MS patients and 18 HCs demonstrated that patients with disability progression during the 3-year follow-up had significantly higher TSPO binding in the thalamus at baseline compared to non-progressed patients (Misin et al., 2022). Using a stepwise logistic regression model (similarly used in Study **III**), the final model

predicted disability progression with a 53% sensitivity and a 94% specificity suggesting that TSPO-PET measurable microglial activation in the thalamus has potential in predicting short-term disability progression in MS (Misin et al., 2022). Notably, a recently published study of our group demonstrated, that a higher T2 lesion burden and an elevated immunoglobulin G (IgG) index at the time of MS diagnosis associate with later microglial activation in the NAWM, the perilesional NAWM and the thalamus, highlighting the significant role for early inflammatory events in the development of later progression-related pathology (Laaksonen et al., 2023).

Due to the limited spatial resolution (~2.5 mm) of PET imaging, the TSPO-signal detected in the perilesional area can be affected by spill-in effects from the lesion that complicates the interpretation of the findings. However, in the context of progressive MS, Study **II** and **III** highlights the importance of the perilesional area TSPO-signal for a worsening of disability and the findings are in line with other previous TSPO-PET studies (Lehto, Sucksdorff, et al., 2023; Rissanen et al., 2018), iron-rim detecting MRI studies (Absinta et al., 2019; Dal-Bianco et al., 2021) and neuropathological studies (Frischer et al., 2015; Kuhlmann et al., 2017; Lassmann et al., 2012; Popescu & Lucchinetti, 2012). These studies place the microglia at the chronic lesion edge. No solid consensus of the width of the perilesional area exists so far, thus varying perilesional areas have been used in previous and recently published TSPO-PET studies (Lehto, Nylund, et al., 2023; Lehto, Sucksdorff, et al., 2023; Nylund et al., 2022; Rissanen et al., 2018). A distance of 3 to 6 mm to the lesion border was used as an ROI in Study **II**, whereas the perilesional ROI in Study **III** was created by dilating the corresponding T1- lesion ROI mask image by six voxels and then removing the core from the resulting image respectively. Future studies will clarify which definition/delineation of the lesion rim will provide the best sensitivity and specificity to capture the correlation with disease accumulation and to predict progression.

In a recently published study of our group, where we evaluated the degree of the brain microglial activation in disease stable RRMS patients compared to an age-matched HC population, a statistically significant difference was observed with the previously described method of detecting clusters of active voxels (Nylund et al., 2022), but not with the method of quantification of radioligand binding using DVR in various ROIs (the method used in studies **I**, **II** and **III**) (Lehto, Nylund, et al., 2023). Hence, detection of clusters of active voxels might provide a more sensitive method in capturing microglial activation compared to the quantification of radioligand binding using DVR in various ROIs, particularly in patients with less active MS where the overall DVR is usually low.

Identifying patients with an elevated risk of highly active MS disease is important, because neuroinflammation in early MS can potentially be controlled with

effective DMTs. As reviewed earlier, there is increasing evidence of the importance of early high efficacy treatment to prevent or postpone accumulation of disability and disease progression (Bergamaschi et al., 2016; Brown et al., 2019; Harding et al., 2019; Kavaliunas et al., 2017). Therefore, novel biomarkers incorporated to clinical work are urgently needed, to identify already at an early stage of the disease those patients with the highest risk of later disease progression. These patients presumably benefit the most from an early onset of high-efficacy DMTs. Furthermore, during the course of the disease, clinical evaluation of disease progression can be challenging. Thus, new biomarkers are needed for evaluation of disease progression to identify patients who are at risk of conversion to progressive disease.

Microglial activation is a critical pathological element that seems to already contribute to disease progression at disease onset (Giannetti et al., 2015) and holds promise as a predictive biomarker of disease progression throughout the disease course as highlighted in Study **III**. However, the appearance of clinical progression in the form of PIRA already in early RRMS, despite the usage of highly effective DMT, implies that a gradual compartmentalised pathological process in the CNS without an eminent relation to focal inflammation plays a significant role in MS already from the onset of the disease. This gradual pathological process in the CNS can possibly be driven by the increased microglial activation (as suggested in Study **III**). Consequently, developing and implementing treatment options to reduce the microglial activation might be a key element in complementing the unmet needs in the treatment field of progressive MS.

6.2 Limitations

The complex nature of the technique of nuclear medicine and the considerable costs make TSPO-PET imaging a demanding technology, and limiting its wider use globally. To follow the general ethical principles of good clinical practice, the number of study subjects in the PET studies should be kept as low as possible, in order to limit the amount of radiation exposure to the study participants. The financial costs of PET studies are substantially high (the listing price as of May 2023 at Turku PET Centre for a single ^{11}C -PK11195 TSPO-PET imaging is 4315 euros). Ethical aspects and high costs restrict the sample sizes, and this can lead to underpowered studies and to results that cannot be replicated.

PET quantification relies on models that are only approximations of the underlying processes. Moreover, the utilization of PET kinetic models is based on estimates, that can be oversimplified. Consequently, the DVR estimates may possibly not entirely correspond to the underlying biological processes at cellular level. Considering, that MS influences the whole brain, the DVR estimates might be

biased due to specific binding in the reference region. Moreover, ^{11}C -PK11195 has a rather modest penetration through the intact BBB leading to a lower brain uptake. Importantly, the ^{11}C -PK11195 radioligand signal in Studies **I–III** does not entirely derive from the activated microglial cells. As previously reviewed, ^{11}C -PK11195 also binds to astrocytes and other TSPO expressing structures in the brain, such as endothelial and smooth muscle cells in the brain vasculature, decreasing the signal-to-noise ratio of the ligand. In addition, to avoid potential artefacts, infratentorial lesions were excluded from the studies presented in this thesis. Infratentorial lesions can potentially cause more severe disability than supratentorial lesions, thus weakening the interpretation of the correlation between the microglial activity of the analysed supratentorial lesions and disability. Moreover, patient head movements in the scanning may induce artefacts to the imaging data and some distortion may also occur in the PET and MRI image co-registration. All the lesion masks were checked and manually corrected (if needed) slice by slice, which could lead to inter- and intra-rater variability. Even though all the above-mentioned matters were observed throughout the study process to minimise the errors, they should be taken into account when interpreting the results.

As presented in Study **I** and **II**, DMTs have an effect on the microglial activity. For ethical reasons, PET studies should not postpone the initiation of DMTs, if clinically indicated. Therefore, while treatment-naïve patients can rarely be recruited, previous or ongoing DMTs can potentially interfere with the interpretation of the total microglial activity detected. This potential bias was taken into account as a confounding factor in the statistical analysis in Studies **I–III**.

In addition to the general methodological limitations described above, the highly heterogenic procedures in TSPO-PET studies performed in different PET Centres throughout the world make their direct comparison challenging. The methodology in analysing TSPO-PET imaging signal can vary considerably between different imaging centres, with different reference regions being chosen. For example, in some studies the reference region used has been the same area as the ROI in other studies (Debruyne et al., 2003; Politis et al., 2012; Versijpt et al., 2005). Moreover, no consensus regarding the best TSPO radioligand for detecting the TSPO uptake has yet been agreed between the different PET centres throughout the world, thus leading to the use of several different TSPO-binding ligands, which has hampered the comparison between the studies.

Considering this, it will be of great importance to harmonise and validate the methodology used in TSPO-PET imaging and to implement multi-centre studies with larger patient cohorts in the future to achieve the maximal benefit of this potential imaging method.

6.3 Clinical implications and future directions

Despite advanced treatment options with the currently available therapies being initiated at an early stage of the disease, many patients with RRMS continue to accumulate disability over time unrelated to relapses (Kappos et al., 2020; Tilling et al., 2016). This represents a significant unmet medical need. As referred to earlier, RRMS is traditionally believed to start in the peripheral tissues by the adaptive immune response of T- and B-cells. However, recent studies have questioned this theory highlighting that already in the very early stage of the disease even before any initial clinical symptoms have manifested the smouldering disease component is present, together with the acute focal inflammation component (Giovannoni et al., 2022). This smouldering disease component, referred to as smouldering MS in the present nomenclature, is characterised by the presence of chronic active lesions and activated microglia (Giovannoni et al., 2022; Guerrero & Sicotte, 2020). Neuropathological, PET and MRI studies have increased our understanding of this insidious smouldering process and its underlying mechanisms of neuroaxonal loss in the pathogenesis of progressive MS. Identifying the chronic inflammation in the CNS *in vivo* with the usage of non-invasive imaging methods, can possibly be the basis of future efforts for more individualised treatments. It can also possibly provide a key element for stratification of suitable patients participating in clinical trials of treatments targeting the biology behind progressive MS.

As demonstrated in this thesis, the detection of microglial activity in the MS brain using TSPO-PET imaging provides a potential method to monitor disease accumulation, to predict disease progression and to measure treatment response. However, there are still great challenges to be solved before TSPO-PET can be more widely used in clinical work or as a surrogate marker in therapeutic studies.

As reviewed earlier, the DMT selection to treat progressive forms of MS is at present limited with only ocrelizumab to PPMS and siponimod to SPMS with a rather modest effect (Kappos et al., 2018; Montalban et al., 2017). Although the DMTs presently available have been shown to decrease the microglial activation to some degree, as presented in the Studies **I** and **II**, the current DMTs primarily effect the peripheral adaptive immunity. This may be due to the fact that they are large proteins in size and likely do not penetrate through an intact BBB into the CNS to any significant degree. Hence, the positive study results in reducing the microglial activation in Studies **I** and **II** are presumable mostly due to efficient blocking of inflammatory cell entry from the periphery into the CNS rather than direct effect of fingolimod (Study **I**) or natalizumab (Study **II**) on the resident innate immune cell population within the CNS. Therefore, considering the compartmentalised processes in the CNS driving the pathology trapped behind a mainly intact BBB, the continual failures or modest results in studies evaluating the effect of the DMTs presently available for treating progressive forms of MS might not come as a surprise.

Consequently, future treatment approaches are urgently warranted that combine an anti-inflammatory drug for the prevention of focal inflammatory activity and relapses together with a compound penetrating into the CNS with a direct effect on microglial activity.

Currently, no treatments that directly target microglial activity exist in clinical use, but such treatments could potentially prevent the neuro-axonal damage and disease progression. In this regard, the CNS-penetrant inhibitors of Bruton's tyrosine kinase (BTK) hold great promise as a tool to treat MS patients in the future. BTK is an intracellular enzyme involved in regulating the maturation, proliferation, survival and activation of both B cells and myeloid cells including microglia meaning that BTK inhibitors have the potential to target both the adaptive immune system and the innate immune system. At present (as of September 2023), there are 17 phase 2 or 3 ongoing studies evaluating the effect of BTK inhibitors both for treating relapsing-remitting and progressive forms of MS. Importantly, recent studies with HCs and patients with RRMS have shown that BTK inhibitors are capable of penetrating the BBB into the CSF at bioactive levels (Owens et al., 2022). Furthermore, inhibition of BTK in *ex vivo/in vivo* experimental mice models favoured remyelination suggesting BTK inhibitors could hold promise as a therapeutic tool for promoting myelin repair (Martin et al., 2020). Consequently, a shift from a pro-inflammatory to a pro-remyelinating phenotype of CNS resident microglia can be a key element in controlling smouldering MS.

Detection of microglial activity in the MS brain using TSPO-PET imaging has a potential for evaluating MS pathology *in vivo* and has increased our understanding of MS pathogenesis. TSPO-PET holds much potential as an imaging biomarker to provide alternative methods in detecting signs correlating to future disease accumulation, as presented in Study III. The potential ability to predict which patients have the greatest likelihood of experiencing disease accumulation in the near future is a highly attractive prospect and opens new vistas for treatment trials with novel treatments aiming to slow down/prevent future disease progression. Furthermore, TSPO-PET imaging for patient cohorts with TSPO-rim-active lesions would additionally improve the odds of therapeutic success in treatment trials of the progressive disease. TSPO-PET imaging has already been used as an outcome measure in treatment trials of neurological diseases (NCT02481674, NCT04066244) but for treating MS, to the best of my knowledge, no such treatment trials has yet been applied (as of September 2023).

Apart from clinical treatment trials, TSPO-PET imaging could also enable more individualised care in clinical settings in order to provide an effective treatment already at an early stage of the disease for those patients with the greatest likelihood of progression. On the other hand, considering the high specificity of TSPO-PET to predict future disease progression as demonstrated in Study III, TSPO-PET imaging

could support the decision to lighten/halt the treatment of a carefully chosen patient group, for example, patients with a stable disease for many years.

Understanding individual differences in disability accrual and the pathology driving such an accrual improves the odds of the successful development of new treatments for progressive MS and can offer more individualised care. In this respect, TSPO-PET imaging holds promise as a potential additional surrogate marker. To harmonise and validate the methodology and to allow multi-centre studies to be performed, the present challenges of TSPO-PET imaging can be diminished, to maximise the benefits of this potential imaging modality in the field of MS as well as in the field of numerous other neurological conditions. Nevertheless, it remains unclear how TSPO-PET imaging and MRI-based iron rim identification methods perform when compared head-to-head on a larger scale and whether their complimentary use will improve the sensitivity of predicting MS progression. The results of ongoing multi-modality serial TSPO-PET/MRI imaging studies evaluating the effect of DMTs on iron accumulation and TSPO-uptake on the rim of chronic active lesions will shed light on these questions.

7 Summary/Conclusions

The purpose of this thesis was 1) to evaluate the effect of fingolimod and natalizumab treatments on microglial activation in MS patients using serial *in vivo* TSPO-PET imaging and ^{11}C -PK11195 radioligand, 2) to examine the possible predictive role of microglial activation in later MS disease progression using *in vivo* TSPO-PET imaging and ^{11}C -PK11195 radioligand. Based on the results presented in this thesis, the following conclusions can be deduced:

- I** Fingolimod treatment reduces microglial activation at the site of focal inflammatory lesions. *In vivo* TSPO-PET imaging can be used as a tool to assess longitudinal changes in microglial activation and therefore opens new vistas for designing future therapeutic studies in MS, that use the evaluation of microglial activation as an imaging outcome measure.
- II** Natalizumab treatment reduces microglial activation behind an intact BBB in the NAWM and at the rim of chronic lesions, in brain areas relevant for MS disease progression. *In vivo* TSPO-PET imaging holds promise as a surrogate outcome measure in studies of progressive MS and can be used as a tool in designing future therapeutic studies in progressive MS.
- III** Higher microglial activation in brain areas relevant for MS disease progression measured with *in vivo* TSPO-PET imaging and ^{11}C -PK11195 radioligand correlate with later disability. This study gives proof of concept that microglial activation is an undesired phenomenon. TSPO-PET, detecting microglial activation holds promise as a biomarker predicting future disease accumulation in MS.

Acknowledgements

This thesis project was conducted in the Turku PET Centre during the years 2013–2023.

First, I would like to express my gratitude to all my supervisors, Professor Laura Airas, Docent Eero Rissanen and Professor Juha Rinne. Laura's genuine enthusiasm for research combined with her social skills in networking and her creative mind in novel ideas in the neuroimmunology field is beyond comparison. Juha's broad knowledge of clinical neuroimaging and neurological research has been of great value in helping me pushing this project forward. Eero's role as a close supervisor in teaching PET imaging and analysing the data has been irreplaceable. I would also like to thank my supervisors for the patience throughout this process. Good things will come in time, although sometimes it can take over a decade.

I am grateful to the former and current Heads of Department of Clinical Neurosciences at the University of Turku, Professor Risto O. Roine and Professor Jaakko Rinne, for providing the opportunity to combine clinical work with research.

The director of Turku PET Centre, Professor and musician Juhani Knuuti, is thanked for giving me the opportunity to carry out this project in such a great facilities. Also, I would like to thank all the Turku PET Centre personnel that have participated in collecting the data of the studies presented in this thesis. I would like to give special thanks to the always so hard-working and down-to-earth Minna Aatsinki, with whom I have spent hundreds of hours collecting imaging data throughout the years.

I would like to thank Docent Johanna Krüger and Professor Jukka Peltola for their constructive and valuable comments during the revision process of this thesis. I would also like to thank Elizabeth Nyman for the skilled English revision of this thesis.

I have had the privilege of working with experienced and competent co-authors and other members of the Airas group while preparing the manuscripts of this thesis. Jouni Tuisku, Salla Nuutinen, Teemu Paavilainen, Johanna Rokka, Markus Matilainen, Anna Vuorimaa, Sarah Smith, Joonas Keitilä, Riitta Parkkola, Marjo Nylund, Eero Polvinen, Eveliina Honkonen and Maija Saraste. Markus and Jouni, your expertise in modelling and analysing the PET data and contribution in the

statistics have been invaluable. Marjo, Eveliina and Maija, I am grateful for your expertise and the assistance in technical issues you all have offered me throughout the years. Above all, you are all very warm-hearted persons and easy to get along with.

I wish to warmly thank all the colleagues, with whom I have had the pleasure to enjoy the clinical work in Jyväskylä and in Turku. I am grateful to the team at the Department of Neurology in the Central Hospital of Central Finland including Taneli Sarasoja, Jouni Ranua, Sari Avikainen and Minna Hälinen. You all warmly welcomed me to neurology and influenced me a lot in the decision to continue in the field. During our Jyväskylä time me and my wife had also the privilege getting acquainted with Jussi and Laura Joukainen, which we are grateful for. I also wish to acknowledge the enjoyable group of colleagues and friends at the Neurocenter at Turku University Hospital for creating a fun and warm atmosphere at work. A special mention goes to my present boss Manu Jokela for maintaining a good team-spirit at work. I also warmly thank my colleagues at Åbolands for maintaining a warm atmosphere and particularly Reijo Grönfors for making it possible for me to work at Åbolands. I also warmly thank Antti Palomäki for helping me with technical issues in finalising this thesis project.

I am also grateful to the hard-working executive secretary Leila Laakso-Kantonen for the help you always provide when needed. I would also like to thank the warm-hearted nurse Liisa Puttaa for the flexibility you offered me with arranging my days at clinical work based on the periodically tight PET imaging schedule if needed.

Of my colleagues, last but certainly not least I would like to thank Markku Päivärinta. Although Markku has not participated in the content of this thesis project in any way, his wisdom and teaching methods have influenced me considerably throughout the years in the path of becoming a neurologist.

I am deeply grateful to my wonderful parents, Annette and Lars, for your endless love and support throughout my life. Sadly, my mother passed away during this thesis project, the one who would have appreciated this day the most. I am grateful to my brother Dan and his wife Henna for the friendship and moments spent together. My parents-in-law, Marjaliisa and Mohamed, are warmly thanked for all the joyful moments spent together, inspiring conversations, delicious dinners and for the help with our children.

Finally, there are no words to express my gratitude and love to my beautiful wife Minna. I have been privileged to find you and share my life with you as loving soulmates already from the beginning of the medical studies. I admire your life values, intelligence and great sense of humour. As a mother, you take excellent care of our three amazing children, Rasmus, Kasper and Linnea, that we have been blessed with together. You four bring so much meaning and joy into my life.

This work was financially supported by scholarships from the Finnish MS Foundation, the Finnish Medical Foundation, the Finnish Medical Society (Finska Läkaresällskapet) and the Finnish Brain Foundation.

Turku, November 2023
Marcus Sucksdorff

References

- Absinta, M., Sati, P., Masuzzo, F., Nair, G., Sethi, V., Kolb, H., . . . Reich, D. S. (2019). Association of Chronic Active Multiple Sclerosis Lesions With Disability In Vivo. *JAMA Neurol.* doi:10.1001/jamaneurol.2019.2399
- Absinta, M., Sati, P., & Reich, D. S. (2016). Advanced MRI and staging of multiple sclerosis lesions. *Nat Rev Neurol*, *12*(6), 358–368. doi:10.1038/nrneurol.2016.59
- Airas, L., Dickens, A. M., Elo, P., Marjamäki, P., Johansson, J., Eskola, O., . . . Rinne, J. (2015). In vivo PET imaging demonstrates diminished microglial activation after fingolimod treatment in an animal model of multiple sclerosis. *J Nucl Med*, *56*(2), 305-310. doi:10.2967/jnumed.114.149955
- Airas, L., Nylund, M., & Rissanen, E. (2018). Evaluation of Microglial Activation in Multiple Sclerosis Patients Using Positron Emission Tomography. *Front Neurol*, *9*, 181. doi:10.3389/fneur.2018.00181
- Ascherio, A., & Munger, K. L. (2007). Environmental risk factors for multiple sclerosis. Part I: the role of infection. *Ann Neurol*, *61*(4), 288–299. doi:10.1002/ana.21117
- Ascherio, A., Munger, K. L., White, R., Köchert, K., Simon, K. C., Polman, C. H., . . . Pohl, C. (2014). Vitamin D as an early predictor of multiple sclerosis activity and progression. *JAMA Neurol*, *71*(3), 306–314. doi:10.1001/jamaneurol.2013.5993
- Baecher-Allan, C., Kaskow, B. J., & Weiner, H. L. (2018). Multiple Sclerosis: Mechanisms and Immunotherapy. *Neuron*, *97*(4), 742–768. doi:10.1016/j.neuron.2018.01.021
- Baird, J. F., Sasaki, J. E., Sandroff, B. M., Cutter, G. R., & Motl, R. W. (2020). Feasibility of "Sit Less, Move More": An intervention for reducing sedentary behavior Among African Americans with MS. *Mult Scler J Exp Transl Clin*, *6*(2), 2055217320932341. doi:10.1177/2055217320932341
- Banati, R. B., Middleton, R. J., Chan, R., Hatty, C. R., Kam, W. W., Quin, C., . . . Liu, G. J. (2014). Positron emission tomography and functional characterization of a complete PBR/TSPO knockout. *Nat Commun*, *5*, 5452. doi:10.1038/ncomms6452
- Banati, R. B., Newcombe, J., Gunn, R. N., Cagnin, A., Turkheimer, F., Heppner, F., . . . Myers, R. (2000). The peripheral benzodiazepine binding site in the brain in multiple sclerosis: quantitative in vivo imaging of microglia as a measure of disease activity. *Brain*, *123* (Pt 11), 2321–2337. doi:10.1093/brain/123.11.2321
- Barry, B., Erwin, A. A., Stevens, J., & Tornatore, C. (2019). Fingolimod Rebound: A Review of the Clinical Experience and Management Considerations. *Neurol Ther*, *8*(2), 241–250. doi:10.1007/s40120-019-00160-9
- Barzegar, M., Najdaghi, S., Afshari-Safavi, A., Nehzat, N., Mirmosayyeb, O., & Shaygannejad, V. (2021). Early predictors of conversion to secondary progressive multiple sclerosis. *Mult Scler Relat Disord*, *54*, 103115. doi:10.1016/j.msard.2021.103115
- Bashinskaya, V. V., Kulakova, O. G., Boyko, A. N., Favorov, A. V., & Favorova, O. O. (2015). A review of genome-wide association studies for multiple sclerosis: classical and hypothesis-driven approaches. *Hum Genet*, *134*(11–12), 1143–1162. doi:10.1007/s00439-015-1601-2
- Benjamin, S. E. (2020). Sleep in Patients With Neurologic Disease. *Continuum (Minneapolis)*, *26*(4), 1016–1033. doi:10.1212/CON.0000000000000887

- Bergamaschi, R., Quaglini, S., Tavazzi, E., Amato, M. P., Paolicelli, D., Zipoli, V., . . . Trojano, M. (2016). Immunomodulatory therapies delay disease progression in multiple sclerosis. *Mult Scler*, 22(13), 1732–1740. doi:10.1177/1352458512445941
- Berger, J. R., & Koralnik, I. J. (2005). Progressive multifocal leukoencephalopathy and natalizumab--unforeseen consequences. *N Engl J Med*, 353(4), 414–416. doi:10.1056/NEJMe058122
- Bezukladova, S., Tuisku, J., Matilainen, M., Vuorimaa, A., Nylund, M., Smith, S., . . . Airas, L. (2020). Insights into disseminated MS brain pathology with multimodal diffusion tensor and PET imaging. *Neurol Neuroimmunol Neuroinflamm*, 7(3). doi:10.1212/NXI.0000000000000691
- Biber, K., Owens, T., & Boddeke, E. (2014). What is microglia neurotoxicity (Not)? *Glia*, 62(6), 841–854. doi:10.1002/glia.22654
- Bjornevik, K., Cortese, M., Healy, B. C., Kuhle, J., Mina, M. J., Leng, Y., . . . Ascherio, A. (2022). Longitudinal analysis reveals high prevalence of Epstein-Barr virus associated with multiple sclerosis. *Science*, 375(6578), 296–301. doi:10.1126/science.abj8222
- Brown, J. W. L., Coles, A., Horakova, D., Havrdova, E., Izquierdo, G., Prat, A., . . . Group, M. S. (2019). Association of Initial Disease-Modifying Therapy With Later Conversion to Secondary Progressive Multiple Sclerosis. *JAMA*, 321(2), 175–187. doi:10.1001/jama.2018.20588
- Brownlee, W. J., Hardy, T. A., Fazekas, F., & Miller, D. H. (2017). Diagnosis of multiple sclerosis: progress and challenges. *Lancet*, 389(10076), 1336–1346. doi:10.1016/S0140-6736(16)30959-X
- Brynedal, B., Duvefelt, K., Jonasdottir, G., Roos, I. M., Akesson, E., Palmgren, J., & Hillert, J. (2007). HLA-A confers an HLA-DRB1 independent influence on the risk of multiple sclerosis. *PLoS One*, 2(7), e664. doi:10.1371/journal.pone.0000664
- Bunai, T., Terada, T., Kono, S., Yokokura, M., Yoshikawa, E., Futatsubashi, M., . . . Ouchi, Y. (2018). Neuroinflammation following disease modifying therapy in multiple sclerosis: A pilot positron emission tomography study. *J Neurol Sci*, 385, 30–33. doi:10.1016/j.jns.2017.12.004
- Chard, D. T., Griffin, C. M., McLean, M. A., Kapeller, P., Kapoor, R., Thompson, A. J., & Miller, D. H. (2002). Brain metabolite changes in cortical grey and normal-appearing white matter in clinically early relapsing-remitting multiple sclerosis. *Brain*, 125(Pt 10), 2342–2352. doi:10.1093/brain/awf240
- Chedid, T., Moisset, X., & Clavelou, P. (2022). Rationale for off-label treatments use in primary progressive multiple sclerosis: A review of the literature. *Rev Neurol (Paris)*, 178(9), 932–938. doi:10.1016/j.neurol.2022.02.461
- Chen, M. K., & Guilarte, T. R. (2008). Translocator protein 18 kDa (TSPO): molecular sensor of brain injury and repair. *Pharmacol Ther*, 118(1), 1-17. doi:10.1016/j.pharmthera.2007.12.004
- Ching, A. S., Kuhnast, B., Damont, A., Roeda, D., Tavitian, B., & Dollé, F. (2012). Current paradigm of the 18-kDa translocator protein (TSPO) as a molecular target for PET imaging in neuroinflammation and neurodegenerative diseases. *Insights Imaging*, 3(1), 111–119. doi:10.1007/s13244-011-0128-x
- Chisari, C. G., Sgarlata, E., Arena, S., Toscano, S., Luca, M., & Patti, F. (2022). Rituximab for the treatment of multiple sclerosis: a review. *J Neurol*, 269(1), 159–183. doi:10.1007/s00415-020-10362-z
- Choi, J. W., Gardell, S. E., Herr, D. R., Rivera, R., Lee, C. W., Noguchi, K., . . . Chun, J. (2011). FTY720 (fingolimod) efficacy in an animal model of multiple sclerosis requires astrocyte sphingosine 1-phosphate receptor 1 (S1P1) modulation. *Proc Natl Acad Sci U S A*, 108(2), 751–756. doi:10.1073/pnas.1014154108
- Chun, J., & Hartung, H. P. (2010). Mechanism of action of oral fingolimod (FTY720) in multiple sclerosis. *Clin Neuropharmacol*, 33(2), 91–101. doi:10.1097/WNF.0b013e3181cbf825
- Cohen, J. A., & Chun, J. (2011). Mechanisms of fingolimod's efficacy and adverse effects in multiple sclerosis. *Ann Neurol*, 69(5), 759–777. doi:10.1002/ana.22426
- Cohen, J. A., Coles, A. J., Arnold, D. L., Confavreux, C., Fox, E. J., Hartung, H. P., . . . investigators, C.-M. I. (2012). Alemtuzumab versus interferon beta 1a as first-line treatment for patients with

- relapsing-remitting multiple sclerosis: a randomised controlled phase 3 trial. *Lancet*, 380(9856), 1819–1828. doi:10.1016/S0140-6736(12)61769-3
- Colasanti, A., Guo, Q., Muhlert, N., Giannetti, P., Onega, M., Newbould, R. D., . . . Matthews, P. M. (2014). In Vivo Assessment of Brain White Matter Inflammation in Multiple Sclerosis with (18)F-PBR111 PET. *J Nucl Med*, 55(7), 1112–1118. doi:10.2967/jnumed.113.135129
- Coles, A. J., Cox, A., Le Page, E., Jones, J., Trip, S. A., Deans, J., . . . Compston, D. A. (2006). The window of therapeutic opportunity in multiple sclerosis: evidence from monoclonal antibody therapy. *J Neurol*, 253(1), 98–108. doi:10.1007/s00415-005-0934-5
- Colonna, M., & Butovsky, O. (2017). Microglia Function in the Central Nervous System During Health and Neurodegeneration. *Annu Rev Immunol*, 35, 441–468. doi:10.1146/annurev-immunol-051116-052358
- Comi, G., Bar-Or, A., Lassmann, H., Uccelli, A., Hartung, H. P., Montalban, X., . . . Foundation, E. P. o. t. t. A. M. o. t. E. C. (2021). Role of B Cells in Multiple Sclerosis and Related Disorders. *Ann Neurol*, 89(1), 13–23. doi:10.1002/ana.25927
- Compston, A., & Coles, A. (2008). Multiple sclerosis. *Lancet*, 372(9648), 1502–1517. doi:10.1016/S0140-6736(08)61620-7
- Confavreux, C., O'Connor, P., Comi, G., Freedman, M. S., Miller, A. E., Olsson, T. P., . . . Group, T. T. (2014). Oral teriflunomide for patients with relapsing multiple sclerosis (TOWER): a randomised, double-blind, placebo-controlled, phase 3 trial. *Lancet Neurol*, 13(3), 247–256. doi:10.1016/S1474-4422(13)70308-9
- Correale, J., Gaitán, M. I., Ysraelit, M. C., & Fiol, M. P. (2017). Progressive multiple sclerosis: from pathogenic mechanisms to treatment. *Brain*, 140(3), 527–546. doi:10.1093/brain/aww258
- Cosenza-Nashat, M., Zhao, M. L., Suh, H. S., Morgan, J., Natividad, R., Morgello, S., & Lee, S. C. (2009). Expression of the translocator protein of 18 kDa by microglia, macrophages and astrocytes based on immunohistochemical localization in abnormal human brain. *Neuropathol Appl Neurobiol*, 35(3), 306–328. doi:10.1111/j.1365-2990.2008.01006.x
- Cree, B. A., Gourraud, P. A., Oksenberg, J. R., Bevan, C., Crabtree-Hartman, E., Gelfand, J. M., . . . University of California, S. n. F. M.-E. T. (2016). Long-term evolution of multiple sclerosis disability in the treatment era. *Ann Neurol*, 80(4), 499–510. doi:10.1002/ana.24747
- Cree, B. A. C., Arnold, D. L., Chataway, J., Chitnis, T., Fox, R. J., Pozo Ramajo, A., . . . Lassmann, H. (2021). Secondary Progressive Multiple Sclerosis: New Insights. *Neurology*, 97(8), 378–388. doi:10.1212/WNL.0000000000012323
- Cree, B. A. C., Hollenbach, J. A., Bove, R., Kirkish, G., Sacco, S., Caverzasi, E., . . . University of California, S. n. F. M.-E. T. (2019). Silent progression in disease activity-free relapsing multiple sclerosis. *Ann Neurol*, 85(5), 653–666. doi:10.1002/ana.25463
- D'Amico, E., Zanghi, A., Chisari, C. G., Fermo, S. L., Toscano, S., Arena, S., . . . Zappia, M. (2019). Effectiveness and safety of Rituximab in demyelinating diseases spectrum: An Italian experience. *Mult Scler Relat Disord*, 27, 324–326. doi:10.1016/j.msard.2018.09.041
- Dal-Bianco, A., Grabner, G., Kronnerwetter, C., Weber, M., Höftberger, R., Berger, T., . . . Hametner, S. (2017). Slow expansion of multiple sclerosis iron rim lesions: pathology and 7 T magnetic resonance imaging. *Acta Neuropathol*, 133(1), 25–42. doi:10.1007/s00401-016-1636-z
- Dal-Bianco, A., Grabner, G., Kronnerwetter, C., Weber, M., Kornek, B., Kasprian, G., . . . Hametner, S. (2021). Long-term evolution of multiple sclerosis iron rim lesions in 7 T MRI. *Brain*, 144(3), 833–847. doi:10.1093/brain/awaa436
- Damani, M. R., Zhao, L., Fontainhas, A. M., Amaral, J., Fariss, R. N., & Wong, W. T. (2011). Age-related alterations in the dynamic behavior of microglia. *Aging Cell*, 10(2), 263–276. doi:10.1111/j.1474-9726.2010.00660.x
- Datta, G., Colasanti, A., Kalk, N., Owen, D., Scott, G., Rabiner, E. A., . . . Matthews, P. M. (2017). C-PBR28 and. *J Nucl Med*, 58(9), 1477–1482. doi:10.2967/jnumed.116.187161

- Datta, G., Colasanti, A., Rabiner, E. A., Gunn, R. N., Malik, O., Ciccarelli, O., . . . Matthews, P. M. (2017). Neuroinflammation and its relationship to changes in brain volume and white matter lesions in multiple sclerosis. *Brain*, *140*(11), 2927–2938. doi:10.1093/brain/awx228
- de Jong, H. W., van Velden, F. H., Kloet, R. W., Buijs, F. L., Boellaard, R., & Lammertsma, A. A. (2007). Performance evaluation of the ECAT HRRT: an LSO-LYSO double layer high resolution, high sensitivity scanner. *Phys Med Biol*, *52*(5), 1505–1526. doi:10.1088/0031-9155/52/5/019
- De Stefano, N., Giorgio, A., Battaglini, M., Rovaris, M., Sormani, M. P., Barkhof, F., . . . Filippi, M. (2010). Assessing brain atrophy rates in a large population of untreated multiple sclerosis subtypes. *Neurology*, *74*(23), 1868–1876. doi:10.1212/WNL.0b013e3181e24136
- De Stefano, N., Stromillo, M. L., Rossi, F., Battaglini, M., Giorgio, A., Portaccio, E., . . . Amato, M. P. (2011). Improving the characterization of radiologically isolated syndrome suggestive of multiple sclerosis. *PLoS One*, *6*(4), e19452. doi:10.1371/journal.pone.0019452
- Debruyne, J. C., Versijpt, J., Van Laere, K. J., De Vos, F., Keppens, J., Strijckmans, K., . . . De Reuck, J. L. (2003). PET visualization of microglia in multiple sclerosis patients using [¹¹C]PK11195. *Eur J Neurol*, *10*(3), 257–264. doi:10.1046/j.1468-1331.2003.00571.x
- Degelman, M. L., & Herman, K. M. (2017). Smoking and multiple sclerosis: A systematic review and meta-analysis using the Bradford Hill criteria for causation. *Mult Scler Relat Disord*, *17*, 207–216. doi:10.1016/j.msard.2017.07.020
- Dendrou, C. A., Fugger, L., & Friese, M. A. (2015). Immunopathology of multiple sclerosis. *Nat Rev Immunol*, *15*(9), 545–558. doi:10.1038/nri3871
- Eriksson, M., Andersen, O., & Runmarker, B. (2003). Long-term follow up of patients with clinically isolated syndromes, relapsing-remitting and secondary progressive multiple sclerosis. *Mult Scler*, *9*(3), 260–274. doi:10.1191/1352458503ms914oa
- Erlandsson, K., Buvat, I., Pretorius, P. H., Thomas, B. A., & Hutton, B. F. (2012). A review of partial volume correction techniques for emission tomography and their applications in neurology, cardiology and oncology. *Phys Med Biol*, *57*(21), R119–159. doi:10.1088/0031-9155/57/21/R119
- Filippi, M., Bar-Or, A., Piehl, F., Preziosa, P., Solari, A., Vukusic, S., & Rocca, M. A. (2018). Multiple sclerosis. *Nat Rev Dis Primers*, *4*(1), 43. doi:10.1038/s41572-018-0041-4
- Filippi, M., Preziosa, P., Meani, A., Dalla Costa, G., Mesaros, S., Drulovic, J., . . . Group, M. S. (2022). Performance of the 2017 and 2010 Revised McDonald Criteria in Predicting MS Diagnosis After a Clinically Isolated Syndrome: A MAGNIMS Study. *Neurology*, *98*(1), e1–e14. doi:10.1212/WNL.0000000000013016
- Foster, C. A., Howard, L. M., Schweitzer, A., Persohn, E., Hiestand, P. C., Balatoni, B., . . . Billich, A. (2007). Brain penetration of the oral immunomodulatory drug FTY720 and its phosphorylation in the central nervous system during experimental autoimmune encephalomyelitis: consequences for mode of action in multiple sclerosis. *J Pharmacol Exp Ther*, *323*(2), 469–475. doi:10.1124/jpet.107.127183
- Frischer, J. M., Bramow, S., Dal-Bianco, A., Lucchinetti, C. F., Rauschka, H., Schmidbauer, M., . . . Lassmann, H. (2009). The relation between inflammation and neurodegeneration in multiple sclerosis brains. *Brain*, *132*(Pt 5), 1175–1189. doi:10.1093/brain/awp070
- Frischer, J. M., Weigand, S. D., Guo, Y., Kale, N., Parisi, J. E., Pirko, I., . . . Lucchinetti, C. F. (2015). Clinical and pathological insights into the dynamic nature of the white matter multiple sclerosis plaque. *Ann Neurol*, *78*(5), 710–721. doi:10.1002/ana.24497
- Frohman, E. M., Racke, M. K., & Raine, C. S. (2006). Multiple sclerosis--the plaque and its pathogenesis. *N Engl J Med*, *354*(9), 942–955. doi:10.1056/NEJMra052130
- Gao, H. M., & Hong, J. S. (2008). Why neurodegenerative diseases are progressive: uncontrolled inflammation drives disease progression. *Trends Immunol*, *29*(8), 357–365. doi:10.1016/j.it.2008.05.002
- Giannetti, P., Politis, M., Su, P., Turkheimer, F. E., Malik, O., Keihaninejad, S., . . . Piccini, P. (2015). Increased PK11195-PET binding in normal-appearing white matter in clinically isolated syndrome. *Brain*, *138*(Pt 1), 110–119. doi:10.1093/brain/awu331

- Gillen, K. M., Mubarak, M., Nguyen, T. D., & Pitt, D. (2018). Significance and. *Front Immunol*, *9*, 255. doi:10.3389/fimmu.2018.00255
- Giovannoni, G., Bermel, R., Phillips, T., & Rudick, R. (2018). A brief history of NEDA. *Mult Scler Relat Disord*, *20*, 228–230. doi:10.1016/j.msard.2017.07.011
- Giovannoni, G., Popescu, V., Wuerfel, J., Hellwig, K., Jacobaeus, E., Jensen, M. B., . . . Scalfari, A. (2022). Smouldering multiple sclerosis: the 'real MS'. *Ther Adv Neurol Disord*, *15*, 17562864211066751. doi:10.1177/17562864211066751
- Giovannoni, G., Soelberg Sorensen, P., Cook, S., Rammohan, K., Rieckmann, P., Comi, G., . . . Vermersch, P. (2018). Safety and efficacy of cladribine tablets in patients with relapsing-remitting multiple sclerosis: Results from the randomized extension trial of the CLARITY study. *Mult Scler*, *24*(12), 1594–1604. doi:10.1177/1352458517727603
- Gold, R., Arnold, D. L., Bar-Or, A., Fox, R. J., Kappos, L., Mokliatchouk, O., . . . Miller, C. (2022). Long-term safety and efficacy of dimethyl fumarate for up to 13 years in patients with relapsing-remitting multiple sclerosis: Final ENDORSE study results. *Mult Scler*, *28*(5), 801–816. doi:10.1177/13524585211037909
- Gold, R., Kappos, L., Arnold, D. L., Bar-Or, A., Giovannoni, G., Selmaj, K., . . . Investigators, D. S. (2012). Placebo-controlled phase 3 study of oral BG-12 for relapsing multiple sclerosis. *N Engl J Med*, *367*(12), 1098–1107. doi:10.1056/NEJMoa1114287
- Goodkin, D. E., Cookfair, D., Wende, K., Bourdette, D., Pullicino, P., Scherokman, B., & Whitham, R. (1992). Inter- and intrarater scoring agreement using grades 1.0 to 3.5 of the Kurtzke Expanded Disability Status Scale (EDSS). Multiple Sclerosis Collaborative Research Group. *Neurology*, *42*(4), 859–863. doi:10.1212/wnl.42.4.859
- Gross, R. H., Sillau, S. H., Miller, A. E., Farrell, C., & Krieger, S. C. (2019). The Multiple Sclerosis Severity Score: fluctuations and prognostic ability in a longitudinal cohort of patients with MS. *Mult Scler J Exp Transl Clin*, *5*(1), 2055217319837254. doi:10.1177/2055217319837254
- Guarnera, C., Bramanti, P., & Mazzon, E. (2017). Alemtuzumab: a review of efficacy and risks in the treatment of relapsing remitting multiple sclerosis. *Ther Clin Risk Manag*, *13*, 871–879. doi:10.2147/TCRM.S134398
- Guerrero, B. L., & Sicotte, N. L. (2020). Microglia in Multiple Sclerosis: Friend or Foe? *Front Immunol*, *11*, 374. doi:10.3389/fimmu.2020.00374
- Guilarte, T. R. (2019). TSPO in diverse CNS pathologies and psychiatric disease: A critical review and a way forward. *Pharmacol Ther*, *194*, 44–58. doi:10.1016/j.pharmthera.2018.09.003
- Hagens, M. H., Killestein, J., Yaqub, M. M., van Dongen, G. A., Lammertsma, A. A., Barkhof, F., & van Berckel, B. N. (2018). Cerebral rituximab uptake in multiple sclerosis: A. *Mult Scler*, *24*(4), 543–545. doi:10.1177/1352458517704507
- Hamzaoui, M., Garcia, J., Boffa, G., Lazzarotto, A., Absinta, M., Ricigliano, V. A. G., . . . Stankoff, B. (2023). Positron Emission Tomography with [Ann Neurol, *94*(2), 366–383. doi:10.1002/ana.26657
- Harding, K., Williams, O., Willis, M., Hrastelj, J., Rimmer, A., Joseph, F., . . . Tallantyre, E. (2019). Clinical Outcomes of Escalation vs Early Intensive Disease-Modifying Therapy in Patients With Multiple Sclerosis. *JAMA Neurol*, *76*(5), 536–541. doi:10.1001/jamaneurol.2018.4905
- Hase, Y., Ding, R., Harrison, G., Hawthorne, E., King, A., Gettings, S., . . . Kalaria, R. N. (2019). White matter capillaries in vascular and neurodegenerative dementias. *Acta Neuropathol Commun*, *7*(1), 16. doi:10.1186/s40478-019-0666-x
- Hauser, S. L., Bar-Or, A., Cohen, J. A., Comi, G., Correale, J., Coyle, P. K., . . . Groups, A. I. a. A. I. T. (2020). Ofatumumab versus Teriflunomide in Multiple Sclerosis. *N Engl J Med*, *383*(6), 546–557. doi:10.1056/NEJMoa1917246
- Hauser, S. L., Bar-Or, A., Comi, G., Giovannoni, G., Hartung, H. P., Hemmer, B., . . . Investigators, O. I. a. O. I. C. (2017). Ocrelizumab versus Interferon Beta-1a in Relapsing Multiple Sclerosis. *N Engl J Med*, *376*(3), 221–234. doi:10.1056/NEJMoa1601277

- Hauser, S. L., Waubant, E., Arnold, D. L., Vollmer, T., Antel, J., Fox, R. J., . . . Group, H. T. (2008). B-cell depletion with rituximab in relapsing-remitting multiple sclerosis. *N Engl J Med*, *358*(7), 676–688. doi:10.1056/NEJMoa0706383
- Hawker, K., O'Connor, P., Freedman, M. S., Calabresi, P. A., Antel, J., Simon, J., . . . group, O. t. (2009). Rituximab in patients with primary progressive multiple sclerosis: results of a randomized double-blind placebo-controlled multicenter trial. *Ann Neurol*, *66*(4), 460–471. doi:10.1002/ana.21867
- He, A., Merkel, B., Brown, J. W. L., Zhovits Ryerson, L., Kister, I., Malpas, C. B., . . . group, M. s. (2020). Timing of high-efficacy therapy for multiple sclerosis: a retrospective observational cohort study. *Lancet Neurol*, *19*(4), 307–316. doi:10.1016/S1474-4422(20)30067-3
- Herranz, E., Gianni, C., Louapre, C., Treaba, C. A., Govindarajan, S. T., Ouellette, R., . . . Mainero, C. (2016). Neuroinflammatory component of gray matter pathology in multiple sclerosis. *Ann Neurol*, *80*(5), 776–790. doi:10.1002/ana.24791
- Heydarpour, P., Amini, H., Khoshkish, S., Seidkhani, H., Sahraian, M. A., & Yunesian, M. (2014). Potential impact of air pollution on multiple sclerosis in Tehran, Iran. *Neuroepidemiology*, *43*(3–4), 233–238. doi:10.1159/000368553
- Hillert, J., Tsai, J. A., Nouhi, M., Glaser, A., & Spelman, T. (2022). A comparative study of teriflunomide and dimethyl fumarate within the Swedish MS Registry. *Mult Scler*, *28*(2), 237–246. doi:10.1177/13524585211019649
- Hochmeister, S., Grundtner, R., Bauer, J., Engelhardt, B., Lyck, R., Gordon, G., . . . Lassmann, H. (2006). Dysferlin is a new marker for leaky brain blood vessels in multiple sclerosis. *J Neuropathol Exp Neurol*, *65*(9), 855–865. doi:10.1097/01.jnen.0000235119.52311.16
- Hollenbach, J. A., & Oksenberg, J. R. (2015). The immunogenetics of multiple sclerosis: A comprehensive review. *J Autoimmun*, *64*, 13–25. doi:10.1016/j.jaut.2015.06.010
- Holloway, O. G., Canty, A. J., King, A. E., & Ziebell, J. M. (2019). Rod microglia and their role in neurological diseases. *Semin Cell Dev Biol*, *94*, 96–103. doi:10.1016/j.semcdb.2019.02.005
- Högel, H., Rissanen, E., Vuorimaa, A., & Airas, L. (2018). Positron emission tomography imaging in evaluation of MS pathology in vivo. *Mult Scler*, *24*(11), 1399–1412. doi:10.1177/1352458518791680
- Iaffaldano, P., Lucisano, G., Butzkueven, H., Hillert, J., Hyde, R., Koch-Henriksen, N., . . . Trojano, M. (2021). Early treatment delays long-term disability accrual in RRMS: Results from the BMSD network. *Mult Scler*, *27*(10), 1543–1555. doi:10.1177/13524585211010128
- Innis, R. B., Cunningham, V. J., Delforge, J., Fujita, M., Gjedde, A., Gunn, R. N., . . . Carson, R. E. (2007). Consensus nomenclature for in vivo imaging of reversibly binding radioligands. *J Cereb Blood Flow Metab*, *27*(9), 1533–1539. doi:10.1038/sj.jcbfm.9600493
- Jakimovski, D., Guan, Y., Ramanathan, M., Weinstock-Guttman, B., & Zivadinov, R. (2019). Lifestyle-based modifiable risk factors in multiple sclerosis: review of experimental and clinical findings. *Neurodegener Dis Manag*, *9*(3), 149–172. doi:10.2217/nmt-2018-0046
- Jonasson, E., & Sejbaek, T. (2020). Diroximel fumarate in the treatment of multiple sclerosis. *Neurodegener Dis Manag*, *10*(5), 267–276. doi:10.2217/nmt-2020-0025
- Junck, L., Olson, J. M., Ciliax, B. J., Koeppe, R. A., Watkins, G. L., Jewett, D. M., . . . Starosta-Rubinstein, S. (1989). PET imaging of human gliomas with ligands for the peripheral benzodiazepine binding site. *Ann Neurol*, *26*(6), 752–758. doi:10.1002/ana.410260611
- Jučaite, A., Cselényi, Z., Arvidsson, A., Ahlberg, G., Julin, P., Varnäs, K., . . . Farde, L. (2012). Kinetic analysis and test-retest variability of the radioligand [¹¹C](R)-PK11195 binding to TSPO in the human brain - a PET study in control subjects. *EJNMMI Res*, *2*, 15. doi:10.1186/2191-219X-2-15
- Kalincik, T., Brown, J. W. L., Robertson, N., Willis, M., Scolding, N., Rice, C. M., . . . Group, M. S. (2017). Treatment effectiveness of alemtuzumab compared with natalizumab, fingolimod, and interferon beta in relapsing-remitting multiple sclerosis: a cohort study. *Lancet Neurol*, *16*(4), 271–281. doi:10.1016/S1474-4422(17)30007-8

- Kalincik, T., Horakova, D., Spelman, T., Jokubaitis, V., Trojano, M., Lugeski, A., . . . Group, M. S. (2015). Switch to natalizumab versus fingolimod in active relapsing-remitting multiple sclerosis. *Ann Neurol*, *77*(3), 425–435. doi:10.1002/ana.24339
- Kalincik, T., Kubala Havrdova, E., Horakova, D., Izquierdo, G., Prat, A., Girard, M., . . . Butzkueven, H. (2019). Comparison of fingolimod, dimethyl fumarate and teriflunomide for multiple sclerosis. *J Neurol Neurosurg Psychiatry*, *90*(4), 458–468. doi:10.1136/jnnp-2018-319831
- Kalincik, T., Sharmin, S., Roos, I., Freedman, M. S., Atkins, H., Burman, J., . . . Group, M. S. (2023). Comparative Effectiveness of Autologous Hematopoietic Stem Cell Transplant vs Fingolimod, Natalizumab, and Ocrelizumab in Highly Active Relapsing-Remitting Multiple Sclerosis. *JAMA Neurol*, *80*(7), 702–713. doi:10.1001/jamaneurol.2023.1184
- Kang, Y., Pandya, S., Zinger, N., Michaelson, N., & Gauthier, S. A. (2021). Longitudinal change in TSPO PET imaging in progressive multiple sclerosis. *Ann Clin Transl Neurol*, *8*(8), 1755–1759. doi:10.1002/acn3.51431
- Kapoor, R., Ho, P. R., Campbell, N., Chang, I., Deykin, A., Forrester, F., . . . investigators, A. (2018). Effect of natalizumab on disease progression in secondary progressive multiple sclerosis (ASCEND): a phase 3, randomised, double-blind, placebo-controlled trial with an open-label extension. *Lancet Neurol*, *17*(5), 405–415. doi:10.1016/S1474-4422(18)30069-3
- Kappos, L., Antel, J., Comi, G., Montalban, X., O'Connor, P., Polman, C. H., . . . Group, F. D. S. (2006). Oral fingolimod (FTY720) for relapsing multiple sclerosis. *N Engl J Med*, *355*(11), 1124–1140. doi:10.1056/NEJMoa052643
- Kappos, L., Bar-Or, A., Cree, B. A. C., Fox, R. J., Giovannoni, G., Gold, R., . . . Investigators, E. C. (2018). Siponimod versus placebo in secondary progressive multiple sclerosis (EXPAND): a double-blind, randomised, phase 3 study. *Lancet*, *391*(10127), 1263–1273. doi:10.1016/S0140-6736(18)30475-6
- Kappos, L., Wolinsky, J. S., Giovannoni, G., Arnold, D. L., Wang, Q., Bernasconi, C., . . . Hauser, S. L. (2020). Contribution of Relapse-Independent Progression vs Relapse-Associated Worsening to Overall Confirmed Disability Accumulation in Typical Relapsing Multiple Sclerosis in a Pooled Analysis of 2 Randomized Clinical Trials. *JAMA Neurol*, *77*(9), 1132–1140. doi:10.1001/jamaneurol.2020.1568
- Kaunzner, U. W., Kang, Y., Monohan, E., Kothari, P. J., Nealon, N., Perumal, J., . . . Gauthier, S. A. (2017). Reduction of PK11195 uptake observed in multiple sclerosis lesions after natalizumab initiation. *Mult Scler Relat Disord*, *15*, 27–33. doi:10.1016/j.msard.2017.04.008
- Kaunzner, U. W., Kang, Y., Zhang, S., Morris, E., Yao, Y., Pandya, S., . . . Gauthier, S. A. (2019). Quantitative susceptibility mapping identifies inflammation in a subset of chronic multiple sclerosis lesions. *Brain*, *142*(1), 133–145. doi:10.1093/brain/awy296
- Kavaliunas, A., Manouchehrinia, A., Stawiarz, L., Ramanujam, R., Agholme, J., Hedström, A. K., . . . Hillert, J. (2017). Importance of early treatment initiation in the clinical course of multiple sclerosis. *Mult Scler*, *23*(9), 1233–1240. doi:10.1177/1352458516675039
- Kobelt, G., Thompson, A., Berg, J., Gannedahl, M., Eriksson, J., Group, M. S., & Platform, E. M. S. (2017). New insights into the burden and costs of multiple sclerosis in Europe. *Mult Scler*, *23*(8), 1123–1136. doi:10.1177/1352458517694432
- Koch, M., Kingwell, E., Rieckmann, P., Tremlett, H., & Neurologists, U. M. C. (2010). The natural history of secondary progressive multiple sclerosis. *J Neurol Neurosurg Psychiatry*, *81*(9), 1039–1043. doi:10.1136/jnnp.2010.208173
- Kreisler, W. C., Jenko, K. J., Hines, C. S., Lyoo, C. H., Corona, W., Morse, C. L., . . . Team, B. C. P. R. P. (2013). A genetic polymorphism for translocator protein 18 kDa affects both in vitro and in vivo radioligand binding in human brain to this putative biomarker of neuroinflammation. *J Cereb Blood Flow Metab*, *33*(1), 53–58. doi:10.1038/jcbfm.2012.131
- Kreutzberg, G. W. (1996). Microglia: a sensor for pathological events in the CNS. *Trends Neurosci*, *19*(8), 312–318. doi:10.1016/0166-2236(96)10049-7

- Kuhlmann, T., Ludwin, S., Prat, A., Antel, J., Brück, W., & Lassmann, H. (2017). An updated histological classification system for multiple sclerosis lesions. *Acta Neuropathol*, *133*(1), 13–24. doi:10.1007/s00401-016-1653-y
- Kurtzke, J. F. (1983). Rating neurologic impairment in multiple sclerosis: an expanded disability status scale (EDSS). *Neurology*, *33*(11), 1444–1452. doi:10.1212/wnl.33.11.1444
- Kutzelnigg, A., & Lassmann, H. (2014). Pathology of multiple sclerosis and related inflammatory demyelinating diseases. *Handb Clin Neurol*, *122*, 15–58. doi:10.1016/B978-0-444-52001-2.00002-9
- Kutzelnigg, A., Lucchinetti, C. F., Stadelmann, C., Brück, W., Rauschka, H., Bergmann, M., . . . Lassmann, H. (2005). Cortical demyelination and diffuse white matter injury in multiple sclerosis. *Brain*, *128*(Pt 11), 2705–2712. doi:10.1093/brain/awh641
- Laakso, S. M., Viitala, M., Kuusisto, H., Sarasoja, T., Hartikainen, P., Atula, S., . . . Soilu-Hänninen, M. (2019). Multiple sclerosis in Finland 2018-Data from the national register. *Acta Neurol Scand*, *140*(5), 303–311. doi:10.1111/ane.13145
- Laaksonen, S., Saraste, M., Sucksdorff, M., Nylund, M., Vuorimaa, A., Matilainen, M., . . . Airas, L. (2023). Early prognosticators of later TSPO-PET-measurable microglial activation in multiple sclerosis. *Mult Scler Relat Disord*, *75*, 104755. doi:10.1016/j.msard.2023.104755
- Lammertsma, A. A. (2002). Radioligand studies: imaging and quantitative analysis. *Eur Neuropsychopharmacol*, *12*(6), 513–516. doi:10.1016/s0924-977x(02)00100-1
- Lassmann, H. (2014). Mechanisms of white matter damage in multiple sclerosis. *Glia*, *62*(11), 1816–1830. doi:10.1002/glia.22597
- Lassmann, H. (2018). Pathogenic Mechanisms Associated With Different Clinical Courses of Multiple Sclerosis. *Front Immunol*, *9*, 3116. doi:10.3389/fimmu.2018.03116
- Lassmann, H., Brück, W., & Lucchinetti, C. F. (2007). The immunopathology of multiple sclerosis: an overview. *Brain Pathol*, *17*(2), 210–218. doi:10.1111/j.1750-3639.2007.00064.x
- Lassmann, H., van Horssen, J., & Mahad, D. (2012). Progressive multiple sclerosis: pathology and pathogenesis. *Nat Rev Neurol*, *8*(11), 647–656. doi:10.1038/nrneuro.2012.168
- Lebrun, C. (2015). The radiologically isolated syndrome. *Rev Neurol (Paris)*, *171*(10), 698–706. doi:10.1016/j.neurol.2015.05.001
- Lehto, J., Nylund, M., Matilainen, M., Sucksdorff, M., Vuorimaa, A., Rajander, J., . . . Airas, L. (2023). Longitudinal stability of progression-related microglial activity during teriflunomide treatment in patients with multiple sclerosis. *Eur J Neurol*. doi:10.1111/ene.15834
- Lehto, J., Sucksdorff, M., Nylund, M., Raitanen, R., Matilainen, M., & Airas, L. (2023). PET-measurable innate immune cell activation reduction in chronic active lesions in PPMS brain after rituximab treatment: a case report. *J Neurol*, *270*(4), 2329–2332. doi:10.1007/s00415-022-11539-4
- Logan, J. (2000). Graphical analysis of PET data applied to reversible and irreversible tracers. *Nucl Med Biol*, *27*(7), 661–670. doi:10.1016/s0969-8051(00)00137-2
- Logan, J., Fowler, J. S., Volkow, N. D., Wang, G. J., Ding, Y. S., & Alexoff, D. L. (1996). Distribution volume ratios without blood sampling from graphical analysis of PET data. *J Cereb Blood Flow Metab*, *16*(5), 834–840. doi:10.1097/00004647-199609000-00008
- Logan, J., Fowler, J. S., Volkow, N. D., Wolf, A. P., Dewey, S. L., Schlyer, D. J., . . . Gatley, S. J. (1990). Graphical analysis of reversible radioligand binding from time-activity measurements applied to [N-11C-methyl]-(-)-cocaine PET studies in human subjects. *J Cereb Blood Flow Metab*, *10*(5), 740–747. doi:10.1038/jcbfm.1990.127
- Lorscheider, J., Buzzard, K., Jokubaitis, V., Spelman, T., Havrdova, E., Horakova, D., . . . Group, M. S. (2016). Defining secondary progressive multiple sclerosis. *Brain*, *139*(Pt 9), 2395–2405. doi:10.1093/brain/aww173
- Lublin, F. D., Häring, D. A., Ganjgahi, H., Ocampo, A., Hatami, F., Čuklina, J., . . . Bermel, R. A. (2022). How patients with multiple sclerosis acquire disability. *Brain*, *145*(9), 3147–3161. doi:10.1093/brain/awac016

- Lublin, F. D., Reingold, S. C., Cohen, J. A., Cutter, G. R., Sørensen, P. S., Thompson, A. J., . . . Polman, C. H. (2014). Defining the clinical course of multiple sclerosis: the 2013 revisions. *Neurology*, 83(3), 278–286. doi:10.1212/WNL.0000000000000560
- Machado-Santos, J., Saji, E., Tröschler, A. R., Paunovic, M., Liblau, R., Gabriely, G., . . . Lassmann, H. (2018). The compartmentalized inflammatory response in the multiple sclerosis brain is composed of tissue-resident CD8⁺ T lymphocytes and B cells. *Brain*, 141(7), 2066–2082. doi:10.1093/brain/awy151
- Magrini, A., Pietroiusti, A., Coppeta, L., Babbucci, A., Barnaba, E., Papadia, C., . . . Bergamaschi, A. (2006). Shift work and autoimmune thyroid disorders. *Int J Immunopathol Pharmacol*, 19(4 Suppl), 31–36.
- Marck, C. H., Aitken, Z., Simpson, S., Weiland, T. J., & Jelinek, G. A. (2019). Does a modifiable risk factor score predict disability worsening in people with multiple sclerosis? *Mult Scler J Exp Transl Clin*, 5(4), 2055217319881769. doi:10.1177/2055217319881769
- Marrie, R. A. (2017). Comorbidity in multiple sclerosis: implications for patient care. *Nat Rev Neurol*, 13(6), 375–382. doi:10.1038/nrneurol.2017.33
- Martin, E., Aigrot, M. S., Grenningloh, R., Stankoff, B., Lubetzki, C., Boschert, U., & Zalc, B. (2020). Bruton's Tyrosine Kinase Inhibition Promotes Myelin Repair. *Brain Plast*, 5(2), 123–133. doi:10.3233/BPL-200100
- Masdeu, J. C., Pascual, B., & Fujita, M. (2022). Imaging Neuroinflammation in Neurodegenerative Disorders. *J Nucl Med*, 63(Suppl 1), 45S–52S. doi:10.2967/jnumed.121.263200
- Mayo, L., Quintana, F. J., & Weiner, H. L. (2012). The innate immune system in demyelinating disease. *Immunol Rev*, 248(1), 170–187. doi:10.1111/j.1600-065X.2012.01135.x
- McGinley, M. P., Goldschmidt, C. H., & Rae-Grant, A. D. (2021). Diagnosis and Treatment of Multiple Sclerosis: A Review. *JAMA*, 325(8), 765–779. doi:10.1001/jama.2020.26858
- Minghetti, L., & Levi, G. (1998). Microglia as effector cells in brain damage and repair: focus on prostanoids and nitric oxide. *Prog Neurobiol*, 54(1), 99–125. doi:10.1016/s0301-0082(97)00052-x
- Misin, O., Matilainen, M., Nylund, M., Honkonen, E., Rissanen, E., Sucksdorff, M., & Airas, L. (2022). Innate Immune Cell-Related Pathology in the Thalamus Signals a Risk for Disability Progression in Multiple Sclerosis. *Neurol Neuroimmunol Neuroinflamm*, 9(4). doi:10.1212/NXI.0000000000001182
- Moll, N. M., Rietsch, A. M., Thomas, S., Ransohoff, A. J., Lee, J. C., Fox, R., . . . Fisher, E. (2011). Multiple sclerosis normal-appearing white matter: pathology-imaging correlations. *Ann Neurol*, 70(5), 764–773. doi:10.1002/ana.22521
- Montalban, X., Hauser, S. L., Kappos, L., Arnold, D. L., Bar-Or, A., Comi, G., . . . Investigators, O. C. (2017). Ocrelizumab versus Placebo in Primary Progressive Multiple Sclerosis. *N Engl J Med*, 376(3), 209–220. doi:10.1056/NEJMoa1606468
- Morrow, S. A., Rosehart, H., Sener, A., & Welk, B. (2018). Anti-cholinergic medications for bladder dysfunction worsen cognition in persons with multiple sclerosis. *J Neurol Sci*, 385, 39–44. doi:10.1016/j.jns.2017.11.028
- Mosser, C. A., Baptista, S., Arnoux, I., & Audinat, E. (2017). Microglia in CNS development: Shaping the brain for the future. *Prog Neurobiol*, 149–150, 1–20. doi:10.1016/j.pneurobio.2017.01.002
- Mukhin, A. G., Papadopoulos, V., Costa, E., & Krueger, K. E. (1989). Mitochondrial benzodiazepine receptors regulate steroid biosynthesis. *Proc Natl Acad Sci U S A*, 86(24), 9813–9816. doi:10.1073/pnas.86.24.9813
- Munger, K. L., Chitnis, T., & Ascherio, A. (2009). Body size and risk of MS in two cohorts of US women. *Neurology*, 73(19), 1543–1550. doi:10.1212/WNL.0b013e3181c0d6e0
- Munger, K. L., Zhang, S. M., O'Reilly, E., Hernán, M. A., Olek, M. J., Willett, W. C., & Ascherio, A. (2004). Vitamin D intake and incidence of multiple sclerosis. *Neurology*, 62(1), 60–65. doi:10.1212/01.wnl.0000101723.79681.38

- Naegelin, Y., Naegelin, P., von Felten, S., Lorscheider, J., Sonder, J., Uitdehaag, B. M. J., . . . Derfuss, T. (2019). Association of Rituximab Treatment With Disability Progression Among Patients With Secondary Progressive Multiple Sclerosis. *JAMA Neurol*, *76*(3), 274–281. doi:10.1001/jamaneurol.2018.4239
- Nutma, E., Gebro, E., Marzin, M. C., van der Valk, P., Matthews, P. M., Owen, D. R., & Amor, S. (2021). Activated microglia do not increase 18 kDa translocator protein (TSPO) expression in the multiple sclerosis brain. *Glia*, *69*(10), 2447–2458. doi:10.1002/glia.24052
- Nutma, E., Stephenson, J. A., Gorter, R. P., de Bruin, J., Boucherie, D. M., Donat, C. K., . . . Amor, S. (2019). A quantitative neuropathological assessment of translocator protein expression in multiple sclerosis. *Brain*, *142*(11), 3440–3455. doi:10.1093/brain/awz287
- Nylund, M., Sucksdorff, M., Matilainen, M., Polvinen, E., Tuisku, J., & Airas, L. (2022). Phenotyping of multiple sclerosis lesions according to innate immune cell activation using 18 kDa translocator protein-PET. *Brain Commun*, *4*(1), fcab301. doi:10.1093/braincomms/fcab301
- O'Connor, P., Wolinsky, J. S., Confavreux, C., Comi, G., Kappos, L., Olsson, T. P., . . . Group, T. T. (2011). Randomized trial of oral teriflunomide for relapsing multiple sclerosis. *N Engl J Med*, *365*(14), 1293–1303. doi:10.1056/NEJMoa1014656
- Okuda, D. T., Kantarci, O., Lebrun-Frénay, C., Sormani, M. P., Azevedo, C. J., Bovis, F., . . . Pelletier, D. (2023). Dimethyl Fumarate Delays Multiple Sclerosis in Radiologically Isolated Syndrome. *Ann Neurol*, *93*(3), 604–614. doi:10.1002/ana.26555
- Olsson, T., Barcellos, L. F., & Alfredsson, L. (2017). Interactions between genetic, lifestyle and environmental risk factors for multiple sclerosis. *Nat Rev Neurol*, *13*(1), 25–36. doi:10.1038/nrneurol.2016.187
- Owen, D. R., Yeo, A. J., Gunn, R. N., Song, K., Wadsworth, G., Lewis, A., . . . Rubio, J. P. (2012). An 18-kDa translocator protein (TSPO) polymorphism explains differences in binding affinity of the PET radioligand PBR28. *J Cereb Blood Flow Metab*, *32*(1), 1–5. doi:10.1038/jcbfm.2011.147
- Owens, T. D., Smith, P. F., Redfern, A., Xing, Y., Shu, J., Karr, D. E., . . . Gourlay, S. G. (2022). Phase 1 clinical trial evaluating safety, exposure and pharmacodynamics of BTK inhibitor tolebrutinib (PRN2246, SAR442168). *Clin Transl Sci*, *15*(2), 442–450. doi:10.1111/cts.13162
- Pachner, A. R., & Steiner, I. (2009). The multiple sclerosis severity score (MSSS) predicts disease severity over time. *J Neurol Sci*, *278*(1–2), 66–70. doi:10.1016/j.jns.2008.11.020
- Pakpoor, J., Disanto, G., Gerber, J. E., Dobson, R., Meier, U. C., Giovannoni, G., & Ramagopalan, S. V. (2013). The risk of developing multiple sclerosis in individuals seronegative for Epstein-Barr virus: a meta-analysis. *Mult Scler*, *19*(2), 162–166. doi:10.1177/1352458512449682
- Palacios, N., Alonso, A., Brønnum-Hansen, H., & Ascherio, A. (2011). Smoking and increased risk of multiple sclerosis: parallel trends in the sex ratio reinforce the evidence. *Ann Epidemiol*, *21*(7), 536–542. doi:10.1016/j.annepidem.2011.03.001
- Palanichamy, A., Jahn, S., Nickles, D., Derstine, M., Abounasr, A., Hauser, S. L., . . . von Büdingen, H. C. (2014). Rituximab efficiently depletes increased CD20-expressing T cells in multiple sclerosis patients. *J Immunol*, *193*(2), 580–586. doi:10.4049/jimmunol.1400118
- Park, E., Gallezot, J. D., Delgado, A., Liu, S., Planeta, B., Lin, S. F., . . . Pelletier, D. (2015). (11)C-PBR28 imaging in multiple sclerosis patients and healthy controls: test-retest reproducibility and focal visualization of active white matter areas. *Eur J Nucl Med Mol Imaging*, *42*(7), 1081–1092. doi:10.1007/s00259-015-3043-4
- Pichler, V., Berroterán-Infante, N., Philippe, C., Vranka, C., Klebermass, E. M., Balber, T., . . . Wadsak, W. (2018). An Overview of PET Radiochemistry, Part 1: The Covalent Labels. *J Nucl Med*, *59*(9), 1350–1354. doi:10.2967/jnumed.117.190793
- Pirttialo, A. L., Soilu-Hänninen, M., & Sipilä, J. O. T. (2019). Multiple sclerosis epidemiology in Finland: Regional differences and high incidence. *Acta Neurol Scand*, *139*(4), 353–359. doi:10.1111/ane.13057

- Pirttialo, A. L., Soilu-Hänninen, M., Sumelahti, M. L., Krökki, O., Murtonen, A., Hänninen, K., & Sipilä, J. O. T. (2020). Changes in multiple sclerosis epidemiology in Finland over five decades. *Acta Neurol Scand*, *142*(3), 200–209. doi:10.1111/ane.13295
- Plavén-Sigray, P., Matheson, G. J., Cselényi, Z., Jucaite, A., Farde, L., & Cervenka, S. (2018). Test-retest reliability and convergent validity of (R)-[EJNMMI Res, *8*(1), 102. doi:10.1186/s13550-018-0455-8
- Politis, M., Giannetti, P., Su, P., Turkheimer, F., Keihaninejad, S., Wu, K., . . . Piccini, P. (2012). Increased PK11195 PET binding in the cortex of patients with MS correlates with disability. *Neurology*, *79*(6), 523–530. doi:10.1212/WNL.0b013e3182635645
- Polman, C. H., O'Connor, P. W., Havrdova, E., Hutchinson, M., Kappos, L., Miller, D. H., . . . Investigators, A. (2006). A randomized, placebo-controlled trial of natalizumab for relapsing multiple sclerosis. *N Engl J Med*, *354*(9), 899–910. doi:10.1056/NEJMoa044397
- Polman, C. H., Reingold, S. C., Banwell, B., Clanet, M., Cohen, J. A., Filippi, M., . . . Wolinsky, J. S. (2011). Diagnostic criteria for multiple sclerosis: 2010 revisions to the McDonald criteria. *Ann Neurol*, *69*(2), 292–302. doi:10.1002/ana.22366
- Polvinen, E., Matilainen, M., Nylund, M., Sucksdorff, M., & Airas, L. M. (2023). TSPO-Detectable Chronic Active Lesions Predict Disease Progression in Multiple Sclerosis. *Neurol Neuroimmunol Neuroinflamm*, *10*(5). doi:10.1212/NXI.0000000000200133
- Popescu, B. F., & Lucchinetti, C. F. (2012). Pathology of demyelinating diseases. *Annu Rev Pathol*, *7*, 185–217. doi:10.1146/annurev-pathol-011811-132443
- Portaccio, E., Bellinva, A., Fonderico, M., Pastò, L., Razzolini, L., Totaro, R., . . . Amato, M. P. (2022). Progression is independent of relapse activity in early multiple sclerosis: a real-life cohort study. *Brain*, *145*(8), 2796–2805. doi:10.1093/brain/awac111
- Preziosa, P., Pagani, E., Meani, A., Moiola, L., Rodegher, M., Filippi, M., & Rocca, M. A. (2022). Slowly Expanding Lesions Predict 9-Year Multiple Sclerosis Disease Progression. *Neurol Neuroimmunol Neuroinflamm*, *9*(2). doi:10.1212/NXI.0000000000001139
- Prosperini, L., Mancinelli, C. R., Solaro, C. M., Nociti, V., Haggiag, S., Cordioli, C., . . . Gasperini, C. (2020). Induction Versus Escalation in Multiple Sclerosis: A 10-Year Real World Study. *Neurotherapeutics*, *17*(3), 994–1004. doi:10.1007/s13311-020-00847-0
- Rae-Grant, A., Day, G. S., Marrie, R. A., Rabinstein, A., Cree, B. A. C., Gronseth, G. S., . . . Pringsheim, T. (2018). Comprehensive systematic review summary: Disease-modifying therapies for adults with multiple sclerosis: Report of the Guideline Development, Dissemination, and Implementation Subcommittee of the American Academy of Neurology. *Neurology*, *90*(17), 789–800. doi:10.1212/WNL.0000000000005345
- Ransohoff, R. M., Hafler, D. A., & Lucchinetti, C. F. (2015). Multiple sclerosis—a quiet revolution. *Nat Rev Neurol*, *11*(3), 134–142. doi:10.1038/nrneurol.2015.14
- Ratchford, J. N., Endres, C. J., Hammoud, D. A., Pomper, M. G., Shice, N., McGready, J., . . . Calabresi, P. A. (2012). Decreased microglial activation in MS patients treated with glatiramer acetate. *J Neurol*, *259*(6), 1199–1205. doi:10.1007/s00415-011-6337-x
- Rissanen, E., Tuisku, J., Rokka, J., Paavilainen, T., Parkkola, R., Rinne, J. O., & Airas, L. (2014). In Vivo Detection of Diffuse Inflammation in Secondary Progressive Multiple Sclerosis Using PET Imaging and the Radioligand ¹¹C-PK11195. *J Nucl Med*, *55*(6), 939–944. doi:10.2967/jnumed.113.131698
- Rissanen, E., Tuisku, J., Vahlberg, T., Sucksdorff, M., Paavilainen, T., Parkkola, R., . . . Airas, L. (2018). Microglial activation, white matter tract damage, and disability in MS. *Neurol Neuroimmunol Neuroinflamm*, *5*(3), e443. doi:10.1212/NXI.0000000000000443
- Rotstein, D., & Montalban, X. (2019). Reaching an evidence-based prognosis for personalized treatment of multiple sclerosis. *Nat Rev Neurol*, *15*(5), 287–300. doi:10.1038/s41582-019-0170-8
- Rotstein, D. L., Chen, H., Wilton, A. S., Kwong, J. C., Marrie, R. A., Gozdyra, P., . . . Tu, K. (2018). Temporal trends in multiple sclerosis prevalence and incidence in a large population. *Neurology*, *90*(16), e1435–e1441. doi:10.1212/WNL.0000000000005331

- Roxburgh, R. H., Seaman, S. R., Masterman, T., Hensiek, A. E., Sawcer, S. J., Vukusic, S., . . . Compston, D. A. (2005). Multiple Sclerosis Severity Score: using disability and disease duration to rate disease severity. *Neurology*, *64*(7), 1144–1151. doi:10.1212/01.WNL.0000156155.19270.F8
- Runia, T. F., Hop, W. C., de Rijke, Y. B., Buljevac, D., & Hintzen, R. Q. (2012). Lower serum vitamin D levels are associated with a higher relapse risk in multiple sclerosis. *Neurology*, *79*(3), 261–266. doi:10.1212/WNL.0b013e31825fdec7
- Sadovnick, A. D., Armstrong, H., Rice, G. P., Bulman, D., Hashimoto, L., Paty, D. W., . . . Murray, T. J. (1993). A population-based study of multiple sclerosis in twins: update. *Ann Neurol*, *33*(3), 281–285. doi:10.1002/ana.410330309
- Salzer, J., Svenningsson, R., Alping, P., Novakova, L., Björck, A., Fink, K., . . . Svenningsson, A. (2016). Rituximab in multiple sclerosis: A retrospective observational study on safety and efficacy. *Neurology*, *87*(20), 2074–2081. doi:10.1212/WNL.0000000000003331
- Saraste, M., Bezukladova, S., Sucksdorff, M., Saunavaara, V., Rissanen, E., Matilainen, M., & Airas, L. (2021). Fingolimod treatment reverses signs of diffuse white matter damage in multiple sclerosis: A pilot study. *Mult Scler Relat Disord*, *48*, 102690. doi:10.1016/j.msard.2020.102690
- Sawcer, S., Hellenthal, G., Pirinen, M., Spencer, C. C., Patsopoulos, N. A., Moutsianas, L., . . . 2, W. T. C. C. C. (2011). Genetic risk and a primary role for cell-mediated immune mechanisms in multiple sclerosis. *Nature*, *476*(7359), 214–219. doi:10.1038/nature10251
- Schweitzer, P. J., Fallon, B. A., Mann, J. J., & Kumar, J. S. (2010). PET tracers for the peripheral benzodiazepine receptor and uses thereof. *Drug Discov Today*, *15*(21–22), 933–942. doi:10.1016/j.drudis.2010.08.012
- Serafini, B., Rosicarelli, B., Veroni, C., Mazzola, G. A., & Aloisi, F. (2019). Epstein-Barr Virus-Specific CD8 T Cells Selectively Infiltrate the Brain in Multiple Sclerosis and Interact Locally with Virus-Infected Cells: Clue for a Virus-Driven Immunopathological Mechanism. *J Virol*, *93*(24). doi:10.1128/JVI.00980-19
- Serafini, B., Scorsi, E., Rosicarelli, B., Rigau, V., Thouvenot, E., & Aloisi, F. (2017). Massive intracerebral Epstein-Barr virus reactivation in lethal multiple sclerosis relapse after natalizumab withdrawal. *J Neuroimmunol*, *307*, 14–17. doi:10.1016/j.jneuroim.2017.03.013
- Sharmin, S., Lefort, M., Andersen, J. B., Leray, E., Horakova, D., Havrdova, E. K., . . . Danish Multiple Sclerosis Registry, O. F. S. E. a. t. M. i. (2021). Natalizumab Versus Fingolimod in Patients with Relapsing-Remitting Multiple Sclerosis: A Subgroup Analysis From Three International Cohorts. *CNS Drugs*, *35*(11), 1217–1232. doi:10.1007/s40263-021-00860-7
- Signori, A., Saccà, F., Lanzillo, R., Maniscalco, G. T., Signoriello, E., Repice, A. M., . . . Sormani, M. P. (2020). Cladribine vs other drugs in MS: Merging randomized trial with real-life data. *Neurol Neuroimmunol Neuroinflamm*, *7*(6). doi:10.1212/NXI.0000000000000878
- Simpson, S., Taylor, B., Blizzard, L., Ponsonby, A. L., Pittas, F., Tremlett, H., . . . van der Mei, I. (2010). Higher 25-hydroxyvitamin D is associated with lower relapse risk in multiple sclerosis. *Ann Neurol*, *68*(2), 193–203. doi:10.1002/ana.22043
- Singhal, T., O'Connor, K., Dubey, S., Pan, H., Chu, R., Hurwitz, S., . . . Bakshi, R. (2019). Gray matter microglial activation in relapsing vs progressive MS: A [F-18]PBR06-PET study. *Neurol Neuroimmunol Neuroinflamm*, *6*(5), e587. doi:10.1212/NXI.0000000000000587
- Sorensen, P. S., & Blinkenberg, M. (2016). The potential role for ocrelizumab in the treatment of multiple sclerosis: current evidence and future prospects. *Ther Adv Neurol Disord*, *9*(1), 44–52. doi:10.1177/1756285615601933
- Spelman, T., Kalincik, T., Jokubaitis, V., Zhang, A., Pellegrini, F., Wiendl, H., . . . Butzkueven, H. (2016). Comparative efficacy of first-line natalizumab vs IFN- β or glatiramer acetate in relapsing MS. *Neurol Clin Pract*, *6*(2), 102–115. doi:10.1212/CPJ.0000000000000227
- Stephenson, J., Nutma, E., van der Valk, P., & Amor, S. (2018). Inflammation in CNS neurodegenerative diseases. *Immunology*, *154*(2), 204–219. doi:10.1111/imm.12922

- Stys, P. K., Zamponi, G. W., van Minnen, J., & Geurts, J. J. (2012). Will the real multiple sclerosis please stand up? *Nat Rev Neurosci*, *13*(7), 507–514. doi:10.1038/nrn3275
- Svenningsson, A., Frisell, T., Burman, J., Salzer, J., Fink, K., Hallberg, S., . . . Lycke, J. (2022). Safety and efficacy of rituximab versus dimethyl fumarate in patients with relapsing-remitting multiple sclerosis or clinically isolated syndrome in Sweden: a rater-blinded, phase 3, randomised controlled trial. *Lancet Neurol*, *21*(8), 693–703. doi:10.1016/S1474-4422(22)00209-5
- Thompson, A. J., Banwell, B. L., Barkhof, F., Carroll, W. M., Coetzee, T., Comi, G., . . . Cohen, J. A. (2018). Diagnosis of multiple sclerosis: 2017 revisions of the McDonald criteria. *Lancet Neurol*, *17*(2), 162–173. doi:10.1016/S1474-4422(17)30470-2
- Thompson, A. J., & Hobart, J. C. (1998). Multiple sclerosis: assessment of disability and disability scales. *J Neurol*, *245*(4), 189–196. doi:10.1007/s004150050204
- Tilling, K., Lawton, M., Robertson, N., Tremlett, H., Zhu, F., Harding, K., . . . Ben-Shlomo, Y. (2016). Modelling disease progression in relapsing-remitting onset multiple sclerosis using multilevel models applied to longitudinal data from two natural history cohorts and one treated cohort. *Health Technol Assess*, *20*(81), 1–48. doi:10.3310/hta20810
- Trapp, B. D., Peterson, J., Ransohoff, R. M., Rudick, R., Mörk, S., & Bö, L. (1998). Axonal transection in the lesions of multiple sclerosis. *N Engl J Med*, *338*(5), 278–285. doi:10.1056/NEJM199801293380502
- Tremblay, M., Stevens, B., Sierra, A., Wake, H., Bessis, A., & Nimmerjahn, A. (2011). The role of microglia in the healthy brain. *J Neurosci*, *31*(45), 16064–16069. doi:10.1523/JNEUROSCI.4158-11.2011
- Tremlett, H., Yinshan Zhao, & Devonshire, V. (2008). Natural history of secondary-progressive multiple sclerosis. *Mult Scler*, *14*(3), 314–324. doi:10.1177/1352458507084264
- Tur, C., Carbonell-Mirabent, P., Cobo-Calvo, Á., Otero-Romero, S., Arrambide, G., Midaglia, L., . . . Montalban, X. (2023). Association of Early Progression Independent of Relapse Activity With Long-term Disability After a First Demyelinating Event in Multiple Sclerosis. *JAMA Neurol*, *80*(2), 151–160. doi:10.1001/jamaneurol.2022.4655
- Turkheimer, F. E., Edison, P., Pavese, N., Roncaroli, F., Anderson, A. N., Hammers, A., . . . Brooks, D. J. (2007). Reference and target region modeling of [¹¹C]-(R)-PK11195 brain studies. *J Nucl Med*, *48*(1), 158–167.
- Turkington, T. G. (2001). Introduction to PET instrumentation. *J Nucl Med Technol*, *29*(1), 4–11.
- Tutuncu, M., Tang, J., Zeid, N. A., Kale, N., Crusan, D. J., Atkinson, E. J., . . . Kantarci, O. H. (2013). Onset of progressive phase is an age-dependent clinical milestone in multiple sclerosis. *Mult Scler*, *19*(2), 188–198. doi:10.1177/1352458512451510
- van den Hoff, J. (2005). Principles of quantitative positron emission tomography. *Amino Acids*, *29*(4), 341–353. doi:10.1007/s00726-005-0215-8
- Veenman, L., & Gavish, M. (2012). The role of 18 kDa mitochondrial translocator protein (TSPO) in programmed cell death, and effects of steroids on TSPO expression. *Curr Mol Med*, *12*(4), 398–412. doi:10.2174/1566524011207040398
- Versijpt, J., Debruyne, J. C., Van Laere, K. J., De Vos, F., Keppens, J., Strijckmans, K., . . . De Reuck, J. L. (2005). Microglial imaging with positron emission tomography and atrophy measurements with magnetic resonance imaging in multiple sclerosis: a correlative study. *Mult Scler*, *11*(2), 127–134. doi:10.1191/1352458505ms1140oa
- Voet, S., Prinz, M., & van Loo, G. (2019). Microglia in Central Nervous System Inflammation and Multiple Sclerosis Pathology. *Trends Mol Med*, *25*(2), 112–123. doi:10.1016/j.molmed.2018.11.005
- Vowinckel, E., Reutens, D., Becher, B., Verge, G., Evans, A., Owens, T., & Antel, J. P. (1997). PK11195 binding to the peripheral benzodiazepine receptor as a marker of microglia activation in multiple sclerosis and experimental autoimmune encephalomyelitis. *J Neurosci Res*, *50*(2), 345–353. doi:10.1002/(SICI)1097-4547(19971015)50:2<345::AID-JNR22>3.0.CO;2-5

- Vukusic, S., & Confavreux, C. (2003). Prognostic factors for progression of disability in the secondary progressive phase of multiple sclerosis. *J Neurol Sci*, *206*(2), 135–137. doi:10.1016/s0022-510x(02)00426-4
- Weinshenker, B. G., Bass, B., Rice, G. P., Noseworthy, J., Carriere, W., Baskerville, J., & Ebers, G. C. (1989). The natural history of multiple sclerosis: a geographically based study. 2. Predictive value of the early clinical course. *Brain*, *112* (Pt 6), 1419–1428. doi:10.1093/brain/112.6.1419
- Weinstein, D. R., Owens, G. M., & Gandhi, A. (2022). Multiple Sclerosis: Systemic Challenges to Cost-Effective Care. *Am Health Drug Benefits*, *15*(1), 13–20.
- Wesnes, K., Myhr, K. M., Riise, T., Cortese, M., Pugliatti, M., Boström, I., . . . Bjørnevik, K. (2018). Physical activity is associated with a decreased multiple sclerosis risk: The EnvIMS study. *Mult Scler*, *24*(2), 150–157. doi:10.1177/1352458517694088
- Wesnes, K., Riise, T., Casetta, I., Drulovic, J., Granieri, E., Holmøy, T., . . . Myhr, K. M. (2015). Body size and the risk of multiple sclerosis in Norway and Italy: the EnvIMS study. *Mult Scler*, *21*(4), 388–395. doi:10.1177/1352458514546785
- Westerlind, H., Ramanujam, R., Uvehag, D., Kuja-Halkola, R., Boman, M., Bottai, M., . . . Hillert, J. (2014). Modest familial risks for multiple sclerosis: a registry-based study of the population of Sweden. *Brain*, *137*(Pt 3), 770–778. doi:10.1093/brain/awt356
- Wiendl, H., Gold, R., Berger, T., Derfuss, T., Linker, R., Mäurer, M., . . . (MSTCG), M. S. T. C. G. (2021). Multiple Sclerosis Therapy Consensus Group (MSTCG): position statement on disease-modifying therapies for multiple sclerosis (white paper). *Ther Adv Neurol Disord*, *14*, 17562864211039648. doi:10.1177/17562864211039648
- Wittayer, M., Weber, C. E., Platten, M., Schirmer, L., Gass, A., & Eisele, P. (2022). Spatial distribution of multiple sclerosis iron rim lesions and their impact on disability. *Mult Scler Relat Disord*, *64*, 103967. doi:10.1016/j.msard.2022.103967
- Wolinsky, J. S., Arnold, D. L., Brochet, B., Hartung, H. P., Montalban, X., Naismith, R. T., . . . Hauser, S. L. (2020). Long-term follow-up from the ORATORIO trial of ocrelizumab for primary progressive multiple sclerosis: a post-hoc analysis from the ongoing open-label extension of the randomised, placebo-controlled, phase 3 trial. *Lancet Neurol*, *19*(12), 998–1009. doi:10.1016/S1474-4422(20)30342-2
- Yaqub, M., van Berckel, B. N., Schuitemaker, A., Hinz, R., Turkheimer, F. E., Tomasi, G., . . . Boellaard, R. (2012). Optimization of supervised cluster analysis for extracting reference tissue input curves in (R)-[(11)C]PK11195 brain PET studies. *J Cereb Blood Flow Metab*, *32*(8), 1600–1608. doi:10.1038/jcbfm.2012.59
- Yong, H. Y. F., & Yong, V. W. (2022). Mechanism-based criteria to improve therapeutic outcomes in progressive multiple sclerosis. *Nat Rev Neurol*, *18*(1), 40–55. doi:10.1038/s41582-021-00581-x
- Zanzonico, P. (2012). Principles of nuclear medicine imaging: planar, SPECT, PET, multi-modality, and autoradiography systems. *Radiat Res*, *177*(4), 349–364. doi:10.1667/tr2577.1
- Zivadinov, R., Weinstock-Guttman, B., Hashmi, K., Abdelrahman, N., Stosic, M., Dwyer, M., . . . Ramanathan, M. (2009). Smoking is associated with increased lesion volumes and brain atrophy in multiple sclerosis. *Neurology*, *73*(7), 504–510. doi:10.1212/WNL.0b013e3181b2a706



**TURUN
YLIOPISTO**
UNIVERSITY
OF TURKU

ISBN 978-951-29-9529-5 (PRINT)
ISBN 978-951-29-9530-1 (PDF)
ISSN 0355-9483 (Print)
ISSN 2343-3213 (Online)